DEVELOPMENT AND VALIDATION OF A DRIVER DISTRACTION ALERT SYSTEM FOR HIGHWAY DRIVING USING A TRUCK DRIVING SIMULATOR

by

Laith Faris Dababneh

A Thesis Submitted in Partial Fulfillment
of the Requirements for the Degree of

Master of Applied Science

In

Automotive Engineering

Faculty of Engineering and Applied Science
University of Ontario Institute of Technology
Oshawa, Ontario, Canada

July 2016

ABSTRACT

Driver distraction is one of the major causes of vehicle accidents, injuries, fatalities and economical losses in Canada and across the world. The main objective of this thesis is to develop a real time driver distraction alert system that can generate early warning signals and prevent vehicle accidents. The proposed system is applied to a truck driving simulator by monitoring the driver response through the steering wheel and accelerator pedal during different driving experiments. In order to ensure an accurate prediction of the driver distraction, the simulation output of the truck driving simulator is compared to that of the commercial TruckSim® software using identical parameters of a given tractor semitrailer during similar driving conditions. Consequently, the driving speed and steering angle profiles for both simulation environments are then compared during standard test maneuvers and found to be in good agreement. Several distraction indicators are proposed in order to predict the driver distraction namely; the jerk profile, spikiness index and the rate of change for both the steering wheel angle and the accelerator pedal position. Several driving experiments are performed considering both the offline and real time assessment of a driver subjected to different types of distraction. The major finding of the thesis emphasizes the effectiveness of using steering wheel rate to estimate driver distraction. Moreover, in comparison to other techniques for predicting driver vigilance, the presented work requires low computational power and has a great potential for developing a real time simple system that can be affordable and reliable.

CONTENTS

LIST OF FIGURES

LIST OF TABLES

LIST OF ABBREVIATIONS

Abbreviation	Expansion
AI	Artificial Intelligence
ANNs	Artificial Neural Networks
AWAKE	Assessment and Warning According to traffic risK Estimation
BCI	Brain Computer Interface
CAPC	Crewman's Associate for Path Control
C.G	Center of Gravity
CISR	Center for Intelligent Systems Research
CSV	Comma Separated Value
DAA	Driver Attention Alert
DI	Distraction Indicator
DMU	Dynamic Measurement Unit
DSS	Driver Safety Solution
DWSs	Driver Warning Systems
EEG	Electroencephalogram (Measuring electrical activity of the brain)
ESP	Electronic Stability Program
ESS	Epworth Sleepiness Scale
GSR	Galvanic Skin Response
HDM	Hypo-vigilance Diagnosis Module
HiLS	Hardware in the Loop Simulator
HM	Hierarchical Manager
IR LEDs	Infrared Light-Emitting Diodes
KSS	Karolinska Sleepiness Scale
LISP	LISt Programming
LMS	Least Mean Squares
LOIS	Likelihood of Image Shape
LSTM	Long Short-Term Memory recurrent neural network
LTV	Linear Time-Variant
MD	Mahalanobis Distance
MFD	Multi-Functional Display

Abbreviation	Expansion
MLP NN	Multilayered Perceptron Neural Network
NHTSA	National Highway Traffic Safety Administration
NIR	Near Infra-Red
OP	Oximetry Pulse
PERCLOS	Percentage of eyelid closure
PPV	Precision of drowsiness prediction
PTDS	Pennsylvania State Truck Driving Simulator
RBPNN	Radial Basis Probabilistic Neural Network
RPROP	Resilient propagation algorithm
SRR	Skin Resistance Response
SSE	Sum Squared Error
SVM	Support Vector Machines
TFALDA	Three Feature based on Automatic Lane Detection Algorithm
TLC	Time to Lane-Crossing
TRE	Traffic Risk Estimation
VDANL	Vehicle Dynamic Analysis Non-Linear

NOMENCLATURE

Symbol	Parameter	Units
Y_i	Steering wheel angle or the accelerator pedal position.	[deg] or [-]
$\dot{Y}_i$	Steering wheel angle or accelerator pedal rate of change	[deg/s]
$\ddot{Y}_i$	Steering wheel angle or accelerator pedal jerk profile	[deg/s^3]
a_{i+n}	Savitzky-Golay filter coefficients.	[-]
C_o	Normalized Savitzky-Golay filter coefficient (Norm)	[-]
Δt	Time step of the middle point	[s]
Ψ	spikiness index	[-]
n_{avg}	Number of data points to find the general trend of jerk	[-]
n	Total number of data points for the entire driving	[-]
$\ddot{Y}_j$	Instantaneous jerk used to calculate the general trend	[deg/s^3]
K	The time at which the driving scenario starts	[s]
N	The time at which the driving scenario ends	[s]
E_{K2}	Represents a point on any driving behaviour curve	[-]
E_{K1}	Represents a point on the baseline driving behaviour	[-]
DI	Distraction indicator	[-]
SSE_{ref}	Reference sum squared error of the alert behaviour	[-]
SSE_a	Sum squared error of any driving experiment	[-]
Sr_i	Steering rate for a specific point (i) in time	[deg/s]
Sw_i	Steering angle for a specific point (i) in time	[deg]
Sw_{i-1}	Steering angle for the point preceding point (i) in time	[deg]
T	Final steering rate threshold for the alert behaviour	[deg/s]
S_{max}	Maximum absolute steering rate for the alert behaviour	[deg/s]
F_a	Allowance factor	[-]
J	Jerk profile of accelerator pedal	[N/s]
A	Amplitude of the jerk	[N/s]
ω	Frequency of the jerk	[1/s]
E	Sum squared error	[-]
$output_i$	neural network output	[-]
$input_i$	neural network input	[-]

Symbol	Parameter	Units
STD	Standard deviation	[-]
x_i	Lateral position or the heading error of the vehicle	[m] or [-]
$\bar{x}$	Arithmetic mean of the time series	[m] or [-]
RSWM	Rapid steering wheel movement	[-]
$h(\dot{s_t})$	A parameter that equals 1 if drowsiness is detected	[-]

ACKNOWLEDGEMENTS

I would like to thank God for guiding me and giving me hope, strength and patience during the course of my academic journey. I would like to express my appreciation to Canada Foundation for Innovation (CFI) and Infrastructure Operating Fund (IOF) for funding the Virage truck driving simulator projects. I would like to express my sincere gratitude to my thesis supervisor Dr. Moustafa El-Gindy for his continuous help, guidance and support during the course of my academic research in the Truck Driving Simulator Laboratory at the University of Ontario Institute of Technology (UOIT). I would also like to thank Virage Simulation Incorporations for their technical support. A special word of thanks to Dr. Alhossein Mostafa Sharaf for his valuable technical contribution and critical editorial revision of this thesis during his post-doctoral fellowship to UOIT. Last but not least, I would like to express my genuine appreciation to my parents Dr. Faris Dababneh and Dr. Sana Naffa for their financial and emotional support. I am also fortunate to have the support and encouragement of my sister Dima and my brother Saif.

CHAPTER 1

INTRODUCTION AND LITERATURE REVIEW

This chapter includes the research thesis motivation, objectives, outline as well as literature review. The literature review gives an overview of the truck simulator validation, the factors resulting in driver vigilance loss as well as the available driver attentiveness monitoring techniques. The information presented in this chapter is provided to give a better understanding of the research problem at hand and to introduce the reader to the future concepts and methodology presented in this thesis. This study has been approved by the Research Ethics Board (REB) at the University of Ontario Institute of Technology (UOIT) and a certificate of completion is provided in Appendix C.

1.1 MOTIVATION

Vehicle accidents have caused deaths, injuries and economic losses worldwide. Drowsiness and distraction are considered as two of the major causes of accidents. The National Highway Traffic Safety Administration (NHTSA) in the USA estimates 56,000 crashes, 40,000 injuries and 1,550 fatalities caused annually by drowsiness/fatigue [1]. This corresponds to $12.4 billion of annual economic losses [2, 3]. In Canada, accidents caused by drowsiness/fatigue are responsible for 20% of all fatal accidents [4]. In addition, accidents caused by drowsiness are estimated to be 35% of fatal motorway crashes in both Australia and Germany [5]. The National Highway Traffic Safety Administration also estimates injuries and fatalities caused by distraction related accidents as 20% of all injuries and 16% of all fatalities [4].

In Canada, a massive accident took place on the 401 highway near Ajax, Ontario on October 29, 2015. Twenty vehicles were involved in the crash and three people including a 12-year-old boy were killed. In addition, other drivers and passengers were critically injured. The accident happened when a transport truck driver did not notice the slowdown of traffic due to a road construction area and smashed into the slow moving traffic. Durham Regional Police Service carried out an investigation to know the reason behind this massive accident and it was concluded that the accident was caused by driver distraction. Durham police investigators said that it took the transport truck driver a moment of being distracted and not paying attention to signs and traffic to cause the fatal collision [6].

Consequently, modern society and automotive companies are now more concerned with safety on roadways. Automotive companies and researchers have worked on developing driver warning systems (DWSs) to prevent accidents before they occur and they have also worked on improving the vehicle's structure and design to avoid driver compartment intrusion during an accident. This research is concerned with developing driver alert systems that can detect driver distraction and issue a warning to avoid accidents.

1.2 OBJECTIVES AND SCOPE

The objective of this thesis is to study the effects of distraction and other factors contributing to vigilance loss on the driving behaviour of commercial truck drivers and to develop a real time distraction detection system that can detect driver distraction at an early stage and issue an audible and visual warning signal that notifies drivers of their reduced vigilance level. A motion base truck driving simulator will be used to study the driving behaviour of the driver and to develop the real time driver distraction detection alert system. Currently, vigilance level detection systems mostly depend on cameras to detect

lane markings or to detect facial features of the driver. The use of cameras requires large computational and image processing power and is affected by environmental conditions such as weather and illumination. Commercially available systems that use cameras to monitor driver vigilance based on facial features are expensive. Other detection systems use the interface between the driver and the vehicle such as the steering wheel and other control panels. However, commercially available systems of this kind are only implemented in high class vehicles and incorporate using other techniques that require cameras to aid in the detection process. In this thesis, the detection system will solely depend on detecting distraction based on the interface of the driver and the vehicle. The main goal of this study is to prove that the car-driver interface is sufficient for detecting differences in driving behaviour and to develop an affordable distraction detection system that can be easily implemented in trucks. The developed system will monitor the steering profile of the driver and build a baseline of the normal driving profile. The system will then issue a warning whenever the driver is outside of their normal driving range. The developed system will alert drivers of their vigilance level without taking any corrective measures on its own resulting in the driver having to act. The developed system is intended for truck drivers who spend long periods of time behind the wheel on expressways with speed limits above 80 km/h.

1.3 OUTLINE OF THESIS

Chapter 2 of this thesis demonstrates the main components of the Virage truck driving simulator used in this study and describes the method implemented in the validation of the truck driving simulator model. Chapter 3 illustrates the methodology used in the development of the real time driver distraction alert system. Chapter 4 presents the results

and discussion of the offline detection of driver distraction. Chapter 5 presents the results and discussion of the real time detection of driver distraction. Chapter 6 discusses the conclusions and future work.

1.4 LITERATURE REVIEW

This section is provided to discuss the driving simulator validation techniques used in previous research. This section is also needed to review the factors contributing to the alertness reduction during driving, alertness level monitoring techniques that are used in accident prevention warning systems and the commercially available vigilance loss detection systems. Alertness monitoring techniques using artificial neural networks (ANNs) are also reviewed since neural networks have been widely used for their ability to classify different levels of alertness.

1.4.1 Validation of Truck Driving Simulators

In this research a truck driving simulator is used to study the effect of distraction on the driving behaviour. As a result, validation is needed to prove that the truck driving simulator model is actually realistic and comparable to real world trucks. Validation is also needed to show that the proposed driver distraction detection system can be commercialized and used in real trucks. Validation is defined as "*the extent to which a model serves its purpose for a particular training device or devices*" [7]. As a result, if the simulator model can generate results that are comparable to a real truck then the model serves its purpose.

Simulator validation can be divided into two primary areas; behavioural and physical. The behavioural validation is concerned with the driver response in real life and the simulation environment. For example, this type of validation compares how fast a driver can respond

to a pedestrian crossing the street in both real life and simulation environments. The physical validation is concerned with the accuracy of the results of the simulation environment compared to that of the typical truck for the same vehicle parameters and driving conditions [8, 9]. This type of validation is essential since it adds accuracy to the model and gives the real driving feel. For example, if a driver is required to perform a certain turn maneuver in real life and in the simulation environment, a valid model would require the driver to have similar steering profiles in both environments.

Panerai et al. [10] presented a study that focused on the behavioural validation of the Renault-V.I truck simulator with real trucks. The speed and safety distance control tasks were used for the validation purposes. Eight professional drivers performed the experiments both on the simulator and in real life. In addition, thirty non-professional drivers performed experiments in the simulation environment only. The drivers were asked to control the vehicle speed without looking at the speedometer as a part of the speed control task. The drivers were then asked to keep a safe distance with preceding vehicles. The simulator used consists of a multi-screen display, a motion base as well as an acoustic feedback. The study concluded that the simulation speed profiles of both driver groups were highly correlated with real world driving. However, professional drivers maintained a safe distance that was as twice as the distance maintained in real world driving. In addition, non-professional drivers maintained a safe distance that was 47% greater than the distance maintained by professional drivers in the simulation environment. It was suggested that the underestimation of the safety distance could be attributed to a poor geometric content in the simulation visual information.

Hoskins et al. [11] presented a validation method that was used for the physical validation of the Pennsylvania State Truck Driving Simulator (PTDS). The validation was done by comparing the results of the PTDS cab motion in the simulation environment with a stand-alone simulation software that uses driving inputs to predict the vehicle response. A Dynamic Measurement Unit (DMU) was placed in the cab and was able to measure the accelerations and angular rate in three directions. The Vehicle Dynamic Analysis Non-Linear (VDANL) was used as the stand-alone simulation software and utilized the driving inputs generated during the PTDS cab real time simulation as illustrated in Figure 1-1. The VDANL was first developed for the National Highway Transportation in the mid 1980's and is capable of predicting vehicle responses for various types of vehicles [12]. The timer synchronization was needed to allow the DMU and the real time simulation run simultaneously.

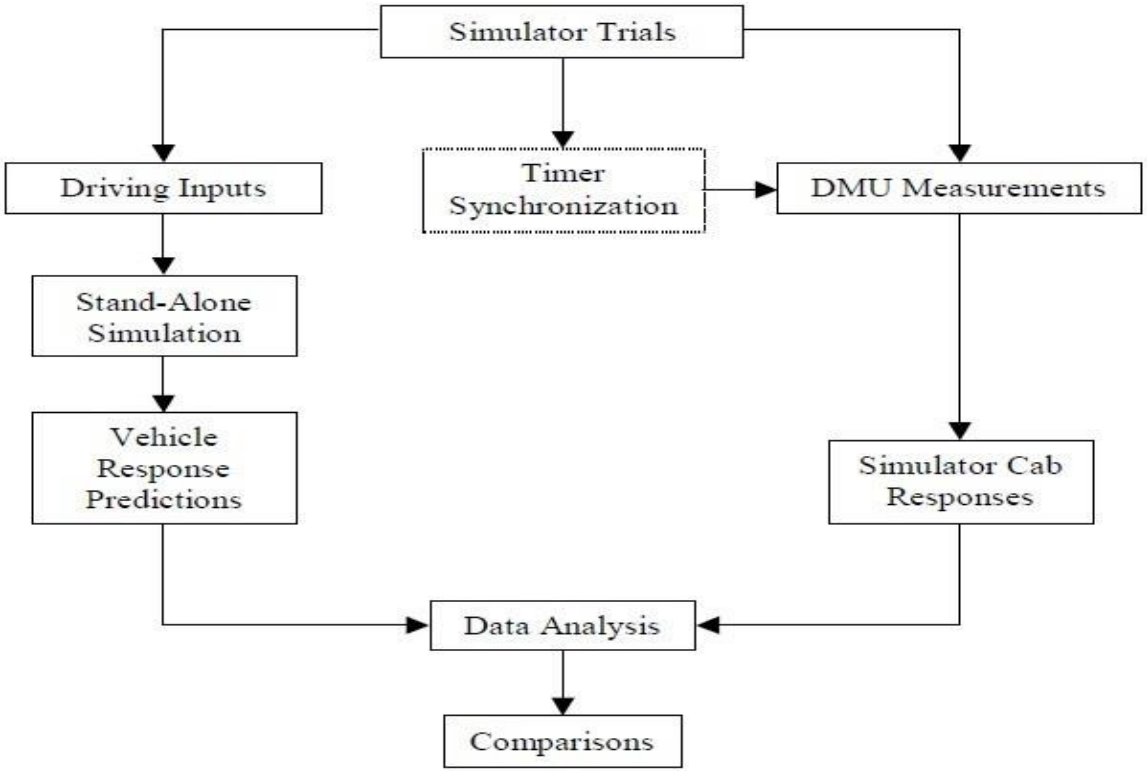

Figure 1-1 Validation method of the PTDS [11]

Two experiments were carried out to validate the PTDS model, the first was the straight-line braking while the second was the double lane change maneuver. The first experiment was needed to evaluate and compare the pitch motion and the lateral acceleration while the second experiment was required to evaluate the roll and lateral acceleration. The drivers were asked to drive down the road until a speed of 65 mph is reached and then apply the brakes as fast as possible during the first experiment. The drivers were asked to perform a double lane change at a speed of 50 mph during the second experiment. Parameters such as braking inputs, vehicle speed, steering wheel inputs and lateral accelerations were recorded during both experiments.

It was found that the braking input, velocity profile as well as the pitch velocity values generated from the simulation were highly correlated with the VDANL predictions. However, a slight variation was observed in the pitch angle and longitudinal acceleration values during the straight-line braking. It was also found that the steering input, roll angle and roll velocity values generated from the simulation were highly correlated with the VDANL predictions. However, a slight variation was observed in the lateral acceleration values. It was suggested that the variation could be attributed to computational delays.

Hoskins et al. [13] presented a literature survey paper on driving simulator validation. The paper first reviewed the definition of validation and discussed the primary types or areas of simulator validation. The primary types are the behavioural and the physical validation. The simulator experiments were validated with real world driving experiments. Several studies investigated the behavioural validation of a fixed-base and motion-base driving simulators. The behavioural validation investigation included driving tasks such as vehicle speed and lateral position control. It was reported that drivers were able to drive the

simulator at speeds that were highly correlated with real world driving experiments. However, experiments performed using fixed-base simulators showed higher vehicle speeds than real world driving experiments. This can be explained by the fact that fixed-base simulators are not capable of providing realistic driving feel so drivers tend to drive faster. In terms of the lateral position, a greater variation was observed between the simulated and the real world driving. The paper also reviewed the steps needed for the physical validation of simulators. The physical validation methodology incorporates data collection from the real world driving experiments and vehicle parameters measurements. The data is then used as an input to the simulator and real world experimental results are compared with simulation predictions.

1.4.2 Factors Contributing to Decreased Driver Vigilance

Decreased driver vigilance may be caused by prolonged inattention such as; sleepiness, fatigue and monotony or short inattention such as distraction (eating while driving, talking) and psycho-physiological factors (anger, influence of drug/alcohol) [14]. This review is concerned with short inattention caused by distraction as well as prolonged inattention related to driving long distances by passenger car and truck drivers.

Sleepiness is defined by the Oxford dictionary as the tendency to fall asleep [15]. Drowsiness and sleepiness are synonymous. Sleepiness is induced by two factors; the circadian rhythm and the homeostatic influence. Circadian rhythms are the regular occurrences which induce sleepiness throughout the day driven by the human internal clock. Circadian rhythms show unintended sleep episodes, most often around 6 am, and in the middle afternoon [16]. The homeostatic influence induces sleepiness if a person stays awake for more than 18 h [17].

Fatigue is defined by the Oxford dictionary as "*the extreme tiredness resulting from mental or physical exertion or illness*" [15]. Fatigue is technically different from sleepiness. Sleepiness is the tendency to fall asleep where fatigue can result from the workload as well as tedious activities which lead to extreme tiredness. Consequently, tiredness causes reluctance to continue performing the task at hand. A driver can get tired without being sleepy, but factors that cause fatigue could also lead to sleepiness [18].

Distraction is defined by the Oxford dictionary as "*a thing that takes your attention away from what you are doing or thinking about*" [15]. Distraction is also defined as "*the diversion of attention away from activities critical for safe driving towards a competing activity*" [19, 20]. Distraction is different than sleepiness. Distraction is generally caused by a triggering event that discerns driver alertness whereas sleepiness does not involve a triggering event and it can be considered as a gradual loss of driver alertness [21].

Monotony is defined by the Oxford dictionary as "*the lack of variety and interest; tedious repetition and routine*" [15]. Monotony affects the driver's physical, cognitive and affective sensations. A monotonous task is often repetitive, predictable and requires low activation of sensory perception. Straight and long road infrastructures are well-known factors that result in an increase of driver monotony [22]. A phenomenon called highway hypnosis is caused by the monotonous road environment. This phenomenon is described as the tendency to become drowsy and to fall asleep while driving an automobile. This phenomenon might also result in driver distraction [23].

1.4.3 Driving Vigilance Monitoring Techniques

The current alertness monitoring techniques can be divided into three categories as suggested by [24]:

- Monitoring the car (such as lane departure warning).
- Monitoring the driver (such as the percentage of eyelid closure).
- Monitoring the car-driver interface (such as steering wheel and pedals).

1.4.3.1 Car Observation Techniques

Kim and Oh [25] used first the Three Feature based on Automatic Lane Detection algorithm (TFALDA) to detect lanes at various road conditions. The TFALDA was first introduced by Yim and Oh [26]. It uses road view images from a camera installed behind a rear view mirror, then the position, intensity and direction on a lane marking are transformed into a three-dimensional vector. The algorithm then detects the current lane by finding a vector which is most similar to the previous lane vector (C_p) as described in Figure 1-2.

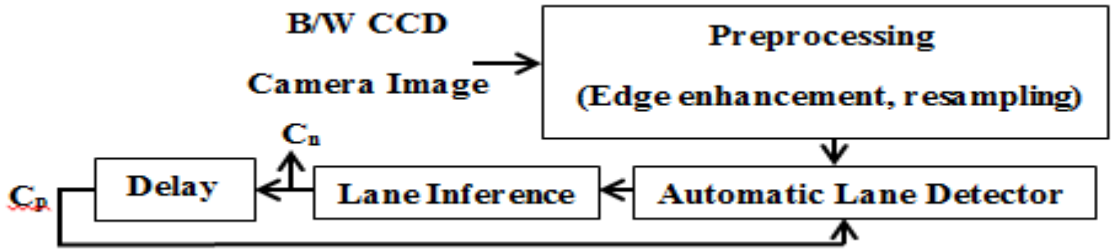

Figure 1-2 TFALDA Flow Chart [25]

An estimation algorithm was then used to estimate the time to lane-crossing (TLC), which represents the future lane information like curvature, and vehicle information like the lateral offset. The lateral offset is "*the distance between a lane center and the nearest front*

wheel and is simply estimated by using the known scale information of vehicle wheels and the nearest distance between a circle model or a straight line model and wheel points". The TLC is the time expected until the vehicle cuts an adjacent lane marking and is simply estimated by intersecting a simply predicted vehicle path and a lane model. After that, the estimated variables were fed to a fuzzy model system that generates the warning. All data were obtained from the Hardware in the Loop Simulator (HiLS) modeled by the Hyundai Motor Company.

Jung and Kelber [27] proposed a lane departure warning system based on "*the lateral offset of the vehicle with respect to the center of the lane*". A linear parabolic model was used first to determine the lane boundaries. The linear part was used for the near distances of 6-30 meters to determine the lateral offset without the need to extract parameters from the camera. The parabolic part was used for far distances as presented in Figure 1-3.

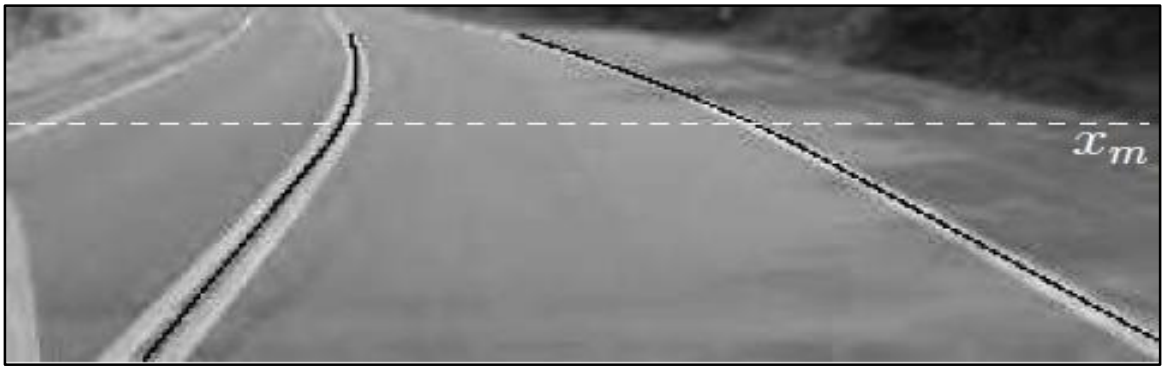

Figure 1-3 Proposed Linear Parabolic Model [27]

The lateral offset data were then analyzed with time and lane departure warning was issued when the vehicle crossed the lane boundaries. The system was tested with video sequences obtained in different driving conditions and has shown a correct and early detection of lane

departure. However, the proposed lane departure system may fail if there is a vehicle traveling closely in front of the camera.

Kreucher et al. [28] used the likelihood of Image Shape (LOIS) algorithm to track the lanes through a sequence of images. The offset of the vehicle was first determined using the LOIS algorithm with respect to right and left lane markings and then examined as a function of time. A Kalman filter was then used to predict the future values of the offset parameters based on past observations. If the vehicle's position was within one meter of the left or right lane markings and if the vehicle's path predicted by the Kalman filter led to it being 0.8 meters to either lane markings in less than a second then the system generates a warning signal. The LOIS algorithm uses a deformable template approach, where a set of shapes comprises the set of all possible conditions that the lane markings could appear within the image. Then a function that is proportional to how well a specific set of lane shape parameters matches with the pixel data of the image. After that, lane tracking is determined based on the shape parameters that maximize the function of the current image.

Leblanc et al. [29] used an automatic road departure warning system called the Crewman's Associate for Path Control (CAPC). He presented the design of the (CAPC) prototype vehicle which is a modified 1994 Ford Taurus SHO. A computer vision was used to sense the roadway up to 100 m in front of the vehicle and a set of transducers provided measurements of the vehicle motion and steering angle. The vehicle path was predicted using an initial condition estimates from a near range linear Kalman filter and current vehicle motion measurements. The road geometry ahead of the vehicle was estimated using a second far range third polynomial Kalman filter. The predicted vehicle path was compared with the sensed roadway geometry to provide the TLC. The TLC was defined as

"*the time until the vehicle's center of gravity crosses either edge of the roadway assuming both the vehicle speed and front wheel steering angle remains unchanged*" as described in Figure 1-4.

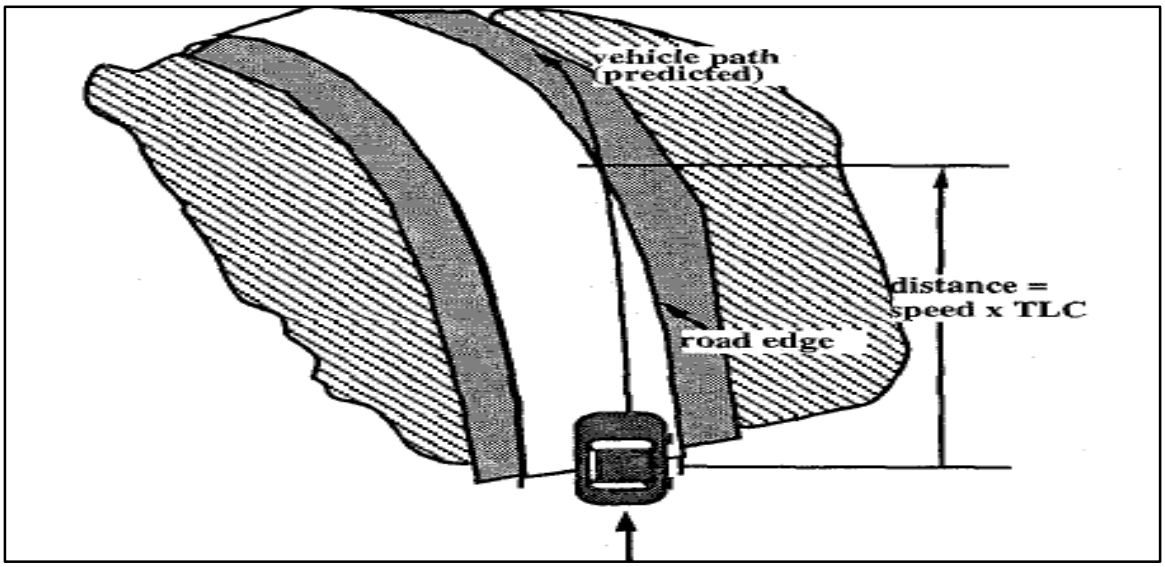

Figure 1-4 Time to lane-Crossing assuming constant steer angle [29]

The experimental results have shown that the system performed well for the set of design conditions and the definition used for TLC allowed for a variety of driving styles to be tolerated while minimizing false alarms.

Both Jung and Kelber [27] and Kreucher et al. [28] have used the lateral offset of the vehicle as a function of time to predict if the vehicle will leave its lane. Jung and Kelber presented a model that only uses the camera to predict far distance lane boundaries and predicts the near lane boundaries without using the camera. However, Kreucher et al. presented an algorithm that comprises of shapes of all possible conditions that the lane boundary might appear in. The algorithm then uses a sequence of images from a camera to predict the lateral offset based on the possible shapes of lane boundaries. Since the Jung

and Kelber method limited the use of a camera, the latter method could be more accurate since the algorithm covers all the possible shapes of lane boundaries.

In addition, both Kim and Oh [25] and Leblanc et al. [29] developed methods that used not only the lateral offset for prediction but also the time to lane-crossing (TLC) which incorporates the road curvature and motion measurements. The method presented by Kim and Oh used images from a camera and converted the data into a vector that was used for prediction based on previous data with the help of curvature and lateral offset data while the Leblanc et al. method incorporated the vehicle motion measurements such as vehicle speed and steering angle to predict the vehicle's path and a computer vision to predict road geometry. The Leblanc et al. method could be more robust since it considers not the only the road profile but also motion parameters of the vehicle.

A lane departure warning and driver alert control system called the Driver Alert System was developed by [30]. The driver alert control measures the distance between the lane markings and the vehicle using a camera, installed between the windshield and the rear view mirror, and various sensors. The sensors record the car's movement and the control unit assesses the driver's alertness level. If the distance between the lane marking and the car decreases, an audible signal and a text message with a coffee cup symbol appears in the car's information display. In addition, the driver can continuously retrieve driving information from the car's trip computer. For example, the driver alertness at the start of the trip is five bars then fewer bars remain if the driving behaviour is inconsistent. The lane departure warning alerts the driver with a gentle audio signal if the car crosses the lane markings at any point. It should be noted that the lane markings must be clearly visible for the camera in poor light, fog and snow conditions which is a drawback of this system.

A lane keeping assist which warns the driver if the car leaves its lane unintentionally was developed by [31]. A camera installed on the inside of the windscreen detects lane markings and evaluates the difference between the lane markings and the road surface. The image processing system sends data to an electronic control unit that determines the car's position and estimates when the car is about to cross its lane. The system also assesses the driver's action in order to be certain if the car has left its lane intentionally or not. For example, if the driver uses the turn indicators and moves back into the original lane after overtaking the system does not issue a warning signal. If the system predicts that the car is leaving its lane without using turn indicators, an electric motor is activated causing the steering wheel to vibrate. Another system called Attention Assist, which is more concerned with an early detection of drowsiness before the car leaves its lane, was developed by Mercedes and will be discussed later on.

Both lane departure warning systems developed by [30] and [31] use a camera to measure the distance between the lane markings and the vehicle as well as using sensors or a control unit to predict the vehicle motion. Both systems allow for lane changes if the driver uses turn indicators. The system presented by [30] offers the driver the ability to continuously check their alertness level and the audible warning is only issued if the level drops significantly while the system developed by [31] warns the driver by vibrating the steering wheel if the vehicle is about to cross its lane. Additionally, the latter system offers a new feature in which an early warning signal is emitted if the lane marking is continuous and the driver is not allowed to cross over it.

The system proposed by [32] improved the lane keeping assist system developed in 2008 for passenger cars by not only vibrating the steering wheel to warn the driver but also

braking one side of the vehicle's tires using the Electronic Stability Program (ESP) if the driver does not respond to the warning. This will force the vehicle back into the right track. However, the lane keeping assist uses an acoustic warning signal in trucks and vans since it would be hard to introduce sudden braking to loaded vehicles. In addition, the system warns bus drivers by vibrating the seat instead of an acoustic signal in order not to frighten the passengers.

It is worth noting that several lane keeping assistance systems were developed by companies in the automotive industry [33, 34, 35, 36, 37]. Some systems warn the driver by audible and visual signals while other systems provide steering correction if the driver does not respond.

Although the lane departure system is practical and non-intrusive since it does not interfere with the driver, the system requires large computational power due to image processing. Additionally, the system may not work properly if the lane markings aren't visible due to severe weather conditions or if other vehicles are travelling closely in front of the camera; since the system depends primarily on the lane markings.

1.4.3.2 Driver Observation Techniques

Lin et al. [38] proposed a real-time wireless Electroencephalogram (EEG)-based Brain Computer Interface (BCI) system for drowsiness detection. The Electroencephalogram (EEG) is a measure of the electrical activity of the brain. The system was comprised of a wireless physiological signal acquisition module and an embedded signal processing module as presented in Figure 1-5. EEG signals were measured by the EEG electrode, which was embedded into a wearable headband, then the EEG amplifier and acquisition

unit in the physiological signal acquisition module was used to amplify and filter the signals. The EEG signals were then pre-processed by the microprocessor unit and transmitted to the embedded signal processing module via Bluetooth. The signals were then monitored and analyzed by the drowsiness detection algorithm implemented in the signal processing unit.

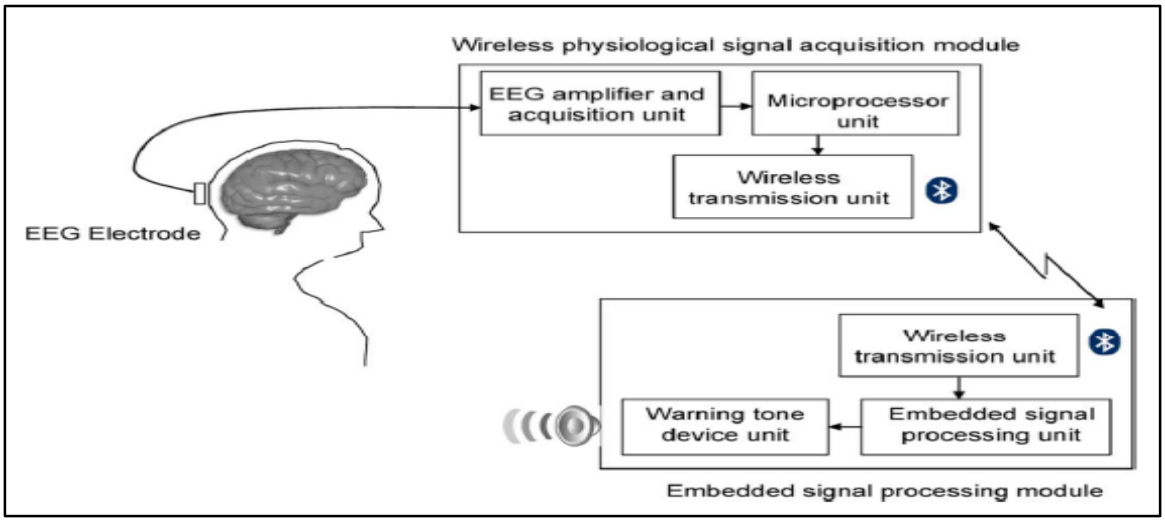

Figure 1-5 EEG-based BCI drowsiness detection system [38]

The theta rhythm (4-7Hz) and the alpha rhythm (8-11Hz) were used by the proposed algorithm to detect the driver alertness. The first few minutes of the EEG recording was assumed as the reference of the driver's alert state. The deviation of the driver's state from the alert state was assessed by using the Mahalanobis distance (MD). If the driver is alert, the EEG spectra in theta and alpha rhythms should match the alert model whereas if the driver is drowsy the MD will increase and trigger a warning tone device. Finally, the system was validated by a lane keeping driving experiment for ten subjects. The precision of drowsiness prediction (PPV) and the sensitivity (Percentage of drowsy people who were identified as having the drowsy condition) values for the ten subjects were 76.9% and 88.7 %, respectively.

Further work has been done by Pal et al. [39], Picot et al. [40] and Lin et al. [41] on using several characteristics of the EEG recordings to detect driver's alertness level.

Savchenko et al. [42] developed an algorithm that monitors operator vigilance using Skin Resistance Response (SRR). The SRR was measured by using two ring-shaped electrodes attached to the operator's left-hand fingers and a direct electric pulse current that measures the physical action was attached to the right-hand fingers. A group of 31 men participated in a test conducted at the Belarusian railroad school to select applicants for the locomotive driver assistant post. Some of the participants were involved in a monotonous activity while others were asked to sit in a comfortable arm-chair in front of a filter device mounted at the subject's eye level at a distance of 2 meters. A visual and sound biofeedback was issued based on the SRR inter-impulse interval parameters. The visual feedback used green, yellow and red colors. If the SRR inter-impulse interval is in the green band the operator's state is interpreted as a high level of alertness, and if the operator's state is in the yellow band then the operator chooses time to control his state since there is a tendency to alertness loss. However, if the SRR inter-impulse interval is at the end of the red band, then a discrete sound signal commands the driver to execute the test algorithm to check their status. It was found that the absolute SRR inter-impulse interval values for subjects that executed a monotonous activity were three times lower than subjects that had to relax.

Azman et al. [43] proposed a method for detecting driver distraction which monitors the mouth and eyes movements of the driver. The eyes and mouth movements were recorded using FaceLab Seeing Machine camera in a laboratory setup. Participants in this study were required to watch a video recording of a real road environment captured in the UK for approximately 8 minutes. The participants were first asked to watch the video without any

source of distractions. The participants were then asked to watch the video while being distracted with specific types of distractions such as answering simple arithmetic questions, listening to music or talking to other occupants. A correlation algorithm called Pearson-r Correlation was used to describe the strength of the relationships between the variables. For example, a value of 0.7 corresponds to a strong correlation between mouth and eye movements. The information was then fed to a Bayesian network in order to determine the alertness state. The network was comprised of nodes representing instances measured with certain values and whenever the driver is distracted some instances will have a measurement that indicates a movement. It was found that there is a high correlation between the eyes and mouth movements when the driver is distracted. It was also found that there is a higher correlation between the right eye height and the mouth movements than the left eye's height.

The PERCLOS, which is the percentage of eyelid closure over time, has been widely used for detecting driver's alertness. It was first established by Wierwille et al. [44] and was defined as "the proportion of time that the eyes are 80% to 100% closed". It was also found that eyelid closure is the most reliable in predicting sleeping episodes among different measures examined. In addition, Wierwille et al. [44] also found a high correlation between the eyelid closures and other the performance measures such as lane deviation, yaw deviation, and steering rate. The use of the PERCLOS was also validated by Dinges and Grace [45] in a controlled laboratory setting.

Park et al. [46] presented an efficient way of measuring eye-blinking levels under various elimination conditions for drowsiness detection systems using a single camera. The camera was installed on the dashboard along with two infrared illuminators that were installed on

the ceiling of the car. The light source of the infrared light was sunlight during the day and Infrared Light-Emitting Diodes (IR LEDs) during the night. The system used here can only detect pupils that appear dark during both the day and the night; therefore, the camera lens had an infrared band-pass filter which removed all visible light and only allowed infrared light in. Eye corner filter method was then applied to detect suitable candidates of the eyes region. Eye shapes that appeared dark (pupils) remained dark while brighter areas were compensated using the illumination compensation algorithm. After that, the filtered candidates of eyes region were first classified into eye groups and non-eye groups. The cascaded Support Vector machines (SVM) was then used to classify eyes groups into two classifiers; open eye classifiers and closed eyes classifiers as illustrated in Figure 1-6.

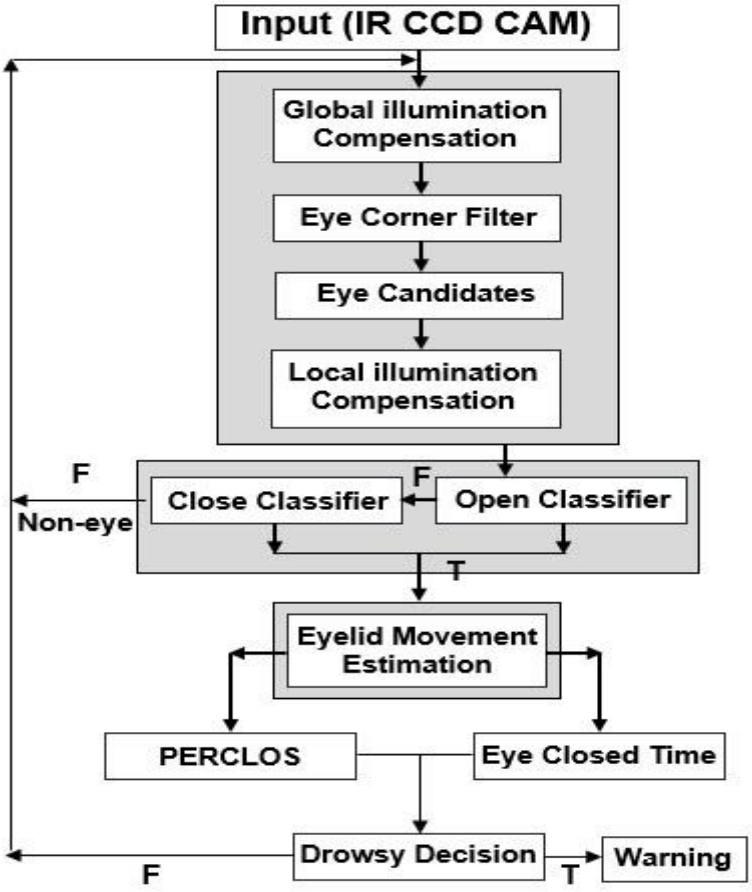

Figure 1-6 Flow chart of the presented drowsiness detection system [46]

If open eyes were detected by open eye classifier, then eyelid movement measurements can be done. However, if open eyes were not detected, closed eyes were sequentially detected by closed eye classifiers. If closed eyes were also not detected, the frame would be ignored. The system was tested under a wide range of illumination conditions during periods of real driving and demonstrated an average detection rate of 98% and an accurate measurement of eye blinking.

Several studies have been done on using the PERCLOS and eye tracking techniques by Tock and Craw [47], Kaneda et al. [48], Erikson and Papanikolopoulos [49], Hong et al. [50], Ueno et al. [51], Ito et al. [52], Hu and Zheng [53], Picot et al. [54], Sugiyama et al. [55] and Dikkers et al. [56]. Researchers have used different techniques to detect the face and then the eyes and they used different algorithms to measure eyelid movements. Researchers also worked on developing a simple and fast system that can be used in real-time and a robust system that can be reliable in several illumination conditions. A fuzzy logic approach was used by some studies to merge the most relevant blinking features (duration, a percentage of eye closure, frequency of blinks and amplitude-velocity ratio). Researchers have also used several facial features to detect alertness levels such as; head motion, mouth occlusion, lips, skin, yawning rate, gaze movement as well as the blinking motion as discussed in Vural et al. [57], Abtahi et al. [58], Smith et al. [59], Ji and Yang [60], Ji et al. [61] as well as Bergasa et al. [62] and [63]. The facial features were extracted using several techniques such as machine learning. The extracted features were also combined using different methods such as the Bayesian networks.

Kelion [64], a news reporter of BBC, reported that Caterpillar is going to sell a product called Driver Safety Solution (DSS) which can detect driver drowsiness in trucks. The DSS

product consists of sensors, alarms, and software. This product uses a camera to detect a driver's pupil size, frequency of blinks and duration of eye closure. The mouth is also detected to see if the driver is looking at the road. Infrared lamps are fitted in truck cabs to monitor employees in the dark and through their safety glasses. An accelerometer and GPS chip are used to check if the truck is being driven at the time of detecting sleepiness. A computer mounted behind the driver's seat is used to process the data. This computer is designed to handle dust and vibrations. If sleepiness is detected from a fraction of a second to up to half a minute, the computer's software issues an audio alarm and vibrates a motor built into the driver's seat. The DSS system will cost up to $ 20,000 to install on each vehicle.

Both Lin et al. [38] and Savchenko et al. [42] have presented systems that can measure the alertness level directly by measuring biological responses from the driver's body. The system presented by Lin et al. [38] monitored the electrical activity of the brain which can be considered more accurate. However, this system achieved an acceptable precision rate which could be improved. The system presented by Savchenco et al. used rings to measure the skin resistance which could be less accurate as monitoring the brain. Drivers may consider both systems to be inconvenient due to the fact that they would need to add wires or electrodes into their bodies. The systems proposed by Park et al. [46] and [64] monitor the eye blinking rate and pupil's size which can be measured without direct contact with the driver's body. The system presented by Park et al. presented a system that monitors the eye blinking rate under various illumination conditions which means that the system can work during day and night. This system achieved a high detection rate of 98%. The system proposed by [64] is much more advanced in which it monitors not only the eyes but also

the mouth to see if the driver is looking straight. It also uses accelerometer and GPS chips to make sure the vehicle is not stationary. The method suggested by [64] could be considered very promising, but the system is not affordable for small companies or for personal use or if used on a fleet of trucks.

In General, the advantage of monitoring the driver is the ability to measure real biological responses that relate directly to drowsiness. However, techniques such as EEG recordings and skin resistance are very intrusive while the facial features techniques are less intrusive but require large computational power due to image processing. This technique had some difficulties with fast head movements and some image frames failed to detect eyes and were ignored.

1.4.3.3 Car-Driver Observation Techniques

Desai and Haque [14] hypothesized that the time derivative of the force (Jerk profile) exerted by the driver at the vehicle driver interfaces (accelerator pedal, steering wheel) can be used to detect different levels of alertness. The accelerator pedal was used as an example case. The jerk profile of the accelerator pedal was determined using the following equation:

$$J = \omega A cos\omega t \qquad \textbf{1-1}$$

Where; A is the amplitude of the jerk, ω is the frequency. The force exerted on the accelerator pedal was represented by a sum of sine functions.

The spikiness index is the deviation of the instantaneous jerk from the general trend as illustrated in Figure 1-7. It was introduced to make the detection algorithm independent of the driving conditions since the general trend captures and characterizes the external

environmental conditions. The spikiness index was determined using the following equation:

$$\Psi = \frac{\sum_{i=n_{avg}+1}^{n} \left(\dddot{Y}_i - \frac{\sum_{j=i-n_{avg}}^{i-1} \dddot{Y}_j}{n_{avg}} \right)^2}{n - n_{avg}} \qquad \textbf{1-2}$$

Where; n_{avg} is the number of data points needed for finding the general trend of the jerk, n is the total number of data points for the entire driving experiment, $\dddot{Y}_i$ is the instantaneous jerk of each data point, $\dddot{Y}_j$ is the instantaneous jerk used to calculate the general trend of the data points.

The spikiness index of the accelerator pedal for an alert driver should have higher amplitudes and frequency than the spikiness of a drowsy driver based on the assumption that an alert driver reacts faster and more often to changes in road patterns.

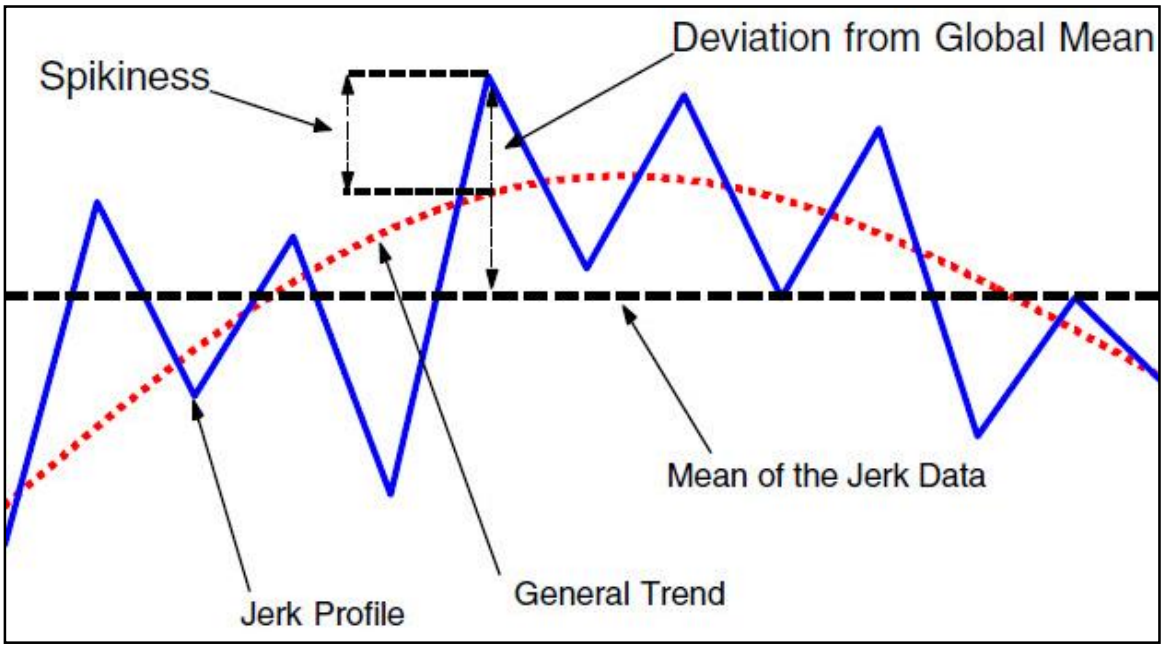

Figure 1-7 The Spikiness Index (deviation from general trend) [14]

The results from simulated environment driving for three drivers are shown in Table 1-1. It was noted that the results were in agreement with the hypothesis. However, the driving experiment in this study was simulated on a personal computer like a video game and the steering wheel and pedals were connected externally to the computer. This simulation environment would not give the real driving feel and conditions.

Table 1-1 Spikiness Index results for alert and drowsy driving [14]

	Driver 1		Driver 2		Driver 3	
	Alert	Drowsy	Alert	Drowsy	Alert	Drowsy
1	2.27E−02	6.09E−03	2.67E−02	8.45E−03	1.36E−01	4.23E−03
2	5.00E−02	8.85E−03	9.93E−03	2.00E−03	2.97E−02	2.42E−02
3	3.67E−02	1.73E−02	8.84E−03	1.79E−02	8.88E−02	3.03E−02
4	1.56E−02	4.60E−03	5.33E−03	2.00E−03	6.58E−02	2.16E−02
5	9.02E−03	3.33E−03	1.11E−02	2.00E−03	4.38E−02	8.97E−02
Average	2.68E−02	8.03E−03	1.24E−02	6.48E−03	7.28E−02	3.40E−02

Chieh et al. [65] described a driver fatigue detection method which monitors the variation of the driver's grip force on the steering wheel. The steering grip force data was obtained using two resistive force sensors that are attached to the steering wheel and connected with the aid of a data acquisition module to a personal computer. A change detection algorithm was used to detect major drops in the steering grip force since there is no absolute steering grip force value to indicate the onset of fatigue/sleep. The log-likelihood ratio, which was used by the change detection algorithm, is the ratio of the probability density based on the mean before a change in steering force and the probability density based on the mean after the change in steering force. Driving was simulated inside a laboratory where subjects had to perform driving sessions on driving simulator software with a computer game steering wheel. The results have shown that the change detection algorithm was able to detect

significant changes in the steering grip force data. However, more tests were required with the advice of medical personals in order to accurately detect the change in steering grip force.

Further work has been done to develop a drowsiness detection method capable of extracting the interval of steering adjustment for lane keeping by means of the steering wheel only [66].

Polychronopoulos et al. [67] presented a multi-sensor system that allowed the information fusion of different sources; vehicle, driver, and environmental sensing parameters. This system was known as the Assessment of driver vigilance and Warning According to traffic risK Estimation (AWAKE) project. The AWAKE project was funded by the European Commission and aimed at increasing traffic safety by achieving a hypo-vigilance diagnosis level over 80% and false alarm rate below 10%. The AWAKE system consisted of three sub systems; the Hypo-vigilance Diagnosis Module (HDM), Traffic Risk Estimation (TRE) and the Driver Warning System (DWS). These subsystems were managed by the Hierarchical Manager (HM) as shown in Figure 1-8.

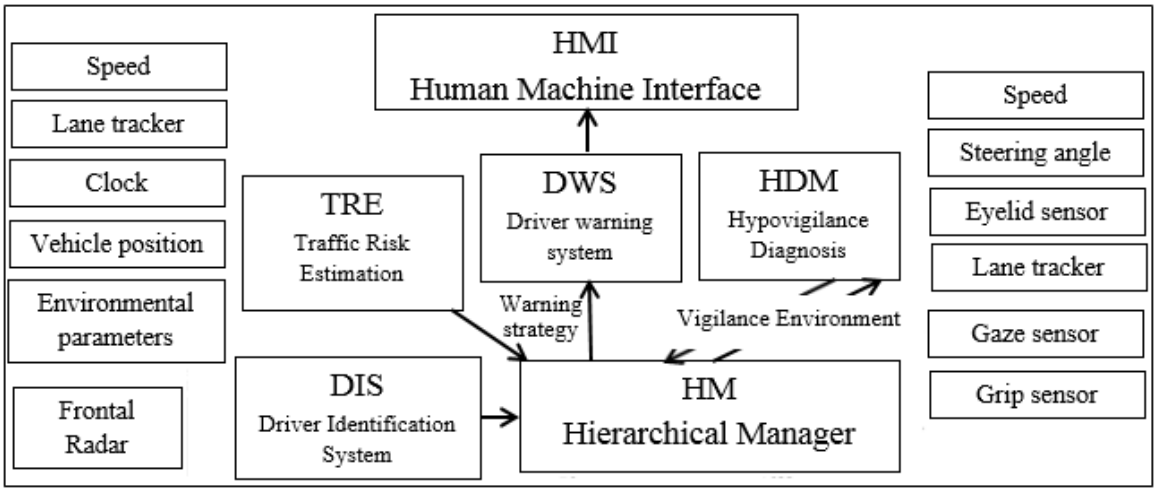

Figure 1-8 Flow chart for the AWAKE system [67]

The HDM detects drowsiness in real-time by monitoring eyelid behaviour, gaze direction, steering wheel grip force, lane tracking, gas/brake pedal positioning and steering wheel positioning using artificial intelligence algorithms. The TRE module assesses the risk of the traffic situation by monitoring data from a map database, global positioning system (GPS), frontal radar, vehicle speed, visibility and driver's gaze direction. The DWS module uses acoustic, visual and haptic output signal to warn the driver. This module has various levels of warning according to the risk level assessment. The HM is responsible for the data exchange between the different subsystems and the information presented to the driver. The HM also uses inputs from the HDM and the TRE to determine the adequate warning level.

A drowsiness detection system developed by [31] warns drivers at an early stage of drowsiness to prevent accidents. This system uses the speed, lateral and longitudinal acceleration and a highly sensitive sensor which monitors the steering wheel rate (speed) and movements. The system also monitors the use of turn indicators and certain control inputs as well as the effects of side winds or road unevenness. This system records the driving style of the driver at the start of every trip and generates an individual profile that is continuously compared with current sensor data. Mercedes engineers carried out intensive tests involving more than 550 drivers. The test results revealed that observing the steering behaviour can very useful for detecting significant changes in alertness levels at an early stage before drowsiness kicks in; since it is hard for drowsy drivers to steer a precise course in their lane and tend to make minor steering errors that are corrected abruptly and quickly. If drowsiness was detected the system emits an audible and flashes up an unequivocal instruction on the display asking the driver to take a break.

A system called Driver Attention Alert (DAA) developed by [68] . This system detects drowsiness or inattention by monitoring the driver's steering inputs using steering angle sensors. The system records the driver's steering inputs for a period of time and then uses the driver's steering pattern as a baseline. The system then compares the subsequent steering inputs with the baseline steering data by finding the steering correction errors. The system accounts for lane changes, the curvature of the road as well as road conditions by using logic in order to prevent false warnings.

Both Chieh et al. [65] and Polychronopoulos et al. [67] have proposed using the steering grip force to monitor alertness. The Chieh et al. method has only focused on using the grip force which depends on driving style. For example, if a driver does not apply a sufficient grip force the system may not be able to detect significant changes. However, the system presented by Polychronopoulos et al. could be more robust since it uses not only the grip force but also monitors the eyelid behaviour and the environmental conditions using artificial intelligence algorithms. Nevertheless, the complexity of the latter's system could result in a higher price.

The detection methods suggested by [14] and [31] focused on using the response of the driver to detect alertness loss. The method presented by [14] used the accelerator pedal jerk profile and spikiness which encapsulates the environmental conditions whereas the method developed by [31] used the steering rate as the main indicator and also incorporated other parameters such as side wind and road unevenness to try to reduce false alarms. It has also been tested on more than 550 drivers which determines the system is robust.

The system presented by [68] is similar to the system presented by [31] in that it monitors the steering behaviour. However, the system developed by [68] only monitors the steering

angle and incorporates logic to prevent false detection caused by lane changes and road curvature and conditions as well as braking whereas the system presented by [31] not only the steering angle but also the steering rate and accounts for a variety of road and driving conditions and checks if the driver is using the control panels. The use of steering rate accounts for lane changes and road curvature since it measures how fast a driver changes the steering angle. Therefore, a driver can have a low steering rate on curves if the angle change is smooth.

Although monitoring the car-driver interface is the most difficult measurement to relate to driver inattention, this technique requires low computational power as compared to image processing techniques and thus cheaper. This system is non-intrusive and practical to drivers.

1.4.4 Driving Vigilance Level Detection Using Artificial Neural Networks

Artificial neural networks (ANNs) are computational models that work in parallel and are comprised of densely interconnected processing units (called neurons). The ANNs are known for their ability to learn by example rather than programming to solve problems [69]. Neural networks were inspired from the studies of the biological nervous system [70]. The main purpose of using a neural network is to map an input to a desired output without using mathematical models and to classify a class of patterns into different categories [71, 72]. Most researchers have used neural networks to classify different levels of driving alertness.

Carswell and Chandran [73] proposed a method of detecting drowsiness based on the hypothesis that the abnormal trajectories of vehicles are indicative of drunk or sleepy

drivers. A single feature of the vehicle such as a tail light was isolated and optical flow was computed only around this feature rather than at each pixel of the image. The optical flow of vehicle velocities was first extracted using a modification of the basic optical flow method then used to train a classifier back-propagation ANN. Each training and testing data set had 50 % normal and 50% abnormal trajectories. Abnormal trajectories were characterized by slowly drifting across a lane and vehicle oscillation around the correct trajectory as illustrated in Figure 1-9. It was noted that the absolute deviation for abnormal trajectories was greater than for the normal trajectories, but some weaving was allowed for a normal trajectory. The ANN with back-propagation learning algorithm converged after 100,000 iterations. The network was tested with 40 test sequences and classified trajectories with 100 % accuracy.

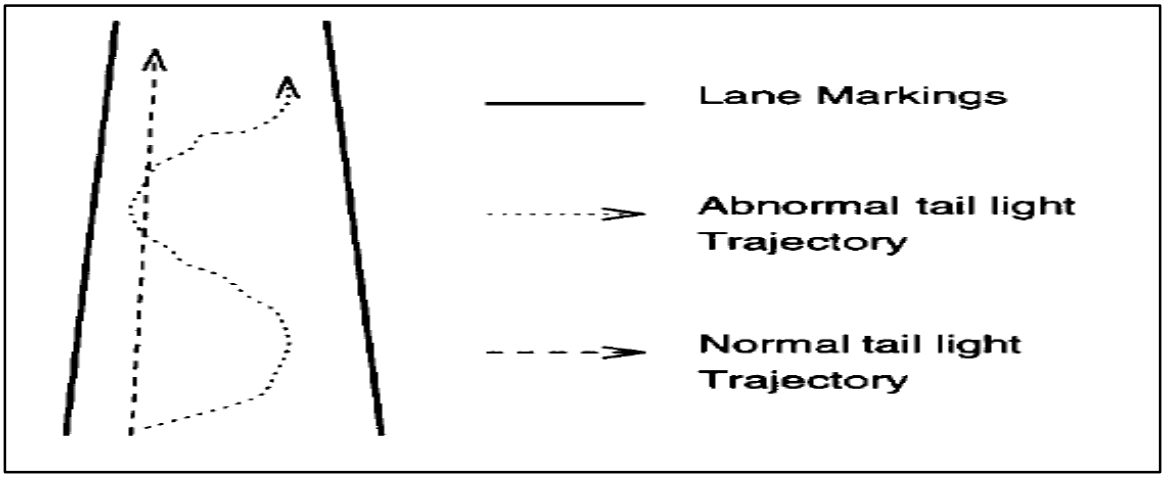

Figure 1-9 Normal and Abnormal Vehicle Trajectories [73]

This method requires using a camera to capture the tail light of the vehicle. As a result, high computational is needed to perform image processing in real time and higher cost as well. In addition, the camera may not be able to get a clear picture in all weather conditions.

The work done by Carswell and Chandran [73] is considered as one of the car observation techniques. However, neural networks were used to classify the vehicle trajectory into normal and abnormal driving for their ability to recognize data patterns.

Hayashi et al. [74] proposed a drivers' drowsiness detection method that focused on analyzing individual differences in biological signals and performance data. An experiment was conducted for six individuals who drove a simulator. The pulse wave and steering data were measured for each individual while driving. The Sympathetic Nerve Activity, Parasympathetic Nerve Activity, Pulse Rate, Lyapunov Exponent, and steering instability were derived from driver's pulse wave and steering data and were used as inputs to an ANN as shown in Figure 1-10.

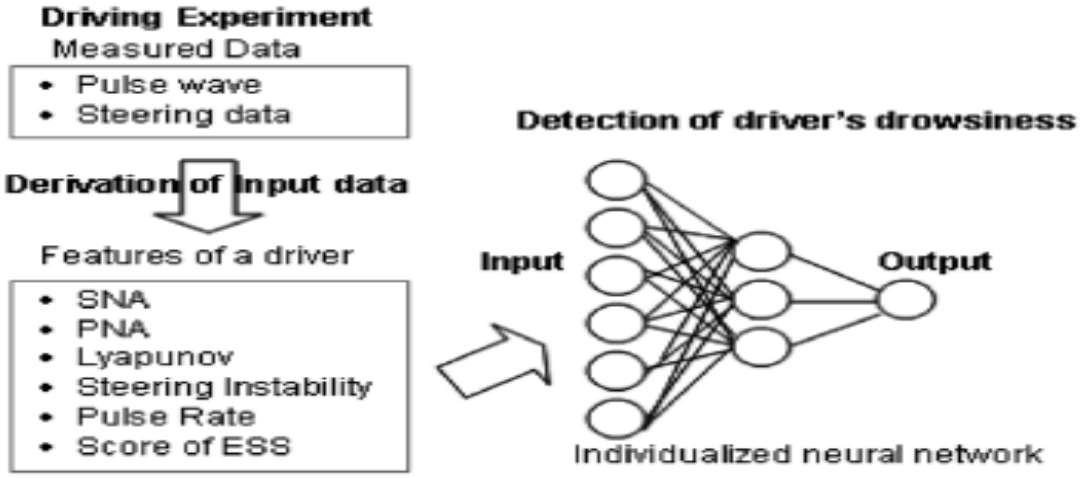

Figure 1-10 Flow Chart of the Drowsiness Detection method [74]

The Epworth Sleepiness Scale (ESS) score, which is a questionnaire used to determine the level of daytime sleepiness, was also used as an input to the neural network. Two drowsiness detection methods were proposed; the individualized drowsiness detection (learning each driver's feature on each network) and the individualized drowsiness

detection with categorization (categorizing drivers' features before their data were used as inputs to the neural network. The first method resulted in 88% detection rate, whereas the latter method resulted in 85% detection rate.

Bundele et al. [75] designed a jacket with embedded sensors that measure physiological body parameters of the driver. These sensors measured signals from the Galvanic Skin Response (GSR) and the Oximetry Pulse (OP) then these signals were recorded using biofeedback signal processing equipment for a pre-driving and post driving states. Signals were then transmitted wirelessly using Bluetooth to a computer tablet (PC) as illustrated in Figure 1-11.

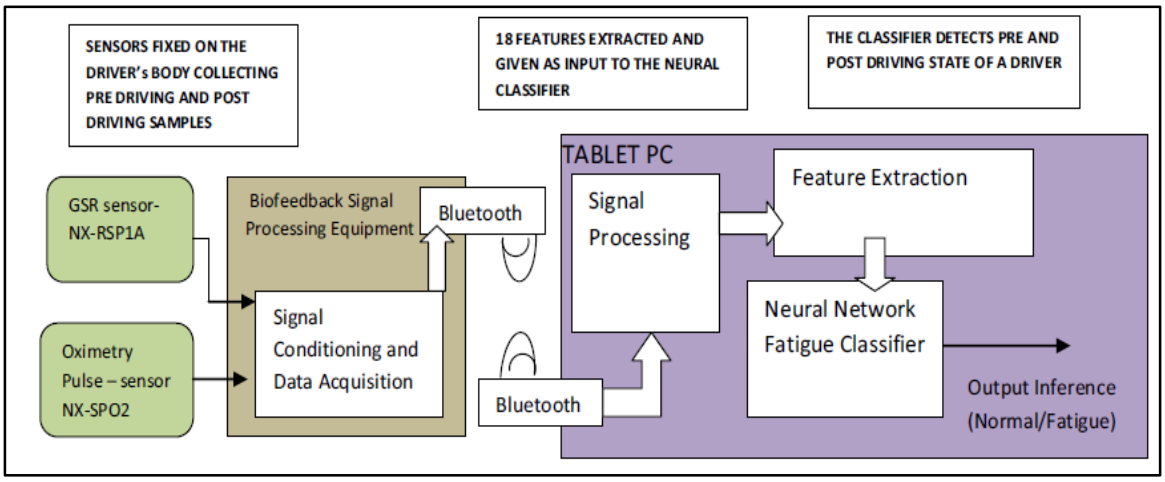

Figure 1-11 Flow chart of the fatigue/drowsiness detection system [75]

After signal processing, eighteen features were extracted. The corresponding data was used as an input to two multilayered perceptron neural networks (MLP NN). The first neural network had a single hidden layer and an output layer. The second neural network had two hidden layers and an output layer. The physiological body parameters were recorded for 3-5 minutes for a group of people of ages varying between 20 and 55 before driving (pre-driving stage). The tests were done by drivers driving taxis, trucks and buses. The

physiological body parameters were also recorded for 3-5 minutes on drivers after a 300-500 km trip (post driving). The single hidden layer network classified data with 92.1% accuracy while the two hidden layers' network classified data with 93.1% accuracy.

Both Hayashi et al. [74] and Bundele et al. [75] measured biological signals from the driver. Hayashi et al. derived features from the driver's pulse wave and the steering data while driving to train the network whereas the latter extracted features from the skin response for a pre-driving and a post driving stages. Although Bundele et al. achieved high classification accuracy, the network compares a non-driving state with a driving state, where it would be more accurate to compare a driver before and after fatigue kicks in while driving. Both methods are intrusive to the driver since real biological signals are collected from the driver body.

Tsai et al. [76] modeled a real-time drowsiness detection system based on Electroencephalogram (EEG) stationary wavelets transform. The system consisted of a six channels active dry electrode, which was mounted on a baseball cap that the driver was supposed to wear, and signal condition circuits, a microcontroller, and a digital signal process module. The EEG characteristics were extracted from the stationary wavelets transform. These characteristics were used as inputs to a back-propagation classifier neural network. Thirty-six features were used as the input vector to the neural network. Ten volunteers of ages between 20 and 25 participated in an experiment. The experiment had two parts; a five-minute baseline period and a 20-minute test period. During the baseline period participants were asked to hold the reaction time button while sitting in a comfortable chair. During the 20-minute test period the subject was asked to look at the projected scenery simulating the front window of a car driving in a monotonous fashion

and try to stay alert. The first part EEG signals were used as a reference for alertness, whereas the second part EEG signals were used to test the drowsiness detection of the system. The accuracy of the network was 79.1% for alertness and 90.91% for the drowsy state.

King and Nguyen [77] described a fatigue driving detection system based on the electroencephalogram (EEG) data for two groups of drivers; professionals and non-professionals. The EEG data were collected using the international 10-20 electrode from a total of 19 sites on the head. The time domain data were processed using the Fast Fourier transform along with a 4-term Blackman-Harris window and a 2 Hz cut-off high-pass filter into alpha, beta, delta and theta bands. These bands were used to train two feed-forward classifier ANNs; the first network was trained based on the professional drivers while the other network was trained based on the non-professional driver. 20 professional drivers and 35 non-professionals were asked to drive a driving simulator continuously until fatigue was observed. Fatigue was judged by an expert based on eye and head movements. The network classified professional drivers with 81.49% accuracy, whereas non-professional drivers were classified with 83.06% accuracy.

Both Tsai et al. [76] and King and Nguyen [77] have used the stationary wavelets transform of the EEG recording to train classifier networks. However, King and Nguyen (2006) not only used the wavelets transform but also judged fatigue based on eye and head movements. Several studies by Sinha et al. [78], Makeig et al. [79], Gevins and Smith [80] and Subasi et al. [81] have been done on using the EEG characteristics to train neural networks to classify alertness levels. Each of these studies used different features extracted

from EEG and different neural network designs. Detection methods that use EEG recordings are considered intrusive and the driver and impractical.

Andreeva et al. [82] treated the driver's body as a mechanical filter structured of springs and dampers as suggested by Tylee et al. [83]. The human body was modeled as springs, dampeners and mass by Rosen and Arcen [84], as can be shown in Figure 1-12.

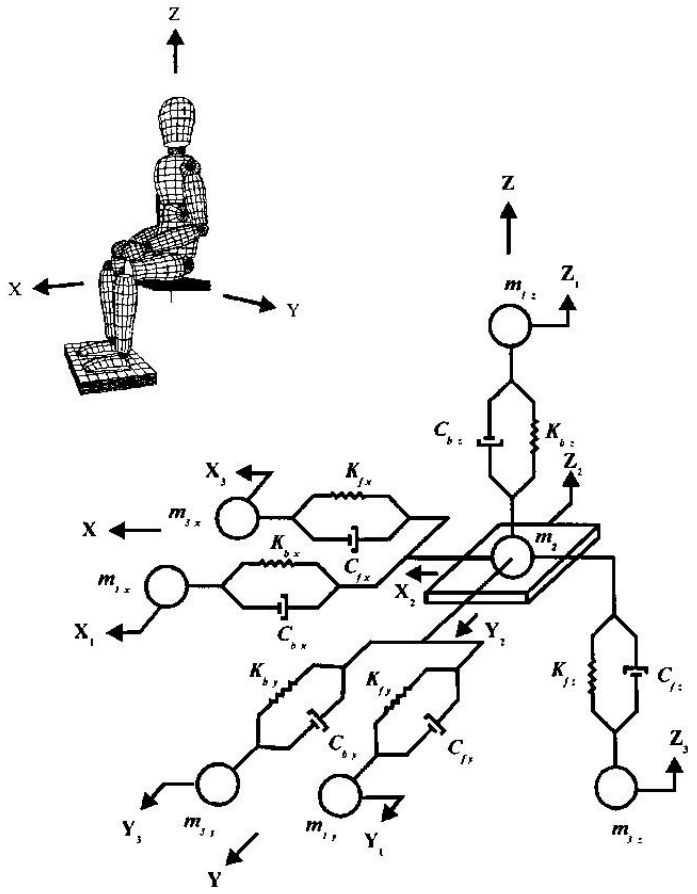

Figure 1-12 Human body model as spring, dampeners and masses [82]

Andreeva et al. [82] also hypothesized that the filtration effects caused by vibrations of the body depends on the sleepiness state of the driver. The driver's body was modeled as a linear time-variant (LTV) system. The driver's upper body was also treated as an unknown plant. Triple axial accelerometers were placed on the driver's seat and head and were used

to monitor the driver's upper body. These accelerometers were used to generate the inputs and signals of the unknown plant and the normalized least mean squares (LMS) algorithm was used for plant identification. Separate filter coefficients (transfer functions) were generated for the awake and sleep states of the subject. The filter coefficients were used to train a feed forward classifier artificial neural network (ANN). The back-propagation algorithm was used to train the network. The adaptive weights were pre-normalized to have a zero mean and unit variance distributions. The system has been tested on 8 subjects and achieved a classification success rate of 95% when tested on the same subject. However, when the system was trained on three subjects and then tested on a fourth subject the classification rate dropped to 90%.

The work done by Andreeva et al. [82] is considered as one of the driver observation techniques. However, it is different in that it monitors driver alertness by studying the human body vibrations and using a neural network to classify the level of alertness based on different body vibrations level. This method is also considered intrusive since accelerometers were added to the head of the driver.

Wollmer et al. [85] described a driver distraction detection method that uses driving and head tracking data. The data is used as inputs to a special type of neural networks called the Long Short-Term Memory recurrent neural network (LSTM). The LSTM allows for the dynamic classification of the driver alertness state for each time step by storing driving information using memory cells over long periods of time and being able to learn the contextual information needed for classification. Driving experiments were done in a real driving environment and drivers used the multimedia interface in the car as a source of distraction. Participants were first asked to drive the vehicle without any source of

distraction and the recorded data was used as a baseline. The participants were then asked to perform tasks such as adjusting the radio, CD or checking the navigation system while driving. The steering wheel angle, throttle position, speed, heading angle as well as lateral deviation and driver head rotation signals were recorded during the driving experiments. The first three signals were considered as directly indicative of the driver alertness state and the lateral deviation and heading angle provided some useful information. The multimedia interface was placed to the right of the driver so whenever the head rotation of the driver was to the right, the driver was assumed to be distracted. The LSTM neural network achieved a classification rate of 96.6%. This method requires using cameras and several sensors to find the lateral deviation, heading angle and the driver head rotation.

Sayed and Eskandarian [86] proposed a method to detect drowsy driving using steering wheel angle signals from a passenger car driving simulator. It was hypothesized that a driver in an alert state makes small amplitude movements of the steering wheel in order to stay in the center of the lane, whereas, a drowsy driver makes larger amplitude movements. The steering signals were pre-processed and then were used to train a classifier artificial neural network (ANN). A validation experiment was conducted at the highway passenger car driving simulator at the Turner Fairbank research center. Twelve subjects (6 males and 6 females) drove a 20 mile (36 km) rural highway test scenario with both straight and curved sections. A test data set was used to test the performance of the trained network. The data set was taken for 6 drivers. The network classified participants into alert and drowsy with 89.9% accuracy.

Eskandarian and Mortazavi [87] developed a drowsiness detection algorithm that used the drivers' steering signals from a truck driving simulator as inputs to a classifier ANN.

Thirteen licensed truck drivers completed an experiment that was conducted at the Center for Intelligent Systems Research (CISR) Truck Driving Simulator Laboratory. Each driver had to drive a 52-mile scenario for morning and night sessions. During each experiment drivers' inputs, eye data and digital video of drivers' face were recorded. First drowsiness was assessed on the subjective basis based on observation data from live recordings and video analysis. Statistical analysis indicated that the steering wheel angle and lateral displacement were significantly correlated with drowsiness levels and that drowsiness was the cause of most accidents during night sessions. It was noted that drowsiness affected steering behaviour in two consecutive phases; Phase-I and phase-II. In Phase-I, the large amplitude of steering correction was observed and while in phase II the driver had no feedback on the steering angle. The steering wheel angle data were pre-processed, by removing the effect of road curvature on steering wheel angles, and converted into a 1 by 8 vector representing 15 seconds of steering activity as shown in Figure 1-13. Phase I steering signals were used to train a classifier neural network. The network was tested and classified drowsiness with 85% accuracy. The network detected drowsiness 3 minutes prior to a crash. Both methods presented in [86] and [87] require preprocessing of the steering wheel angle to account for road curvature. This issue could be simplified by using the time derivative of the steering wheel angle and the effects of road curvature can be eliminated.

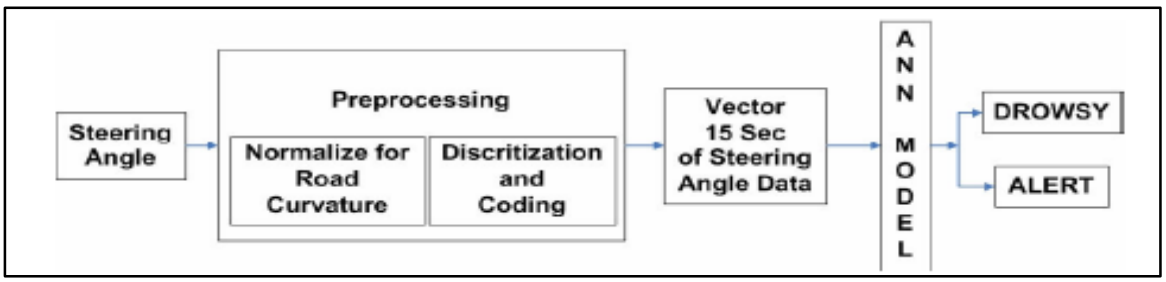

Figure 1-13 Flow chart of the Drowsiness Detection Algorithm [87]

Son et al. [88] presented a driver distraction detection method that uses steering wheel angle and lane position signals. The steering reversal rate and the standard deviation of the lane position were derived from the steering angle and the lane position signals and fed as inputs to a Radial Basis Probabilistic Neural Network (RBPNN). Distraction is characterized by a reduction in lateral position variation and an increase in smaller steering wheel movements. The steering reversal rate was defined as "the number, per minute, of steering wheel reversals larger than a certain minimum angular value". The driving experiments were performed on a fixed-based driving simulator. Participants of age 25-35 were first asked to drive the simulator in a highway environment for 10 minutes to become more familiar with the driving experiment. The participants were then asked to drive for few minutes without any kind of distraction and the data was used as a reference for the alert state. After that, the drivers were asked to listen to audio recordings and try to recall what was said. The neural network was trained to classify the cognitive workload into low workload and high workload. It was found that the steering wheel reversal rate and the standard deviation of the lane position were indicative of the alertness state and the neural network achieved a classification rate of 73.3 %. The lane position in this method requires a camera and high computational power for the image processing.

Culp et al. [24] presented a non-intrusive method of detecting drowsiness based on "the hypothesis that the time derivative of force (jerk) exerted by the driver at the steering wheel and accelerator pedal could be used to detect different level of alertness" as illustrated in Figure 1-14. The steering wheel angle and the accelerator pedal position data were first collected using optical encoders and pre-processed using numerical differentiation to find the jerk profile.

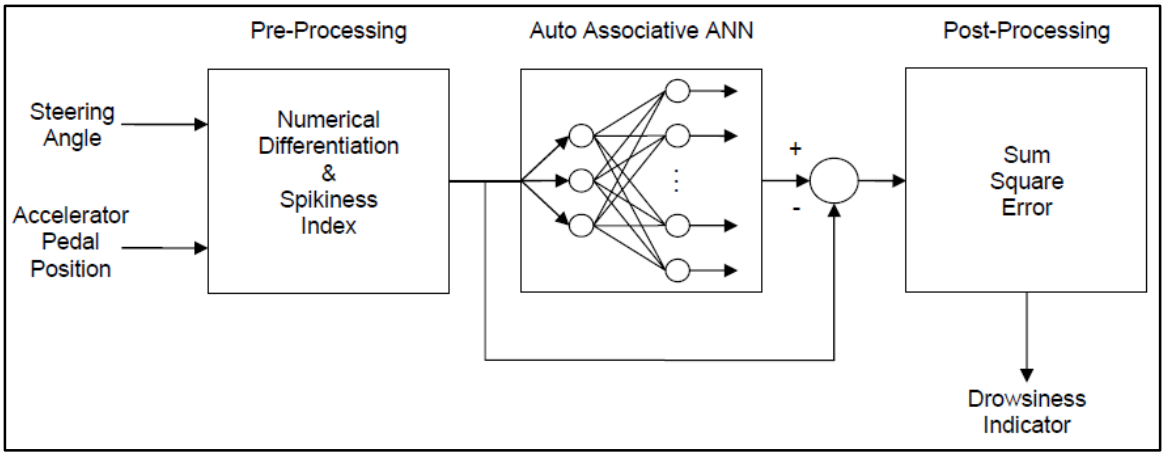

Figure 1-14 Flow Chart for the drowsiness detection method [24]

The jerk profile for the steering wheel angle and accelerator pedal position was determined using the following equation:

$$\dddot{Y}_i = \frac{(Y_{i+3} - Y_{i+2} - Y_{i+1} + Y_{i-1} + Y_{i-2} - Y_{i-3})}{6\Delta t^3} \qquad \textbf{1-3}$$

Where; Y_i represents the steering wheel angle or the accelerator pedal position and Δt is the time step of the middle point at which the derivative is determined.

The spikiness index (deviation of jerk from the general trend of data) suggested by Desai and Haque [14] was also calculated using equation 1-2 and used along with the jerk profile to train ANNs. A special type of neural networks called the Auto Associative ANN inspired by Thompson et al. [89] was used in this approach, where the difference between the input and output of an ANN was used to detect abnormal system behaviour. The advantage of using the auto-associative network is that only one type of input was required to train the network, where a classifier network would require both drowsy and alert data sets. Two feed-forward networks trained with resilient propagation (RPROP) algorithm and two radial basis networks each with different inputs (jerk profile and spikiness index) were used. The network was tested with datasets that were not used in training and the inputs to

the network were then subtracted from the outputs. The difference, which was quantified by the sum squared error, was used as a drowsiness indicator. The sum squared error was determined using the following equation:

$$E = \sum_{i=1}^{n} (output_i - input_i)^2 \qquad \textbf{1-4}$$

Where; $output_i$ is the neural network output, $input_i$ is the input to the neural network and n is the number of data points in the time series.

The drowsiness indicator was normalized by dividing the sum squared error of each experiment by the highest sum squared error value. The highest value represents the worst case of drowsiness. The steering wheel angle and accelerator pedal position data were collected during an experiment conducted at the Pennsylvania State Truck Driving Simulator Laboratory, where a group of volunteers (males and females) of ages 20-30 participated. During each experiment, two participants remained awake for 24 h and each drove on a highway scenario for 20 minutes. Results from the jerk profile and spikiness index networks strayed further from the general drowsiness indicator trend line the further the driver stayed awake as shown in Figure 1-15 and Figure 1-16, respectively. The radial basis network gave similar results to the feed-forward network, but the radial basis needed less time to train and fewer neurons which reduced the network's size. It was also noted that the spikiness index network had different outputs than the jerk profile network, but the drowsiness was predicted at similar times for both networks. The neural networks used in this method were trained on eight drivers and cannot accommodate all driving styles. The work presented in this thesis is a continuation of the research efforts carried out previously by Culp et al. and Dr. Moustafa El-Gindy at the Pennsylvania State University.

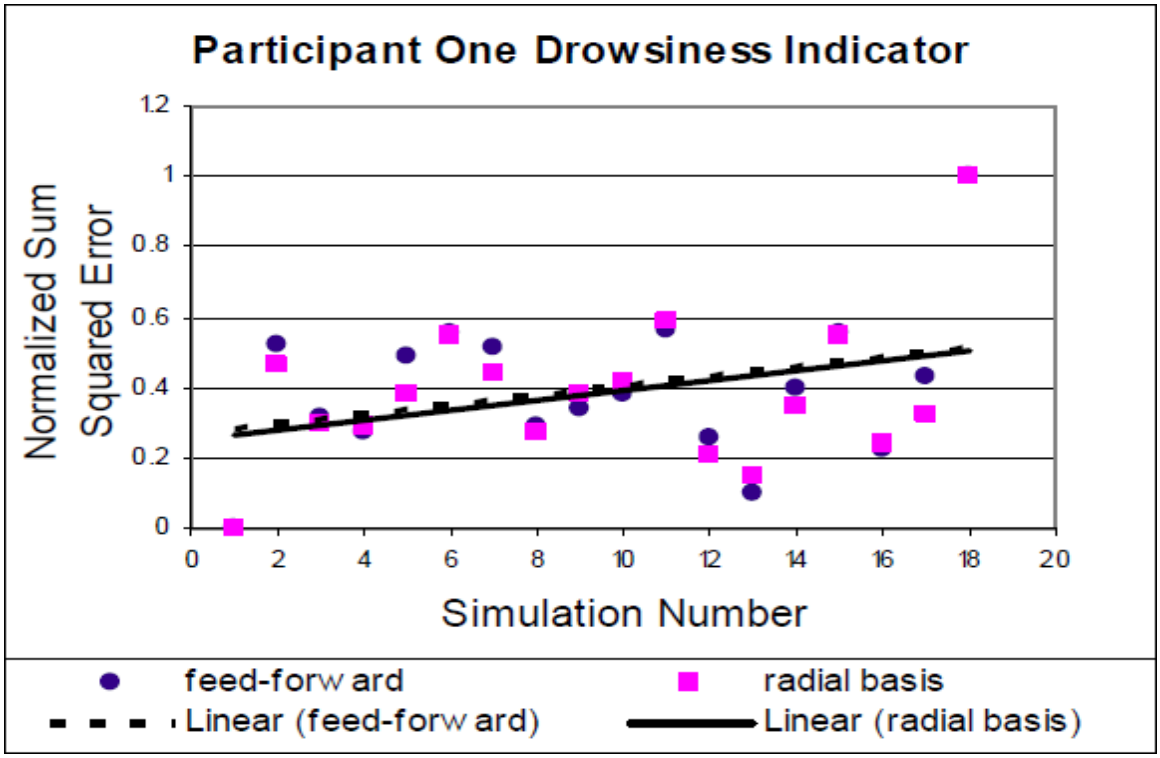

Figure 1-15 Jerk profile drowsiness indicator [24]

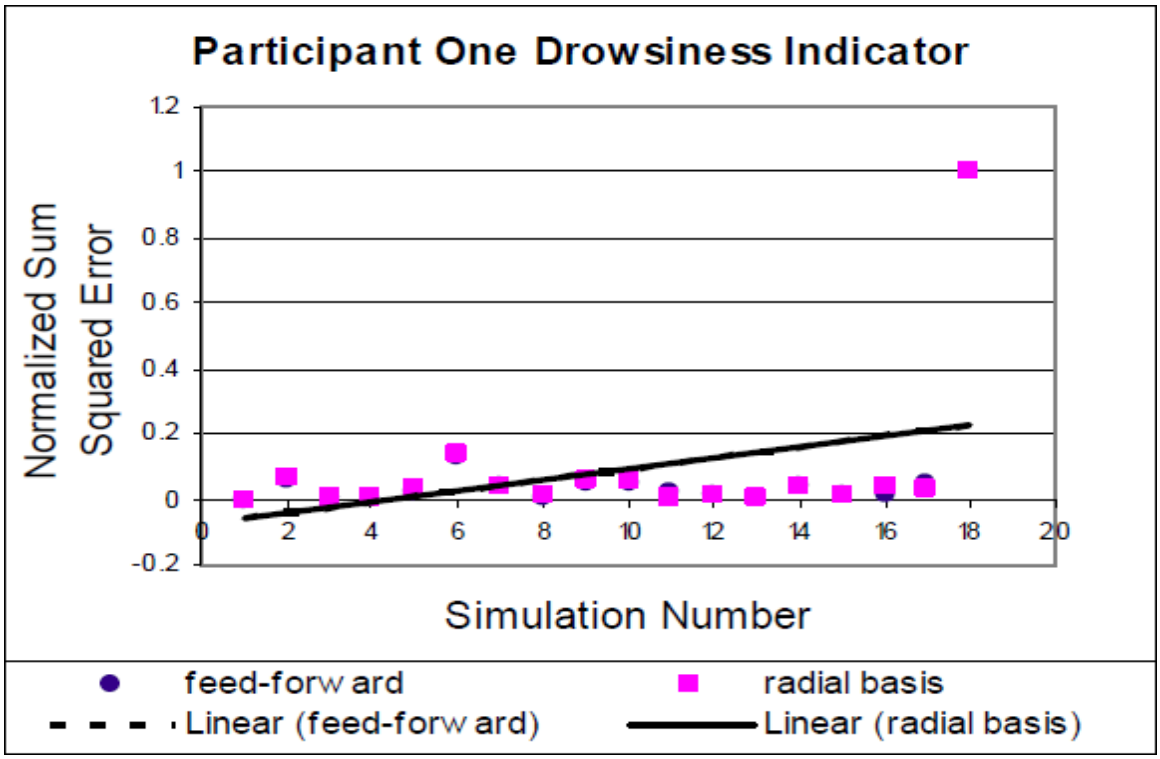

Figure 1-16 Spikiness index drowsiness indicator [24]

Sayed and Eskandarian [86], Eskandarian and Mortazavi [87], Son et al. [88] as well as Culp et al. [24] presented a method that uses the steering wheel angle to train neural networks on different driving behaviour. However, work presented by Eskandarian and Mortazavi [87] accounted for the effects of road curvature on the steering angle and realized that drowsiness affects the steering behaviour in two consecutive phases while Son et al. [88] incorporated the lane position with the steering angle. Nonetheless, Culp et al. [24] eliminated the effects of road curvature and other environmental factors by taking the third derivative of the steering wheel angle and used a special type of neural network which only needs alert driver datasets to be trained and used as reference.

Daza et al. [90] proposed a drowsiness detection system which uses an optimized combination of different driver and driving physical indicators as shown in Figure 1-17.

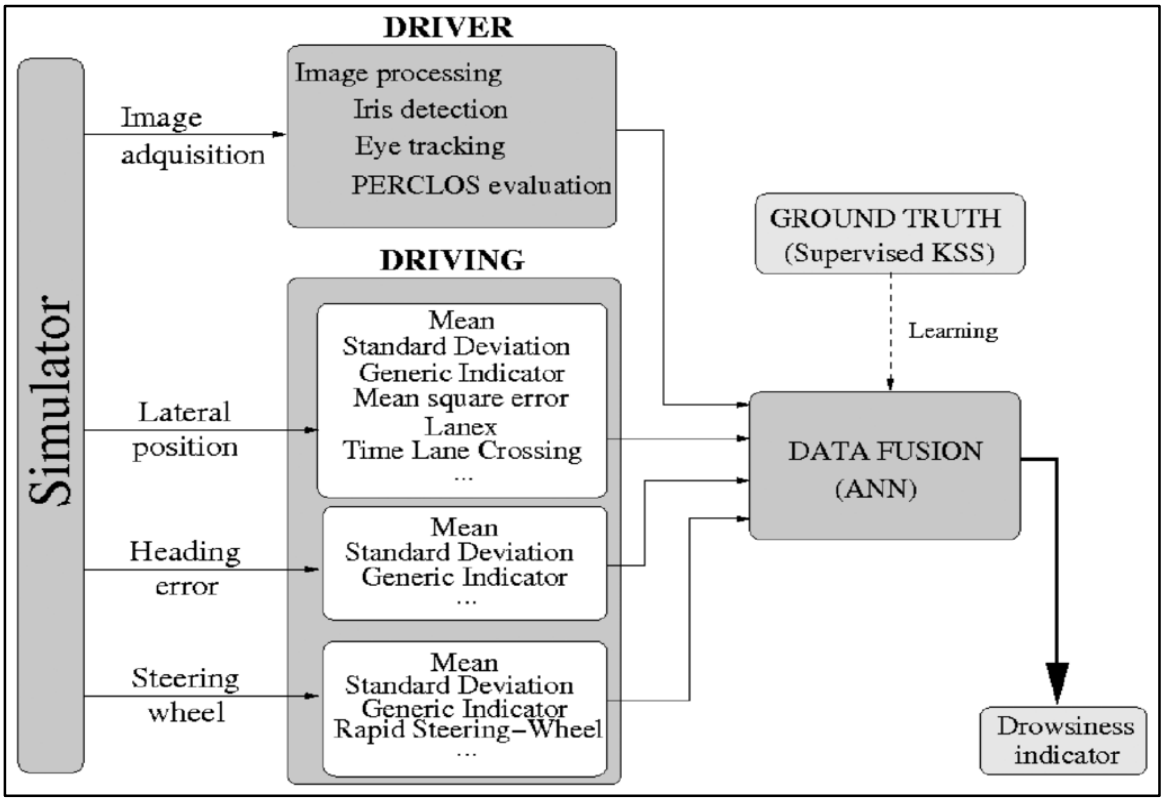

Figure 1-17 Proposed drowsiness detection system architecture [90]

The driver indicators are obtained using a camera and a Near Infra-Red (NIR) illuminator placed on the dashboard. The camera takes images of the driver's face and the NIR illuminator is used when the light is needed. After that, the percentage of eyelid closure (PERCLOS), blink duration, frequency and face position indicators are derived from the images. It was found that the PERCLOS is sufficient to be used for drowsiness since the other driver's indicators provide only a slight improvement over the PERCLOS. In terms of the driving indicators, the lateral position, heading error and the steering angle data were obtained during an experiment which was done on a truck driving simulator. Nine drivers were asked to drive the simulator for 3 hours. Each driver was asked to drive for one hour when sleep deprived, one hour when the driver is not sleep deprived and the last hour was done after a long working day. The drivers were asked to report their alertness level to an expert every 5 minutes in order to use the Karolinska Sleepiness Scale (KSS) in detecting the drowsiness state. It should be noted that the KSS is a subjective method of determining the alertness level. The mean standard deviation and the mean square error were determined for the lateral position and heading error. The mean standard deviation was determined using the following equation:

$$STD = \sqrt{\frac{\sum_{i=1}^{n}(x_i - \bar{x})^2}{n-1}} \qquad \textbf{1-5}$$

Where; x_i represents either the lateral position of the vehicle or the heading error, $\bar{x}$ is the arithmetic mean of the time series and n is the number of data points involved.

The mean squared error was calculated using equation 1-5 but $\bar{x}$ was replaced by a parameter p. This parameter guarantees that the lateral position error or the heading error is equal to zero if the vehicle is in the center of the lane or there is no heading error.

In addition, the Lanex and time to lane crossing were calculated for the lateral position whereas the rapid steering-wheel was calculated for the steering wheel movement. The lateral position was determined by measuring the perpendicular distance between a point on the right lane marking and the center of the vehicle. Moreover, the heading error was defined as "the angle between the direction of heading of the vehicle and the tangent line of the driving lane" whereas the rapid steering wheel movement was defined as "the fraction of the steering-wheel rate that exceeds a specific threshold value during a given time interval". The rapid steering wheel movement (RSWM) was determined using the following equation:

$$RSWM = \frac{1}{n-1}\sum_{i=2}^{n} h(\dot{s_i}) \qquad \textbf{1-6}$$

Where; n is the number of data points in the time series, $h(\dot{s_i})$ equals to 1 if the steering rate exceeds a specific threshold.

Nevertheless, the Lanex was defined as "the fraction of a given time interval spent outside the driving lane" [90]. Some indicators were then optimized using Genetic Algorithm to find the best threshold value for each indicator. After that, the optimized, the non-optimized, as well as the KSS indicators were fed to a feed forward neural network with backpropagation algorithm in order to classify the data into alertness or drowsiness states. It was found that there is a direct correlation between the PERCLOS and the driving behaviour and that any single driving behaviour combined with the PERCLOS result in better detection. It was also found that the best combination was obtained by the fusion of PERCLOS and the mean square error of the heading error. This combination achieved a classification rate of 96%. This method requires cameras and sensors and is good for the simulation environment since this system requires cameras and a variety of sensors. This

will require high computational power and expensive hardware and will make the detection system unaffordable.

Li et al. [91] developed a drowsiness detection method which uses soft computing algorithms to extract features from multiple sensors and feeds these features to a classifier feed forward neural network. The system comprises of a steering angle sensor, a pulse rate sensor as well as a Kinect sensor. The Kinect's sensor comprises of a depth camera with active illumination and was used for eyes tracking, blink detection, head pose as well as the face tracking. More than 40 features were extracted from the pulse rate, Kinect and steering angle sensors. For example, the steering velocity feature was extracted from the steering angle sensor whereas the mean pulse rate and the mean blink frequency features were extracted from the pulse rate sensor and the Kinect sensor, respectively. The sensor data were collected during an experiment done on five drivers with a valid driver's license using a PC-based driving simulator. Each driver was asked to drive the simulator for 588 minutes and to report their alertness level. The subjective driver alertness score was combined with other features extracted from sensors and used as an input vector to the neural network. The system classified the alertness level into three categories (Alert, little drowsy, deep drowsy) and achieved a 98.9% accuracy.

Both Li et al. [91] and Daza et al. [90] presented methods that combine the results of a set several driver and driving sensors to detect drowsiness. However, the system proposed by Li et al. is intrusive since drivers have to attach the pulse rate sensor to the tip of their fingers. In addition to that, the experiment was done on a computer driving environment which does not give the real-life driving feel. Daza et al. have used a driving simulator that is more realistic and accounts for different road and driving conditions.

1.5 CHAPTER SUMMARY

This chapter provided an overview of the truck simulator validation studies and discussed the causes of prolonged alertness loss such as; sleepiness, fatigue, and monotony and short inattention such as distraction. Vigilance loss is usually related to driving long distances and spending hours behind the wheel. The literature also reviewed the alertness monitoring techniques and the commercially available systems used in vehicles. The alertness monitoring techniques were divided into three categories; vehicle, driver, and vehicle driver observation techniques. The vehicle monitoring technique, such as lane departure, has the advantage of being practical since it does not disturb the driver, but road conditions can reduce the reliability of such a system. The driver monitoring technique, such as monitoring facial features, has the advantage of monitoring real biological responses which can be easily related to inattentiveness. However, the system is intrusive in some cases as in electroencephalogram (EEG) recordings, where in other cases the system has some difficulties with eye detection and different illumination conditions. Both the vehicle and the driver monitoring techniques use image processing. As a result, large computational power is required in order for the system to be fast enough to work in real time. The large computational power also contributes to the price of such systems. The vehicle driver interface monitoring technique, such as the steering wheel, has the advantage of being non-intrusive, cheap and simple since the system requires small computational power. Nonetheless, the measurements of this system are hard to relate to vigilance loss. Artificial neural networks have been widely used by researchers for their ability to represent complex relationships and classify different levels of driving alertness. The literature review concluded that further work should be done using the vehicle driver interface to relate this

technique to distraction and to validate its reliability. The latter technique has a great potential for developing a real time simple system that can be affordable and reliable. Consequently, this system can be commercially available; since there are only a few available products.

CHAPTER 2

TRUCK DRIVING SIMULATOR VALIDATION

This chapter describes each component of the Virage VS600M truck driving simulator. The simulator will be used as the main tool to study driver distraction. This chapter also illustrates the main steps used in validating the truck simulator model and the results of the validation process. In addition, this chapter presents a validation for the steering rate algorithm used in the truck simulator.

2.1 MAIN COMPONENTS OF THE TRUCK SIMULATOR

The simulator consists of the operator station unit, computational unit, three display screens and the motion base. Mounted on the motion base is what would be inside the cabin of the truck: driver's seat, steering wheel, instrument cluster, accelerator pedal, brake pedal, clutch pedal, as well as a Multi-Functional Display (MFD). The main components of the truck driving simulator are shown in Figure 2-1.

The computational unit consists of five personal computers (PC) units labeled as PC 1 to PC 5 as shown in Figure 2-2. The first unit (PC 1) represents the operator station unit which allows the operator to select and edit different driving scenarios. It also allows the operator to select different vehicle configurations and simulation environment parameters. In addition, the driver steering wheel and pedals inputs are connected to PC1. The image generation for the left, middle and right screens is controlled by PC2, PC3 and PC4, respectively. The fifth computer unit (PC5) controls the dynamics of the motion base, steering wheel feedback force, audio effects as well as the instrument cluster and the Multi-Functional Display (MFD).

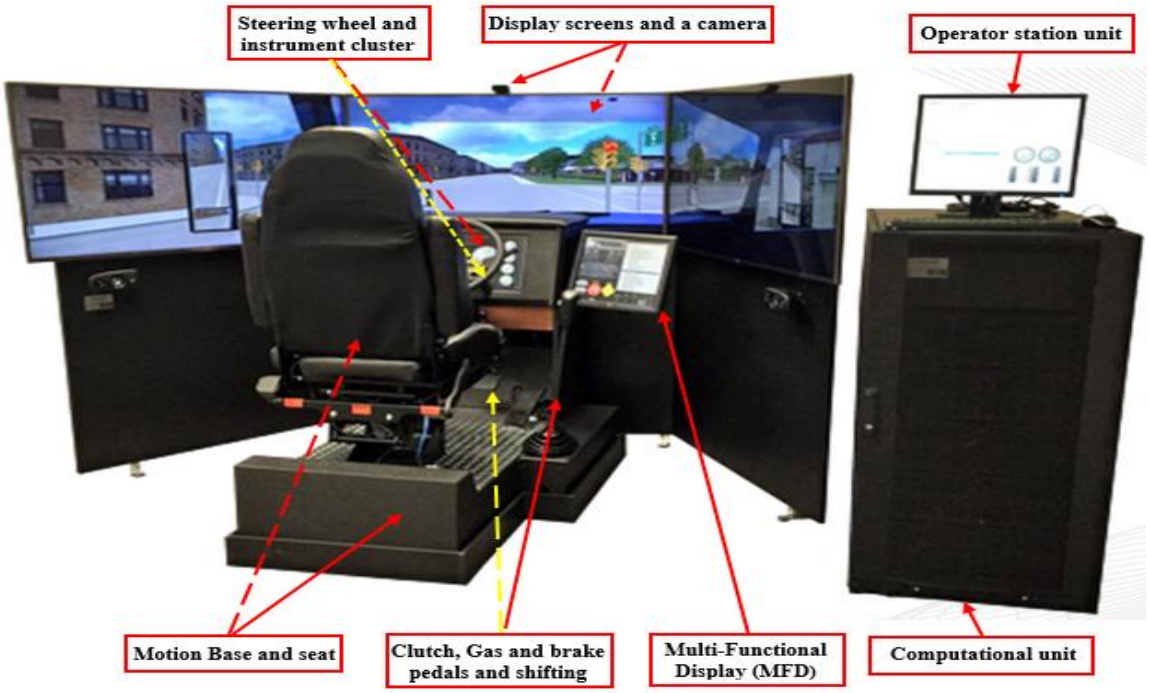

Figure 2-1 Virage VS600M Truck driving simulator main components (Photo courtesy of Virage Simulations, Montreal QC [92]

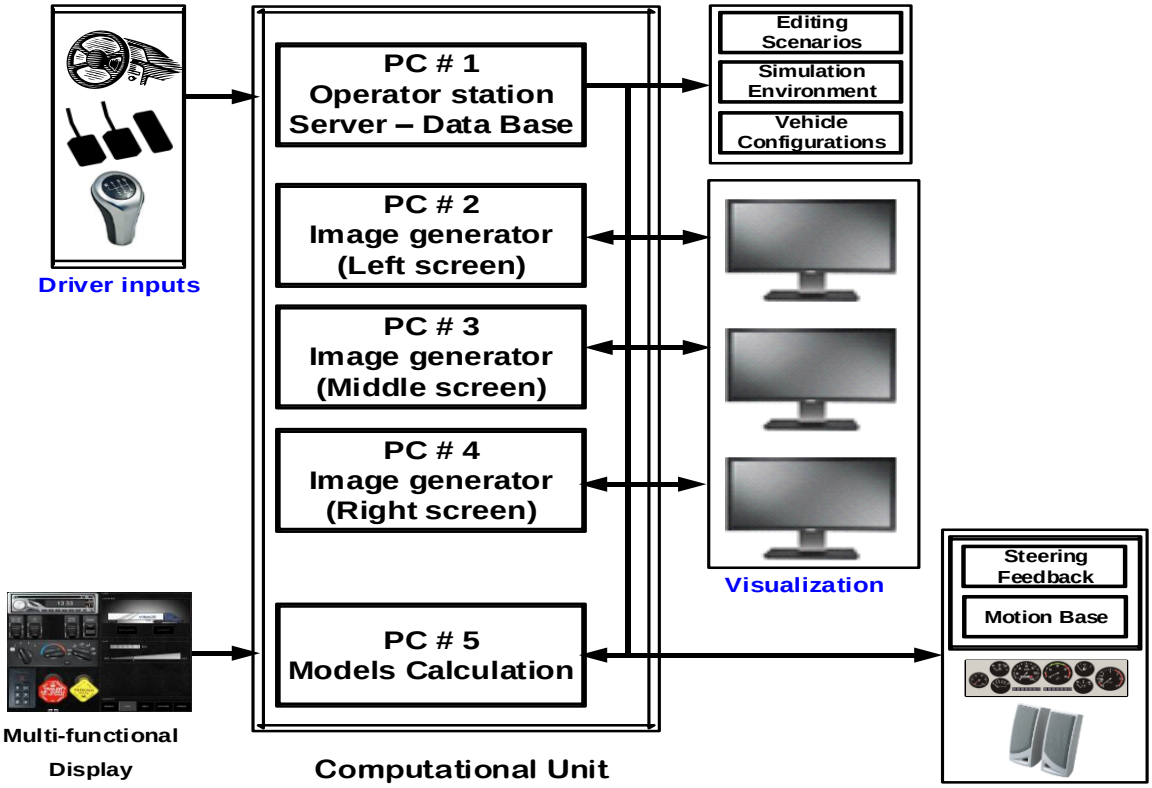

Figure 2-2 Schematic diagram of the truck driving simulator subsystems

The motion base has three degrees of freedom (pitch, roll and yaw) and gives a realistic driving sensation such as the road roughness, negotiating a turn as well as the pitch motion during braking or acceleration. The steering wheel angle is collected from the simulator as a ratio of the maximum steering angle, where a full left rotation of the steering wheel has a value of -1 whereas a full right rotation has a value of 1. The maximum steering angle in this simulator is 720˚ degrees from the center to full right or full left position. The accelerator pedal value is also measured as a ratio where a full throttle, half throttle and no throttle have values of 1, 0.5 and zero, respectively.

In addition, the simulator has a clutch and a manual gear shift lever which offers different transmission modes such as automatic transmission as well as the 10-speed, 13-speed and 18-speed manual transmission modes.

The three display screens are used to give the feeling of driving in a truck cabin, where the center screen shows the road ahead of the driver while the left and right side screens show the left and right sides of the road. The two side screens each have mirrors to show the right and left side lanes whereas the center screen has two small mirrors that show the overall position of the truck.

The Multi-Functional Display (MFD) shown in Figure 2-3 has several functions. The driver can select the added payload weight to the vehicle. The driver can also release the brakes of the tractor and the trailer as well as select the drive mode such as reverse, neutral and drive in the automatic transmission mode. In addition, the driver can select different vehicle configuration such as the straight truck or the tractor semitrailer as well as selecting the engine types and transmission modes.

The MFD also gives the driver the option to select different scenarios from the library, control the sensitivity of the clutch for manual transmission as well as recharge the brake system since air brakes are used in trucks.

Figure 2-3 Multi-Functional Display (MFD)

The virtual instrument cluster shown in Figure 2-4 displays the speedometer and tachometer. Furthermore, there are different sets of indicators for the brake air pressure, coolant temperature, among others.

Figure 2-5 shows a screen shot of the main operator unit used in the simulator. The main operator unit is the main user interface where the operator can run any scenario from the

scenario library, change vehicle configuration, transmission modes as well as control the weather conditions and the time of the day.

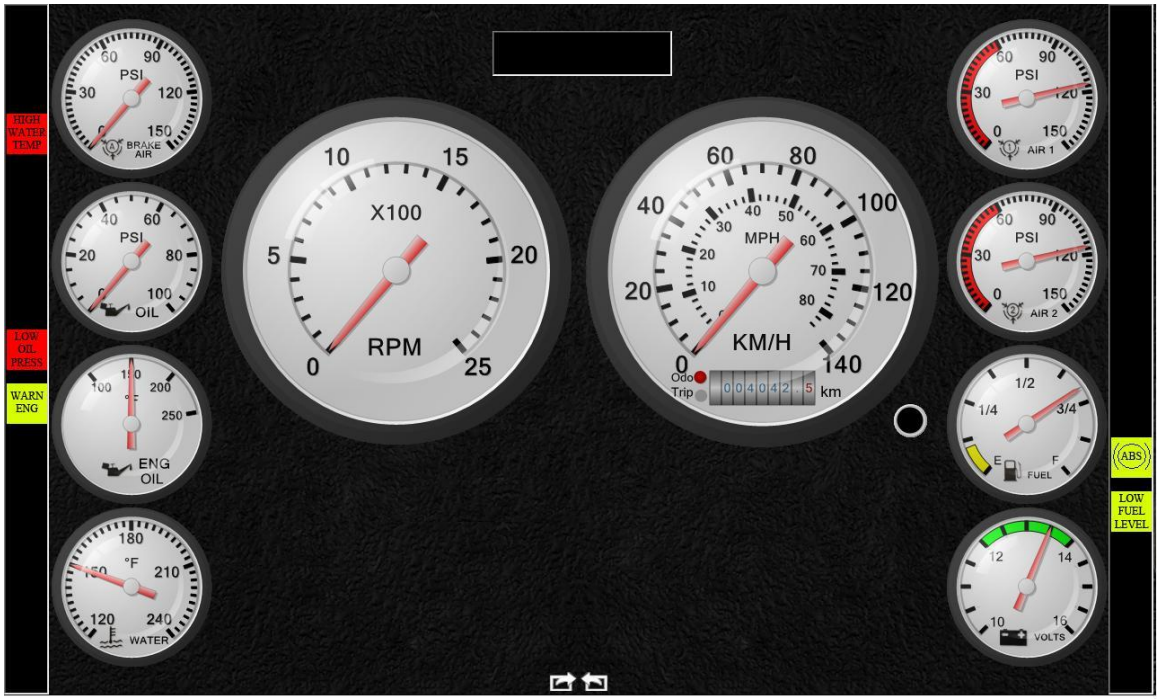

Figure 2-4 Virtual instrument cluster display

The main operator unit also offers different screen views that can be changed while the scenario is running and a map for each scenario. The map can be used to run the new scenarios that do not exist in the scenario library. For example, the operator can modify one of the scenarios for the purposes of collecting data or do specific changes to any scenario and then run it by clicking on the map icon and then clicking the open scenario tab. The main operator unit also controls the camera and allows the operator to do modifications on the vehicle model. For example, the operator can change parameters such as the length of the vehicle, width, center of gravity location, among other parameters. The operator station scenario library offers scenarios that can be used to train drivers on economy driving, manual transmission stick shifting with usage of the clutch, steering,

vigilance, obstacle avoidance, rollover prevention, and emergency situations such as tire blowout.

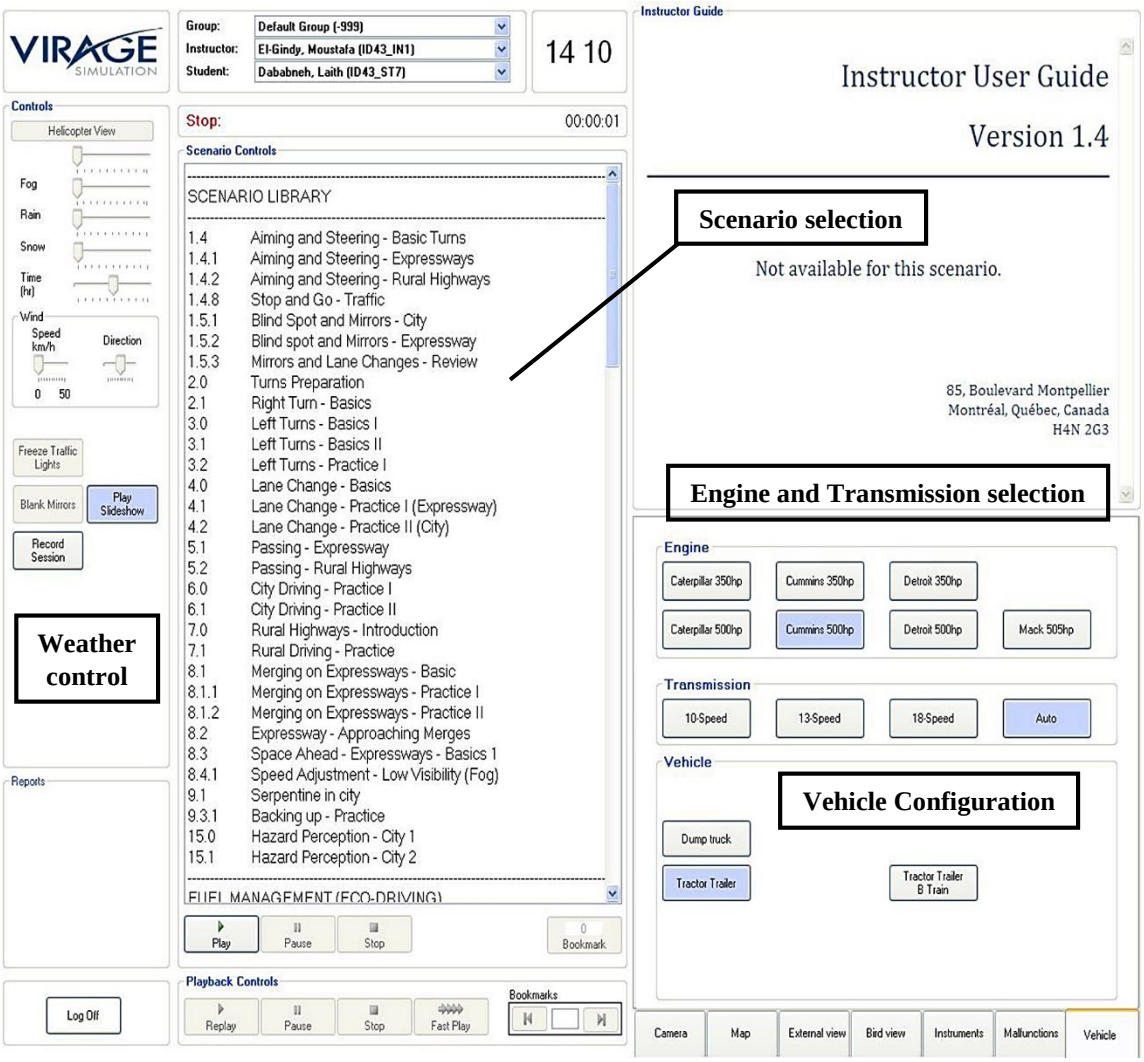

Figure 2-5 Simulator operator station unit

In addition, the library offers a variety of scenarios that can simulate city driving, highway driving, driving in rural areas, mountain driving as well as driving on icy roads. The library also has evaluation scenarios that can be used to test drivers after training and points are allocated for each task to show the driver's competency. Furthermore, each scenario can

be modified by adding or removing objects, controlling traffic and driving conditions. For example, vehicles can be removed from any scenario to reduce traffic.

It should be noted that the Virage car driving simulator VS500M was used in a previous study [93] to evaluate the effects of the cannabis drug on the driving performance.

2.2 TRUCK SIMULATOR VALIDATION PROCEDURE

The purpose of validating the truck driving simulator model is to show that the simulator model is actually reliable and comparable to real world trucks and as a result can be used to study driver distraction effectively and obtain accurate results.

As mentioned earlier in CHAPTER 1, there are two primary areas of truck simulator validation; physical and behavioural validation [8, 9]. This section is mainly concerned with the physical validation of the truck driving simulator. The behavioural validation will require comparing simulator experiments with field testing of real trucks and is out of the scope of this study. The truck simulator model will be physically validated using TruckSim software. The validation process is carried out by comparing the results of two different simulation environments considering the same technical data of the tractor semitrailer and the same driving conditions such as driving speed and path following maneuver as discussed in [13]. The first simulation environment is the truck simulator which represents a typical closed loop real time control system. Different driving scenarios can be chosen and the driver has to control the speed via pedals and shifting lever as well as controlling the direction via the steering wheel to cope with the prescribed scenario. Correction of the path is carried out by the driver from the real time comparison between the direction of the simulated vehicle and the targeted direction defined by the scenario. The second simulation

environment is TruckSim software, which is developed by the Mechanical Simulation Corporation and is widely used to analyze and simulate the dynamic behaviour of trucks and other commercial vehicles. TruckSim has a driver model or auto-pilot to control both the speed and direction of the vehicle during the course of simulation. It should be known that, TruckSim has been validated with field testing of typical vehicles over a period of twenty years [94].

For the purpose of validation, the output data from the truck simulator such as time step, speed profile and maneuver coordinates (x, y and z) are collected from the simulator and used by the auto-pilot of the TruckSim to control similar driving conditions. The first stage of validation guarantees that the same vehicle technical data is used in both TruckSim and the simulator. The second stage assures that the same path maneuvers and driving conditions such as the speed are used in both TruckSim and the simulator. After that, the steering wheel angle of both the simulator and TruckSim is compared to evaluate the validity of the simulator model as illustrated in Figure 2-6 . The steering input has been used in previous studies to evaluate the validity of simulators [11].

The axis system in TruckSim is different than the axis system of the truck simulator as illustrated in Figure 2-7. In TruckSim, the x, y and z axes correspond to the longitudinal, lateral and vertical axes, respectively. Additionally, the motion about the x, y and z axes correspond to the roll, pitch and yaw motions, respectively. However, the x, y and z axes in the truck simulator correspond to the lateral, longitudinal and vertical axes, respectively. Furthermore, the motion about the x, y and z axes in the simulator correspond to the pitch, roll and yaw motions, respectively.

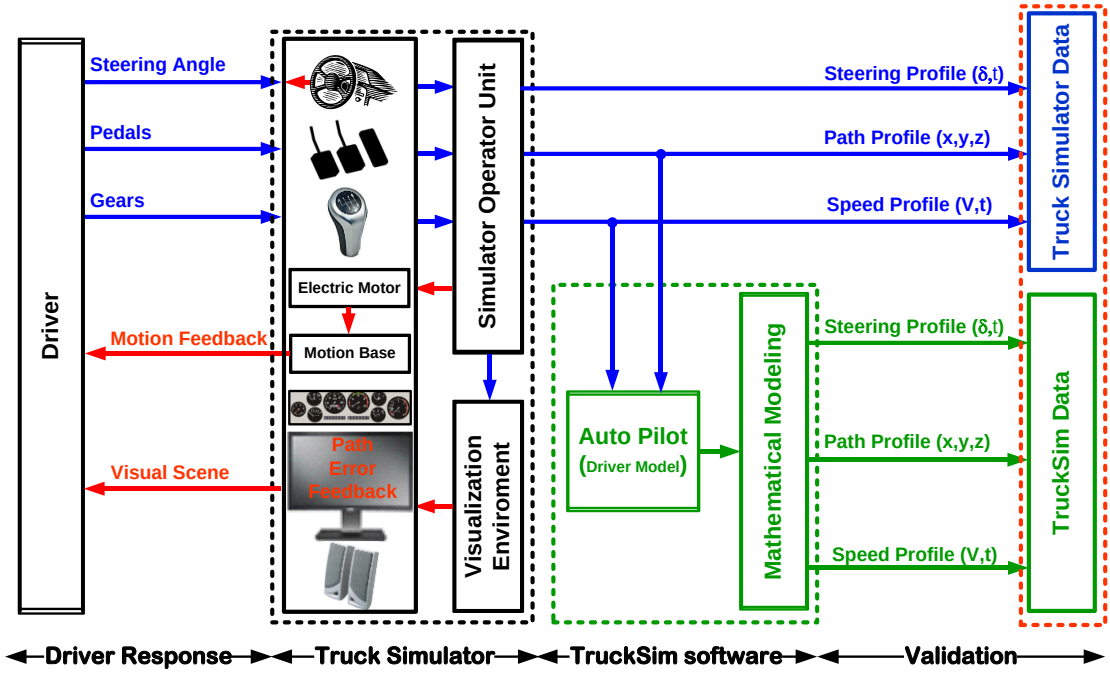

Figure 2-6 Simulator validation procedure

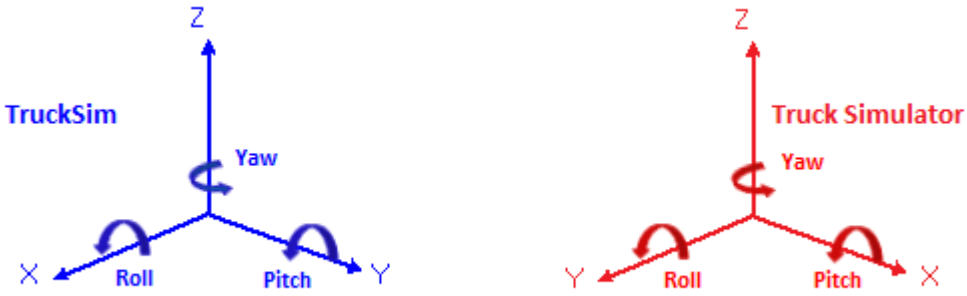

Figure 2-7 Axis system for both TruckSim and the truck simulator

The validation process will be done in two consecutive stages. The following sections will discuss the validation process in details.

2.2.1 First Stage: Implementing Identical Technical Specifications

In order to be able to validate the truck simulator model, the technical data obtained from TruckSim has been extracted and used as inputs into the simulator. It is noted that there are

differences between the data format in TruckSim and the simulator when it comes to inputting data. For example, the location of the Center of Gravity (C.G) is determined in TruckSim as the distance from the front axle, whereas in the simulator it is determined by the total weight distribution on the front and rear axles. As a result, the total weight on each axle in TruckSim has been used to determine the location of C.G based on the total weight in the simulator.

The technical data of the simulator model can be tuned by changing the values of the parameters in the “Interactive.Tod” and “Interactive_trailer.Tod” files. After that, the new values become active once you save and run any scenario. The first file represents the tractor data while the second file shows the trailer data, respectively. The tractor semitrailer vehicle configuration has been used in both TruckSim and the simulator. In addition, the same number of axles has been used to validate the model. This vehicle configuration will be also used to study distraction later on.

Figure 2-8 shows the tractor semitrailer vehicle configuration used in both TruckSim and the simulator. The vehicle on top represents the TruckSim model whereas the vehicle at the bottom represents the simulator model used.

Table 2-1 demonstrates the vehicle parameters that have been used in the simulator and TruckSim. The total weight of the unloaded tractor semitrailer has been calculated by finding the weight on each axle of both the tractor and the semitrailer in TruckSim and then using the values as inputs to the simulator. The total weight of the added load represents the extra weight that has been added to the trailer. It has been determined by subtracting the total weight of the unloaded vehicle from the total weight of the loaded vehicle and has been used as an input to TruckSim.

Figure 2-8 Tractor semitrailer configuration in TruckSim and the simulator

The center of gravity height, axle loads, yaw moment of inertia, wheel radius, tire friction factor and the position of the added load have been taken from TruckSim and used as inputs to the simulator. The suspension spring stiffness, steering box ratio, coefficient of rolling resistance as well as the engine power value have been extracted from the simulator and used as inputs to TruckSim.

Figure 2-9 shows the schematic diagram and the dimensions of the tractor semitrailer vehicle configuration used in TruckSim and the simulator for the validation process. This figure has been added as an illustration to the dimensions discussed previously in Table 2-1. The left side of Figure 2-9 represents the tractor part whereas the right side represents the trailer part. The black square with the cross sign is the articulation point while the circle with the cross sign on the trailer is the point where the extra weight has been added to the trailer. The wheel base of the tractor is the distance between the front axle and the center

of the two rear axles. The wheel base of the trailer is the distance between the articulation point and the center axle of the three rear trailer axles.

Table 2-1 All parameters used in TruckSim and Simulator models

Parameter	Units	Tractor	Trailer
Total weight of the unloaded tractor semitrailer	kg	16014	
Total weight of added load	kg	29986	
Total weight of the loaded tractor semitrailer	kg	45000	
Length of vehicle	mm	6270	14450
Width of vehicle	mm	2438	2438
Load on first axle	kg	5317	1628
Load on second axle	kg	3118	1477
Load on third axle	kg	3126	1348
Center of gravity height	mm	1020	1936
Yaw moment of Inertia	$Kg\text{-}m^2$	34823	150000
Suspension spring stiffness	N/mm	300	600
Articulation point (longitudinal distance from rear axle)	mm	635	13250
Articulation point (height)	mm	1100	1100
Track width of first axle	mm	2030	1863
Track width of second axle	mm	1863	1863
Distance between first and second axle	mm	5000	1200
Distance between second and third axle	mm	1270	1200
Coefficient of rolling resistance	-	0.008	0.008
Wheel radius	mm	510	510
Tire friction factor	-	1.0	1.0
Steering gear box ratio	-	21.95	-
Position of added load (distance from the middle axle)	mm	-	2000
Engine Power	kW	372	-

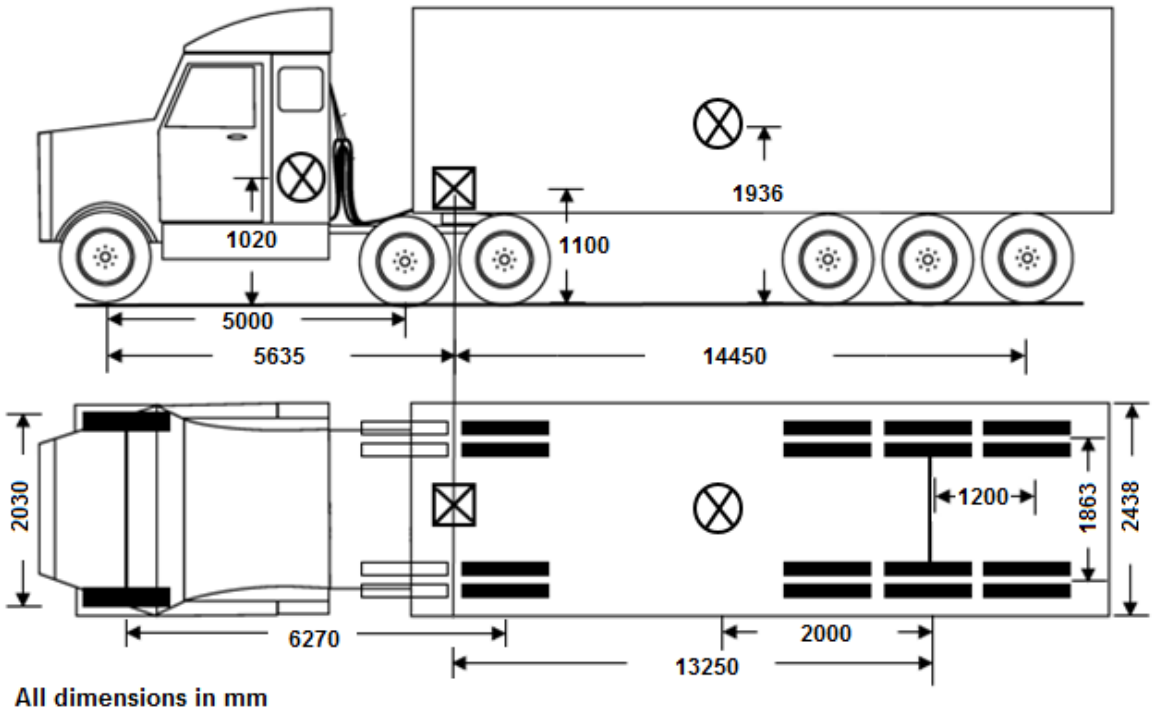

Figure 2-9 Schematic diagram of the tractor semitrailer configuration

The following section will discuss the driving maneuvers and scenarios that have been used to test the simulator model for validity.

2.2.2 Second Stage: Implementing Identical Testing Scenarios and Maneuvers

The highway and the city driving scenarios have been used to test the dynamics of the simulator during critical maneuvers for the purpose of validation. The highway scenario has been used to complete the high speed driving maneuver whereas the city driving scenario has been used to complete the low speed turn maneuver as well as the double lane change maneuver.

The low speed turn maneuver has been done on a tight left turn at a constant speed of 20 km/h. The double lane change maneuver has been done at a speed of 40 km/h and the driver

moved from the rightmost lane to the leftmost lane and then moved back again to the rightmost lane.

The low speed turn, double lane change and the high speed driving maneuvers implemented in this study were inspired by the methods of evaluating the performance measures of heavy vehicles proposed by El-Gindy [95]. Three speed ranges were used in the validation to show that the simulator is valid for various speeds and maneuvers. Based on the methods of evaluating the performance measures, the low speed turn maneuver was performed on a tight turn at speed of 5 km/h while the double lane change maneuver was performed at a speed of 100 km/h. In addition, the high speed driving maneuver was performed on a shallow turn of 393 m radius at a speed of 100 km/h. However, the low speed turn maneuver used in the validation was performed at a speed of 20 km/h instead of 5 km/h while the double lane change maneuver was performed at a speed of 40 km/h instead of 100 km/h. The validation of the high speed driving maneuver was performed at the same speed used to evaluate the performance measures of heavy vehicles but the highway scenario used was comprised of shallow turns of various radii as well as straight sections. It should be noted that the low speed turn maneuver used in the validation was performed at speed of 20 km/h since it was difficult for the driver to achieve a very low speed of 5 km/h in the simulator. Therefore, a speed of 20 km/h was the most suitable to negotiate the tight turn and at the same time the driver was able to successfully maintain a constant speed throughout the driving maneuver.

The vehicle has been tested twice on each maneuver, once to test the vehicle when the trailer is empty and the second time to study the effect of adding the payload to the trailer. The weight of the empty tractor semitrailer vehicle configuration represents the weight of

the tractor and the empty trailer. In contrast, the weight of the fully loaded tractor semitrailer vehicle configuration represents the weight of the empty tractor semitrailer plus the weight of the added payload to the trailer.

The time step, speed and the coordinates (x, y and z) of each maneuver have been collected from the simulator and used as inputs to TruckSim. The data collection from the simulator is done by editing any scenario from the library using the NotePad++ program and then adding the data collection script to that scenario.

Two scripts for the same scenario were investigated. The first script encompassed the collecting data block whereas the second script encompassed the scenario script without the data collection block. After that, WinMerge tool was used to compare the two scripts. This tool places each file either to the left or right of the screen and highlights the parts of the script that differ from one another, indicating a change in the code. The operator can then add the different parts to any scenario using the NotePad++ and save it as a different name in order to keep the original files unmodified.

In order to check the data that will be collected from the data collection scenario, the operator has to double click on the scenario. After that, the main script and the data library shows up. The operator has then to click on the data collection block to the left side of the library screen. By doing that, two tabs having the labels of “Normal code” and “When becomes active” will appear.

The operator can check which data will be collected by looking at the last line of script under the “Normal code” tab. The last line of the script will have the “get-steering” code template. The “get-steering” code is used to collect the steering angle. The operator can

change the data collected by looking at the code templates on the upper side of the screen and then placing another template instead of "get-steering" such as "get-position".

The data is collected by running the scenario that has the data collection script and the data will be saved in an excel sheet that will be available right after stopping the scenario. Each column in this sheet represents one of the selected parameters. For example, the first column is reserved for the steering angle whereas the second column is reserved for the position of the vehicle.

As a result, the operator has to check the last line of the script under the "When becomes active" tab to label the column for each data set collected. The labels should follow the same sequence presented in the last line of script under the "Normal code" tab.

However, the collected data has been modified before using it as inputs to the TruckSim software. The collected data has been modified by adding time steps to find the total time of the simulation or the time at a certain point of the simulation. In addition, TruckSim uses speed units of km/h whereas the speed collected from the simulator has a unit of meter per second. As a consequence, the collected data has been modified by converting the speed units to km/h in order to be used in TruckSim. Furthermore, the x, y and z coordinates collected from the simulator starts from a specific reference point and has been modified to start from the (0, 0, 0) reference point which represents the start of the maneuver in TruckSim. The steering wheel angle has also been modified by multiplying each angle by the maximum steering angle of 720˚ degrees since the steering angle is collected as ratio of the maximum steering angle.

The path coordinates of the driving maneuvers used for the validation of the tractor semitrailer model in both TruckSim and the simulator are shown in Figure 2-10. The path coordinates collected from the simulator are used as inputs to the road generator in TruckSim. The driver model in TruckSim then follows the same exact path by controlling the steering wheel angles of the simulated tractor semitrailer.

An optional feature of Trucksim software is to visualize the prescribed simulation in terms of the vehicle (tractor semitrailer) and the track in a high definition graphics environment. This feature aids the user to fully interpret different aspects of simulation dynamics and therefore be able to analyze the results properly.

The low speed turn maneuver path coordinates and the associated visualization for this maneuver are shown in Figure 2-10 (a). The driver in this maneuver was asked to make a left turn at a speed of 20 km/h. However, the driver had first to move to the leftmost lane of the three-lane road section in order to make the left turn while keeping a constant speed profile. The driver in the double lane change maneuver moved to the leftmost lane of the three-lane road section and then returned to the initial lane while maintaining a constant speed of 40 km/h as displayed in Figure 2-10 (b). It should be noted that the negative lateral position values for the low speed turn and double lane change maneuvers correspond to the direction of the vehicle with respect to the initial reference position. The initial reference position is the position of the vehicle at the beginning of the simulation in the simulator. Therefore, driving to the left side of the initial reference position results in a negative lateral position values while driving to right side results in positive lateral position values. The high speed driving maneuver is comprised of both straight and curved road section as shown in Figure 2-10 (c).

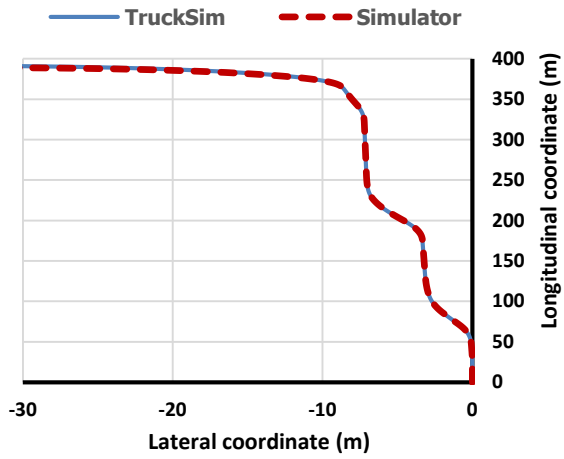

(a) Low speed turn maneuver path coordinates (20 km/h)

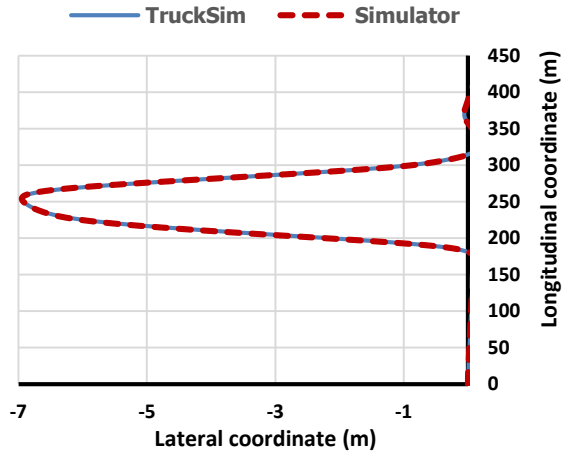

(b) Double lane change maneuver path coordinates (40 km/h)

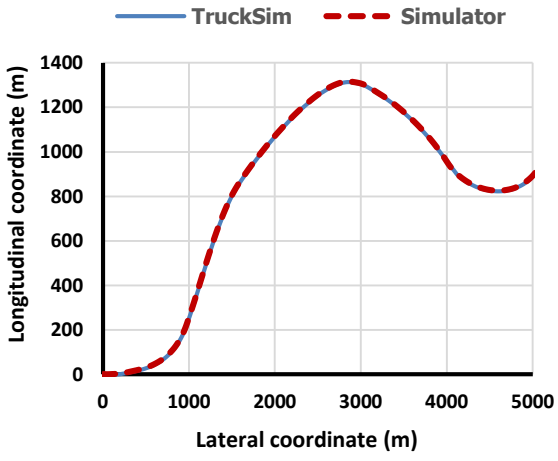

(c) High speed driving maneuver path coordinates (100 km/h)

Figure 2-10 Path coordinates for the validation driving maneuvers

The curved road sections were needed to evaluate the lateral characteristics of the tractor semitrailer model through the steering wheel angle profile. In this maneuver, the driver was required to maintain a constant speed of 100 km/h.

The speed profiles of the driving maneuvers used for the validation of the tractor semitrailer model in both TruckSim and the truck simulator are displayed in Figure 2-11. For the purposes of validation, the driving speed profile in both simulator and TruckSim environments should be identical. The driving speed profile of the driver is collected from the simulator and added as an input to the speed controller in TruckSim. The driver model in TruckSim controls the driving torque to follow similar speed profile.

The speed controller in TruckSim maintained a constant speed profile of 20 km/h throughout the low speed turn maneuver for both the empty and loaded tractor semitrailer vehicle configurations as indicated in Figure 2-11 (a). However, the speed profile obtained from the speed controller in TruckSim showed a slight deviation from the 40 km/h speed profile of the simulator for the loaded tractor semitrailer configuration during the double lane change maneuver as shown in Figure 2-11 (b). Additionally, the speed profile of the loaded tractor semitrailer configuration obtained from TruckSim indicated a variation from the 100 km/h speed profile obtained from the simulator as presented in Figure 2-11 (c). In conclusion, increasing the vehicle speed in conjunction with adding payload to the trailer results in a deviation between the speed profile of the speed controller in TruckSim and the vehicle speed collected from the simulator. The difference between the speed profiles of both the simulator and TruckSim is mainly attributed to differences in the vehicle model and other simulation parameters such as the accuracy of the speed controller in TruckSim.

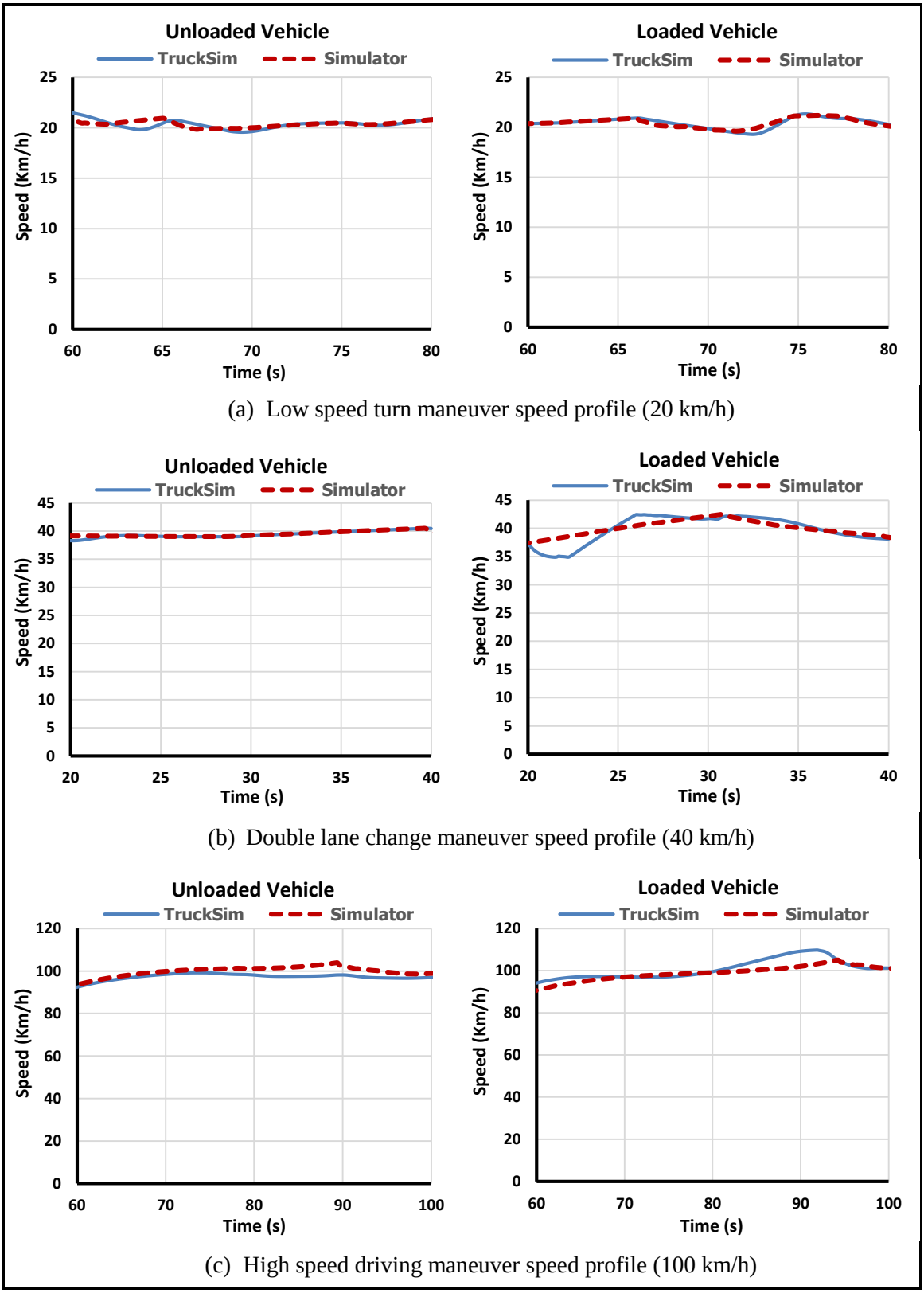

(a) Low speed turn maneuver speed profile (20 km/h)

(b) Double lane change maneuver speed profile (40 km/h)

(c) High speed driving maneuver speed profile (100 km/h)

Figure 2-11 Vehicle speed profile for the validation driving maneuvers

2.2.3 Results of the Truck Driving Simulator Validation Process

The steering wheel angle collected from the simulator is compared with the steering wheel angle output from TruckSim. The steering wheel angles are to be compared for the previously discussed maneuvers using the loaded and the unloaded tractor semitrailer vehicle configurations. The results of this section are considered to be conclusive to whether or not the simulator model is actually valid and whether or not it can be actually used as a tool to study distraction.

The steering wheel angle profiles of the driving maneuvers used for the validation of the tractor semitrailer model in both TruckSim and the simulator are shown in Figure 2-12. The steering wheel angle profile of the low speed turn maneuver for the empty and loaded vehicle configurations is shown in Figure 2-12 (a). The steering angle profile for this maneuver indicates a time delay between TruckSim and the simulator. The time delay can be attributed to the difference between the driver model in TruckSim and the human driver in the simulator. For instance, the driver of the simulator in this maneuver started to turn earlier and over steered on the turn whereas the steering angle profile in TruckSim is smooth. The steering wheel angle profile for the double lane change maneuver has negative steering angle values as shown in Figure 2-12 (b). The negative sign corresponds to turning the steering wheel clockwise from the center point whereas the positive sign corresponds to the counter clockwise motion of the steering wheel. The steering angle profile of the high speed driving maneuver for the tractor semitrailer model is displayed in Figure 2-12 (c). It can be observed that the steering angle profile for all the presented driving maneuvers is higher for the loaded vehicle configuration. Increasing the weight of the vehicle results in having higher tire cornering forces and hence higher steering angles are required [96].

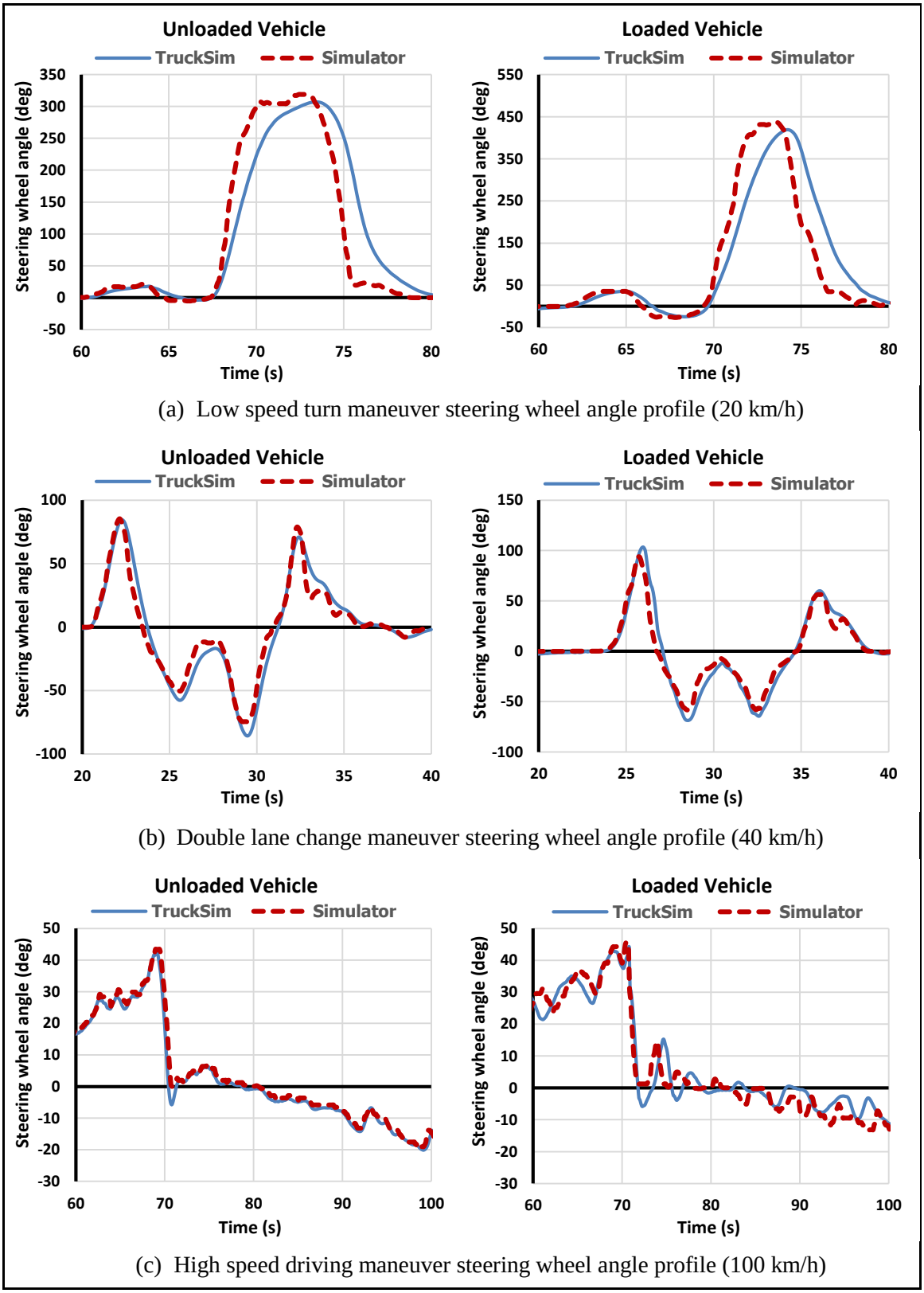

(a) Low speed turn maneuver steering wheel angle profile (20 km/h)

(b) Double lane change maneuver steering wheel angle profile (40 km/h)

(c) High speed driving maneuver steering wheel angle profile (100 km/h)

Figure 2-12 Steering angle profile for the validation driving maneuvers

2.3 CHAPTER SUMMARY

This chapter has summarized the main components of the Virage Truck Simulator and the steps that have been taken to validate the Virage simulator vehicle model. For the purposes of validation, identical technical specifications of the tractor semitrailer vehicle model were used in both TruckSim and the truck simulator simulation environments. Additionally, identical driving maneuvers and vehicle speed profiles have been used in both simulation environments. The steering angle profile generated from the truck simulator driver was compared with the steering angle profile generated from the driver model in TruckSim. The validation was evaluated by the comparison of the steering angle profile in TruckSim with the steering angle profile in the simulator. Based on the validation evaluation results of the steering wheel angle profile, it was concluded that the simulator model is valid for the low speed turn, double lane change as well as the high speed driving maneuvers. It was also noted that the three aforementioned driving maneuvers are sufficient for validating the model and cover most of the cases that a driver could be exposed to while driving. Finally, the discrepancies in the steering angle between the simulator and TruckSim is explained by the fact that the driver model in TruckSim is more accurate on turns since it follows the exact path and does not involve a human driver while in the simulator the steering angle depends on the driver performance and experience.

CHAPTER 3

DRIVER DISTRACTION DETECTION ALERT SYSTEM METHODOLOGY

This chapter describes the methodology used to evaluate driver distraction. The distraction detection analysis is divided into two parts; offline distraction detection analysis and real time distraction detection analysis. The offline analysis means that the driving experiments are still performed in real time but distraction is detected after the driving experiment is over. The research starts with the offline analysis before the development of the real time driver distraction alert system. The offline distraction detection method section includes a description of the jerk profile, spikiness index and the rate of change that are used to evaluate driver distraction. The offline method uses both the steering wheel and the accelerator pedal as the main driver inputs for detecting the distraction of the driver. However, based on the findings of the offline analysis the real time method will only use the steering input as the main driver input to estimate driver distraction. The steering input is chosen for the real time analysis since a high correlation has been found between the steering input and driver distraction. The real time analysis means that distraction is detected in real time while driving. Real time analysis is done directly on the driving simulator using List Programming (LISP) language and is comprised of two methods. The first method incorporates using a single steering rate threshold value to issue the distraction warning. This single threshold value is generated based on previous driving experiments and the value is entered manually into the simulator through the programming language

library. The second method monitors the normal driving behaviour for the first few minutes for any driver and generates a threshold value in real time.

3.1 OFFLINE DISTRACTION DETECION METHOD

The offline analysis studies the effect of driver distraction on the steering wheel angle and the accelerator pedal position. The data is first collected in excel sheets and then MATLAB is used to perform further processing calculations which will be given in this chapter. The main goal of the offline analysis is to determine which parameter is the most suitable for detecting driver distraction in real time. As a result, the findings of this section will help in the development of the real time driver distraction alert system.

3.1.1 Jerk Profile and Rate of Change

The Jerk profile is the third time derivative of the steering wheel angle and accelerator pedal position. It was first introduced by Desai and Haque [14] to discern different levels of driver alertness. It was concluded that the jerk profile was able to discern different levels of alertness and can be used in driver alertness detection systems.

The time derivatives of the steering wheel angle and accelerator pedal position are determined using the Savitzky-Golay numerical differentiation technique [97]. The numerical differentiation is needed to find the derivatives of the numerical data since there is no direct function that represents the steering angle and accelerator pedal position profiles for drivers. The Savitzky-Golay technique uses filter coefficients to find the least square fit for a polynomial within a moving window. The moving window finds the derivative of a point relative to the other points around that point, so the more points involved the more accurate the derivative will be. In order to preserve the characteristics

of the steering angle and accelerator pedal position raw data, a 7-point moving window is used where the middle point is preceded by 3 points and followed by 3 other points. The 7-points moving window was also recommended by [24]. The Savitzky-Golay technique uses a cubic polynomial to fit the data and find derivatives.

Now based on the basics of understanding the Savitzky-Golay numerical differentiation technique presented in [97], the first, second and third derivatives of the raw data are derived as follows:

$$\dot{Y}_i = \frac{(\, a_{i+3}\, Y_{i+3} \; + a_{i+2}\, Y_{i+2} + a_{i+1}\, Y_{i+1} + a_{i-1}\, Y_{i-1} + a_{i-2}\, Y_{i-2} + a_{i-3} Y_{i-3})}{c_o \Delta t} \quad \textbf{3-1}$$

$$\ddot{Y}_i = \frac{2(a_{i+3}\, Y_{i+3} \; + a_{i+2}\, Y_{i+2} + a_{i+1}\, Y_{i+1} + a_{i-1}\, Y_{i-1} + a_{i-2}\, Y_{i-2} + a_{i-3} Y_{i-3})}{c_o \Delta t^2} \quad \textbf{3-2}$$

$$\dddot{Y}_i = \frac{6(\, a_{i+3}\, Y_{i+3} \; + a_{i+2}\, Y_{i+2} + a_{i+1}\, Y_{i+1} + a_{i-1}\, Y_{i-1} + a_{i-2}\, Y_{i-2} + a_{i-3} Y_{i-3})}{c_o \Delta t^3} \quad \textbf{3-3}$$

Where;

Y_i: represents the steering wheel angle or the accelerator pedal position.

a_{i+n}: is the Savitzky-Golay filter coefficients.

C_o: is the Normalized Savitzky-Golay filter coefficient (Norm).

Δt: is the time step of the middle point at which the derivative is determined.

The Savitzky-Golay filter coefficient along with the normalized coefficient numerical values are taken from [97] and are given in Appendix A. It should be noted that filter

coefficients differ based on the derivative class and the number of data points in the moving window.

The filter coefficient values obtained from Appendix A under the 7-point window and cubic polynomial fit for the first and third derivative are substituted into equation 3-1 and equation 3-3 to determine the rate of change and the jerk profile of the steering angle or the accelerator pedal position. The rate of change and the jerk profile are determined using the following equations:

$$\dot{Y}_i = \frac{(-22Y_{i+3} + 67Y_{i+2} + 58Y_{i+1} - 58Y_{i-1} - 67Y_{i-2} + 22Y_{i-3})}{252\Delta t} \quad \textbf{3-4}$$

$$\dddot{Y}_i = \frac{(Y_{i+3} - Y_{i+2} - Y_{i+1} + Y_{i-1} + Y_{i-2} - Y_{i-3})}{\Delta t^3} \quad \textbf{3-5}$$

It should be noted that equation 3-5 has been previously used in [24] to find the jerk profile. However, after reviewing the Savitzky-Golay numerical differentiation technique presented in [97] , the jerk profile equation presented in [24] had to be modified into equation 3-5.

The steering wheel angle rate of change has been used in previous studies and commercially to discern different levels of driver alertness. The steering rate of change is highly correlated with the percentage of eyelid closure (PERCLOS) [44]. As mentioned earlier in CHAPTER 1, the PERCLOS is a method that monitors driver alertness by observing the rate of eyelid closure. The steering angle rate of change and other parameters measured through sensors are also commercially used by Mercedes Benz [31] to detect driver drowsiness. As a result, the steering angle rate of change is also studied and compared with the jerk profile.

3.1.2 Spikiness Index

The spikiness index is determined by finding the general trend of the jerk profile and then calculating the deviation of instantaneous jerk from the general trend of the jerk. It was first introduced in [14] to discern different levels of driver alertness and at the same time make the detection algorithm independent of driving conditions. The spikiness index, general trend of the jerk profile and the instantaneous jerk are presented in Figure 3-1.

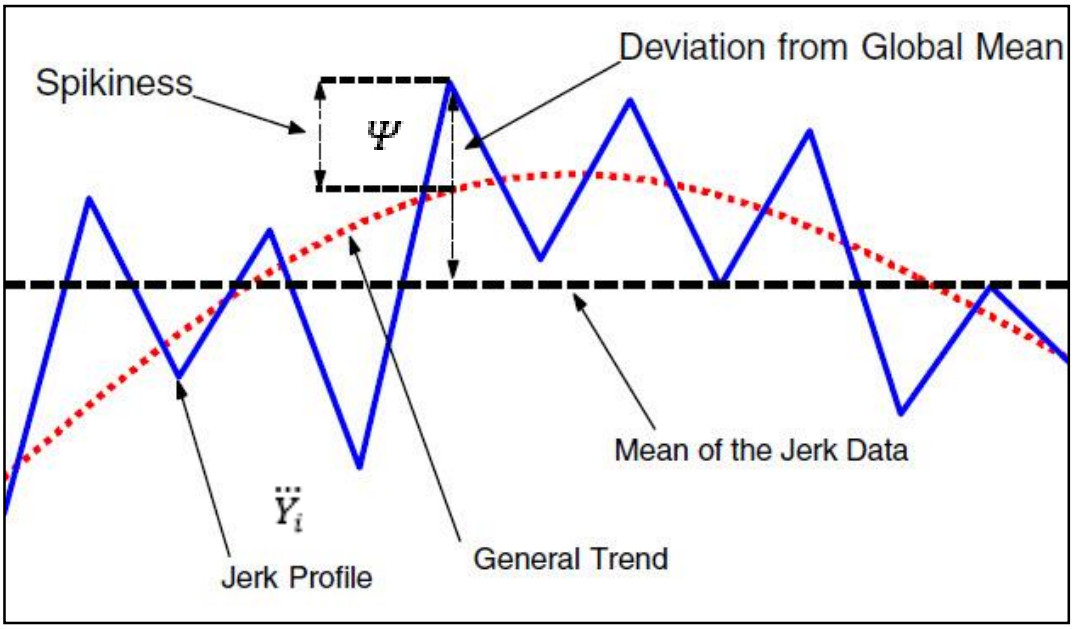

Figure 3-1 Difference between jerk profile and spikiness index [14]

The spikiness index equation presented by [14] is used to find the spikiness index of both the steering wheel angle and the accelerator pedal position as follows:

$$\Psi = \frac{\sum_{i=n_{avg}+1}^{n} \left(\dddot{Y}_i - \frac{\sum_{j=i-n_{avg}}^{i-1} \dddot{Y}_j}{n_{avg}} \right)^2}{n - n_{avg}} \qquad \textbf{3-6}$$

Where;

Ψ : is the spikiness index.

n_{avg} : is the number of data points needed for finding the general trend of the jerk.

n : is the total number of data points for the entire driving experiment.

$\ddot{Y}_i$: is the instantaneous jerk of each data point.

$\ddot{Y}_j$: is the instantaneous jerk used to calculate the general trend of the data points.

It should be noted that n_{avg} determines how close the general trend plot is to the actual jerk profile. If n_{avg} increases the plot becomes flat and eventually it will represent the mean of the jerk profile instead of representing the general trend of the data. In this study, n_{avg} is equal to the number of data points corresponding to 1.5 seconds of drive time.

In addition, the spikiness index requires a fair amount of data points to generate accurate results. As a result, the spikiness index requires a number of data points that is equivalent to at least 30 seconds of drive time to be able to detect driver inattention. It should be also noted that the spikiness index will not be suitable for the real time detection since 30 seconds of drive time is considered to be a large time frame and will generate late warnings [98].

3.1.3 Distraction Detection Indicators

The jerk profile, spikiness index as well as the rate of change of the steering wheel angle and the accelerator pedal position need to be quantified to indicate a change in the driving behaviour. The Sum Squared Error (SSE) equation suggested by [24] is employed here as shown in equation 3-7. It is used in the offline analysis for quantifying driver distraction. The SSE is evaluated for the same driving scenario and time period. The main goal is to have the same driver driving under the same conditions and use the normal driving

behaviour as a baseline and then notice how the distraction will affect the driving behaviour.

$$SSE = \sum_{K=0}^{N} (E_{K2} - E_{K1})^2 \qquad \textbf{3-7}$$

Where;

K: is the time at which the driving scenario starts and the driving profile starts building up.

N: is the time at which the driving scenario ends and the driving profile is ready for evaluation.

E_{K2} : represents a point on any driving behaviour curve (Jerk profile, spikiness index or rate of change).

E_{K1} : represents a point on the baseline driving behaviour curve (Jerk profile, spikiness index or rate of change).

The driving behaviour curve refers to the time history of the jerk profile, spikiness index or rate of change curves. First technique for distraction detection requires two driving experiments at first for the same driving maneuver and driver to find the reference value for the SSE as illustrated in Figure 3-2. After that, the SSE of any other driving experiment for the same driving maneuver and driver is determined by replacing the baseline driving reference #2 curve with the driving behaviour curve of any driving experiment while keeping the same baseline driving reference #1 curve. The new SSE value is compared with the reference SSE value and distraction will be detected if the driver is distracted.

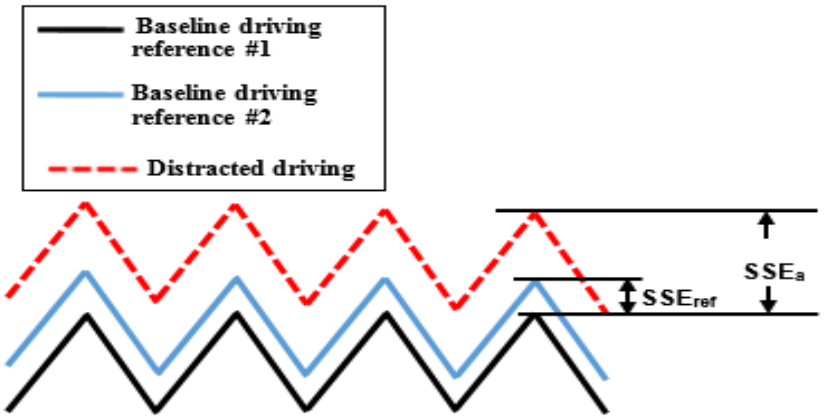

Figure 3-2 First technique for finding the reference SSE

The second technique for distraction detection requires one driving experiment to find the reference value for the SSE as illustrated in Figure 3-3 . After that, the SSE of any other driving experiment for the same driving maneuver and driver is determined by replacing the baseline driving reference #1 curve with the driving behaviour curve of any driving experiment while keeping the same zero line as a reference ($E_{K1} = 0$). The new SSE value is compared with the reference SSE value and distraction will be detected if the driver is distracted.

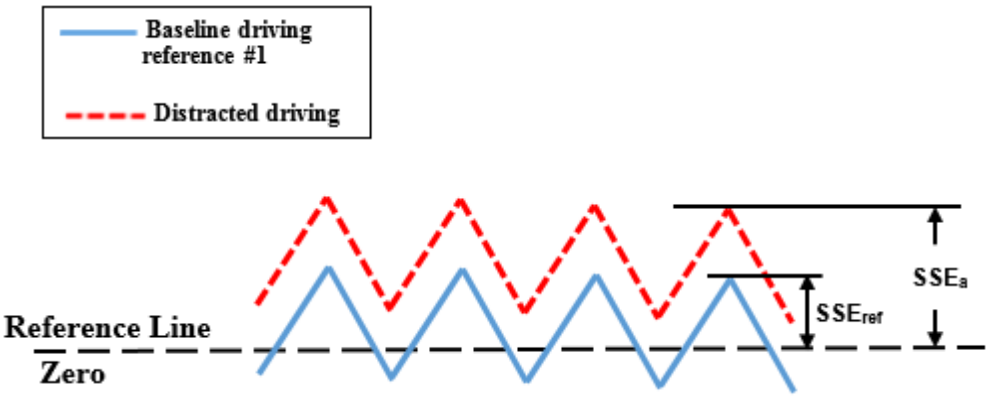

Figure 3-3 Second technique for finding the reference SSE

In a study by [24], the SSE was used to detect driver drowsiness during a 24 h driving experiments. Drivers were asked to drive for 20 minutes each hour and the SSE value was

determined for each driving experiment where the SSE of the last experiment was used as the reference. After that, the SSE of each driving experiment was divided by the maximum SSE to determine alertness level over time. The maximum SSE was considered as the worst case of drowsiness.

Although dividing the SSE of each driving experiment by the SSE of the worst case scenario shows gradual reduction of the alertness level, the warning system will not be able to function without having the worst case scenario as a reference or it will generate a late warning. As a result, this thesis suggests using the SSE of the first driving experiment as the baseline. This way the alert system will be able to issue a warning whenever the driver is outside of the baseline range. This approach also provides different alertness levels where a lower alertness level will indicate a higher deviation from the baseline. This new approach is suitable for distraction detection where the warning system cannot wait for the worst case of distraction and the warning should be issued instantly when needed. This improved approach is summarized as follows:

$$DI = \frac{SSE_a}{SSE_{ref}} \qquad \textbf{3-8}$$

Where;

DI: is referred to as the distraction indicator.

SSE_{ref} : is the reference sum squared error of the non-distracted driving experiment.

SSE_a : is the sum squared error of any driving experiment.

It should be noted that equations 3-7 and 3-8 are used with the jerk profile, spikiness index as well as the rate of change. As result, three distraction indicators are used in this analysis:

jerk distraction indicator, spikiness index indicator and rate of change indicator. The distraction indicator (DI) for a non-distracted driver takes a value of 1 or less while the DI for a distracted driver takes a value higher than 1.

The offline distraction detection method is vital to the development of a real driver distraction alert system. The offline analysis led to important findings that helped in shaping the design of the real time driver distraction alert system as will be discussed in the following section. The flow chart of the offline distraction detection algorithm implemented in MATLAB is shown in Figure 3-4. The steering angle and accelerator pedal position data are first collected for two baseline and one distracted driving experiments.

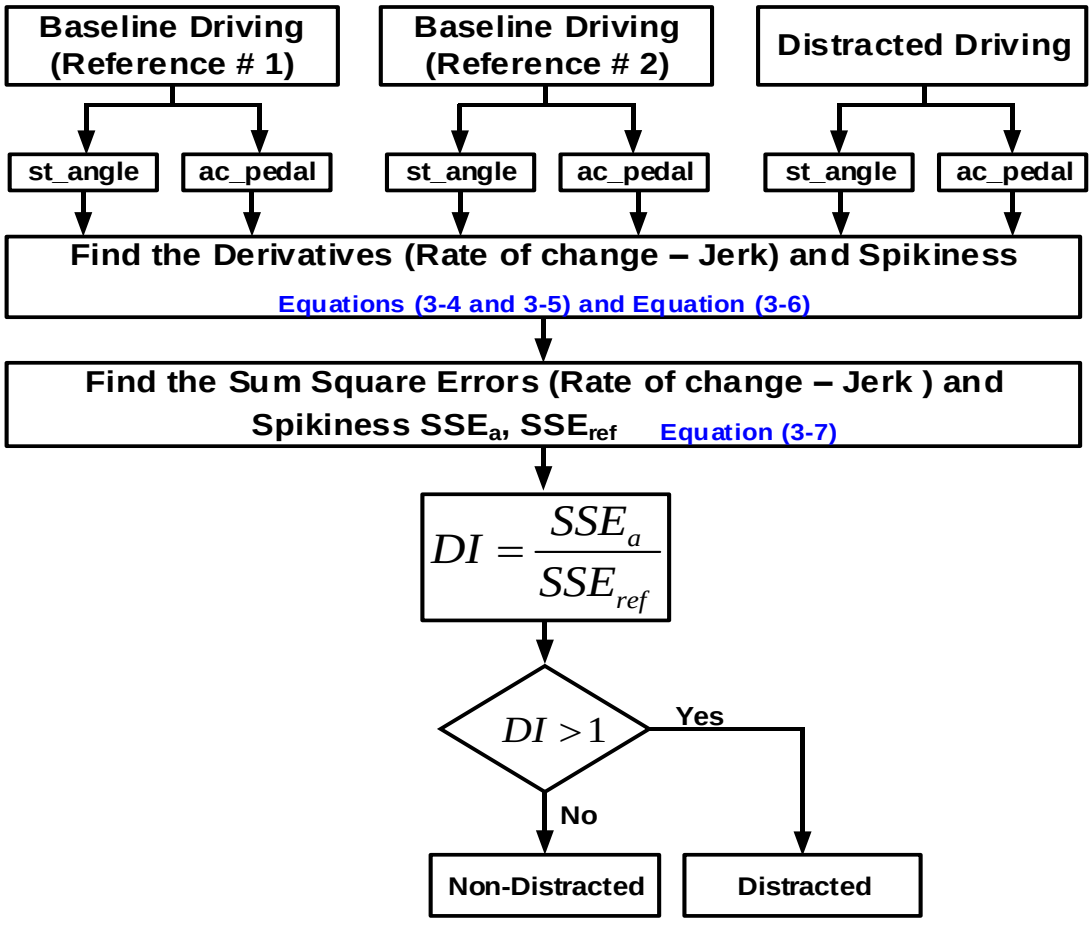

Figure 3-4 Flow chart of the offline distraction detection algorithm (MATLAB)

After that, the first and third time derivative of the steering angle and accelerator pedal are calculated to find the rate of change and jerk profile, respectively. The spikiness index is then determined from the jerk profile. The sum squared error of the rate of change, jerk profile and spikiness index is determined using the first and second SSE techniques discussed previously. The distraction indicator is determined by dividing the SSE of a distracted driving experiment to the SSE of baseline driving experiments. As a result, if the distraction indicator is higher than 1 then the driver is considered to be distracted.

3.2 REAL TIME DISTRACTION DETECTION METHODS

In order to apply the theoretical concepts discussed previously to real time simulations a set of decisions are made based on the findings of the offline analysis. First, the accelerator pedal position is excluded from the real time analysis since it did not show a significant variation that could be indicative of driver distraction. Second, the spikiness index is also excluded from the real time analysis since it requires at least 30 seconds of drive time to generate one data point and it does not issue an instant warning. Third, the steering rate will only be used in real time since the steering jerk profile and the steering rate indicate driver distraction at the same instant in time.

In addition, the steering rate of change presented previously in equation 3-4 is modified to the steering rate algorithm shown below.

$$S_{r_i} = \frac{S_{w_i} - S_{w_{i-1}}}{\Delta t} \qquad \textbf{3-9}$$

Where;

Sr_i : is the steering rate for a specific point (i) in time.

Sw_i : is the steering angle for a specific point (i) in time.

Sw_{i-1} : is the steering angle for the point preceding point (i) in time.

Δt: is the time difference between points (i) and (i-1).

Equation 3-4 is modified to accommodate the requirements of the real time application. It requires at least 7 data points to find the steering rate of the middle point which in turn requires the data to be stored over a period of time to be able to generate a steering rate profile. This process takes a longer period of time and it affects the efficiency of the driver distraction warning system since it would generate late warnings. In addition, the Savitzky-Golay numerical differentiation implemented in the offline analysis uses a 7-point moving window in order to preserve the characteristics of the raw data. This is needed when finding the third derivative since a higher derivative will significantly affect the characteristics of the raw data while the first derivative will not affect the characteristics of the raw data significantly. However, equation 3-9 only requires two data points to find the steering rate instantly and does not demand storing data over a period of time which makes it suitable for real time applications.

The real time analysis is performed directly in the simulator using the List Programming (LISP) language. The steering rate and the real time distraction detection algorithm is added to the simulator through the LISP programming language library. The LISP language was first introduced by John McCarthy in 1958 to check for the correctness of programs. The LISP was developed shortly after the development of the FORTRAN programming language. It has been widely used for its simplicity, ability to generate different data structures in real time and uniformity of syntax. The LISP programming has been applied to Artificial Intelligence (AI), robotics as well as automatic programming applications [99, 100].

The real time approach monitors the driving behaviour during the same driving experiment while the offline analysis compares different driving experiments using the same route and driving time in each experiment where the driving behaviour is the only variable. The offline analysis requires using the same conditions for each driving experiment to make sure that the steering rate is indicative of driver distraction and the variation in the steering rate is only caused by the distraction.

The real time general approach utilizes the first few minutes of driving to build a baseline of the driver's non-distracted state. The baseline is generated by establishing a range of steering rates for the non-distracted driving behaviour based on the maximum and minimum values of the steering rate signal as illustrated in Figure 3-5.

The sum squared error (SSE) requires comparing the steering rate error for the same period of time. For example, if the baseline period is five minutes then the comparison can only be made for the five minutes following the baseline period. In addition, the SSE of the steering rate for the real time application should be compared over a small period of time of 1-2 seconds. The steering rate SSE obtained from the baseline period is not sufficient to detect different driving behaviour since 2 seconds of the SSE is considered as a small time frame and the SSE requires more data points to generate accurate results. As a result, the SSE method could not be implemented and the amplitude of the steering rate signal is used instead. It should be noted that the amplitude of the lateral acceleration has been used in a previous study to detect driver distraction where sudden steering corrections resulted in high spikes in the amplitude of the lateral acceleration [101].

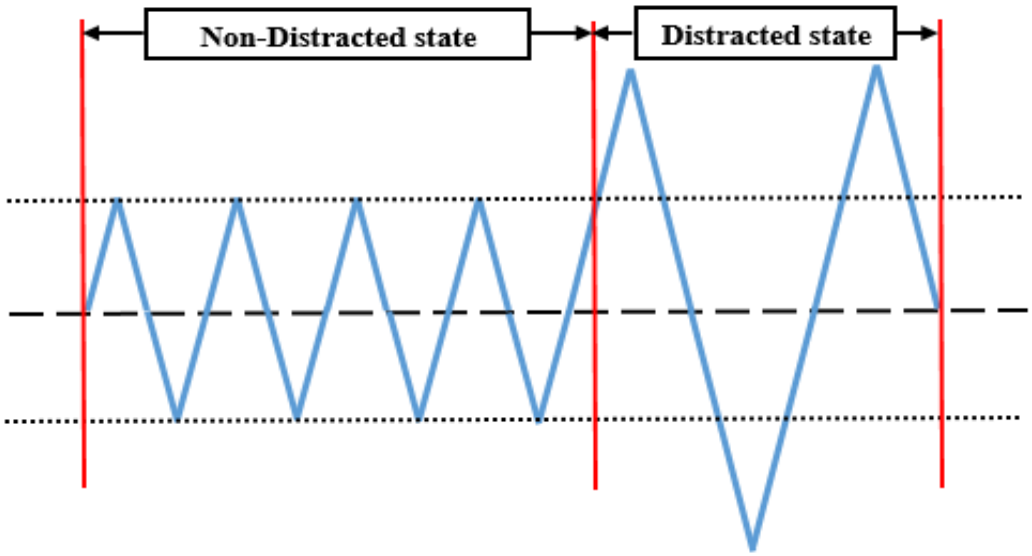

Figure 3-5 Real time distraction detection general approach

3.2.1 First Distraction Detection Method

The first distraction detection method builds a steering rate profile during a driving experiment in which the driver is not subjected to any source of distraction. The driver was first asked to drive the simulator for multiple times to get familiar with the simulator environment until a consistent steering rate profile was obtained. A range for the steering rate of a non-distracted driver is determined based on the maximum and minimum values of the steering rate obtained during the driving experiment. The absolute values of the maximum and minimum steering rate are compared. After that, the highest steering rate value between the two is used as a threshold value. The threshold value has to be multiplied by an allowance factor as illustrated in Figure 3-6 since the driver already reached that value during the non-distraction driving experiment. This method of detection uses a single threshold value to issue a warning signal. The single threshold value is determined through a set of driving experiments for drivers in their non-distracted driving state. The driving experiments are analyzed offline to find the final threshold value which will be added to

the simulator through programming. It should be noted that the threshold range concept has been used in previous studies to detect the inattentive driving behaviour [90, 101].

The final threshold value presented in equation 3-10 is determined by finding the maximum absolute value of the steering rate and then multiplying this value by the allowance factor.

$$T = F_a S_{max} \quad \textbf{3-10}$$

Where;

T: is the final threshold value of the steering rate for the non-distracted driving behaviour.

S_{max}: is the maximum absolute value of the steering rate for the non-distracted driving behaviour.

F_a: is the allowance factor used to amplify the maximum absolute value of the steering rate.

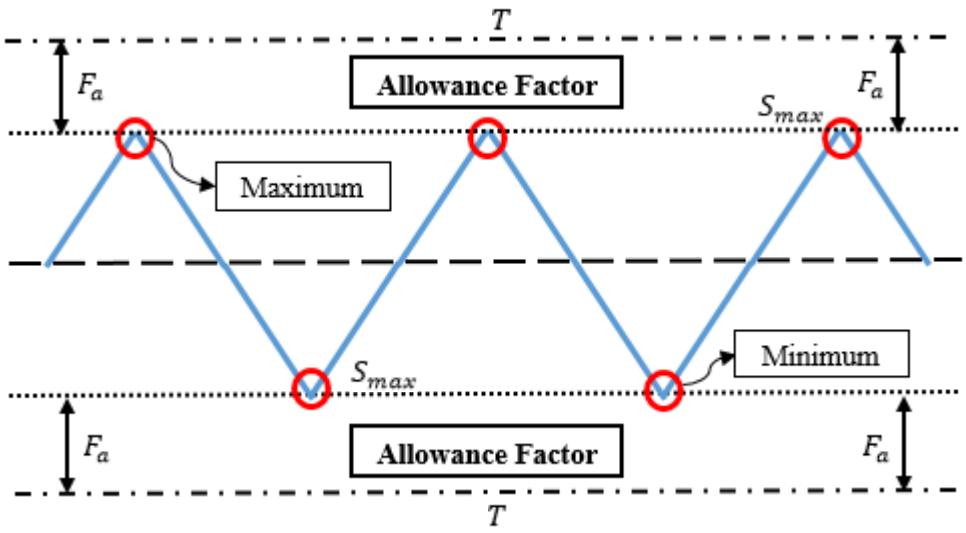

Figure 3-6 First real time distraction detection method

It should be noted that the allowance factor is determined through several driving experiments to obtain the optimum allowance factor. In addition, the final threshold value

takes a positive and negative sign in the programming environment to make sure that the threshold applies to both the right and left steering movements.

The advantage of the first real time distraction detection method is that distraction can be detected without requiring a baseline driving period in the beginning of each driving experiment. This can be achieved by having a threshold value that is determined through several driving experiments and is suitable for different driving styles. However, this threshold value may vary for different vehicle configurations.

3.2.2 Second Distraction Detection Method

The second distraction detection method monitors the driver behaviour during the first few minutes of driving and builds a baseline in real time. It should be noted that the baseline concept has been implemented in previous studies to build a driving pattern for the alert driving state [31, 68, 85]. The second method uses the same technique implemented in the first detection method where the maximum and minimum steering rate is determined during the baseline period and then the highest absolute value of the steering rate is multiplied by the allowance factor. However, the second method does not require any previous knowledge of the driver and the baseline is built in real time while the first method requires offline analysis of driving experiments to determine the final threshold value. In addition, the simulator steering rate algorithm presented in equation 3-9 and the final threshold value shown in equation 3-10 are added to the driving simulator through programming where all calculations are done in real time and no offline analysis is required. It should be noted that the allowance factor of the second method will have a constant value in equation 3-10 which is determined based on the driving experiments of the first method. The experiments of the first method give an idea of the appropriate allowance factor that can reduce false

warnings. The second method is able to detect distraction whenever the baseline period is over, so if the driver steering rate starts to stray outside the final threshold range a warning signal is issued as illustrated in Figure 3-7.

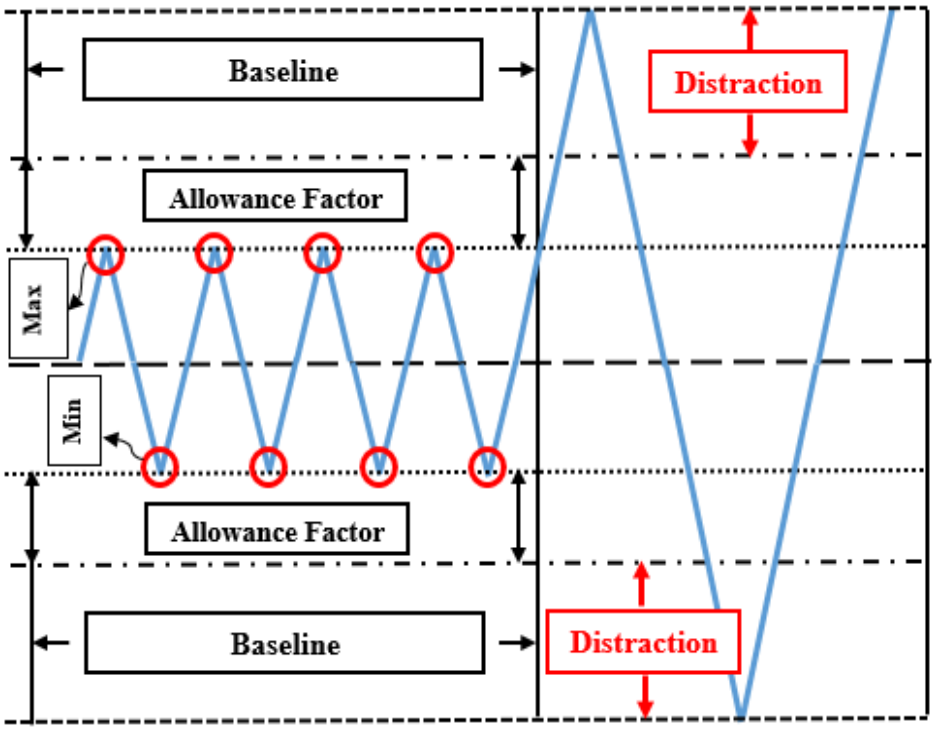

Figure 3-7 Second real time distraction detection method

The advantage of the second real time detection method is that it can generate a final threshold value automatically in real time. However, the second method requires a perfect baseline to detect distraction effectively. This system is intended for long journeys in monotonous environments (highway infrastructure) where drivers are more susceptible to distraction [102]. The flow chart of the real time distraction detection algorithm implemented in List Programming (LISP) language is shown in Figure 3-8. The steering rate is determined in real time from the steering angle and time step using equation 3-9. The maximum absolute steering rate is recorded for the first five minutes of the simulation time to build a baseline. The simulator displays a message on the screen and notifies the

driver whenever the baseline is ready. The final steering rate threshold range for the baseline is determined by multiplying the maximum absolute steering rate by an allowance factor as illustrated in equation 3-10. The simulator continues to calculate the steering rate in real time and issues audible and visual warning messages whenever the steering rate is exceeding the final steering rate threshold range.

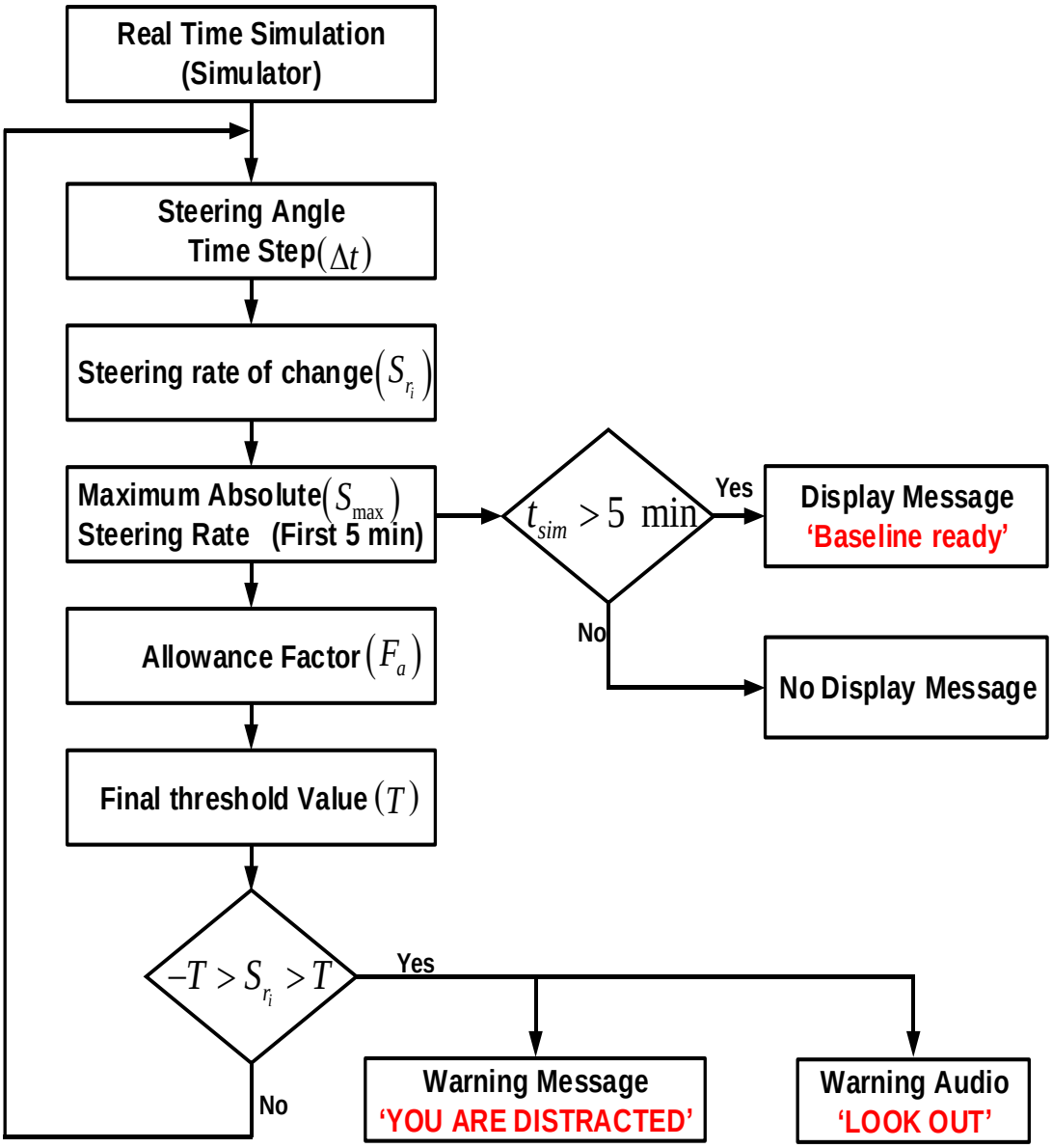

Figure 3-8 Flow chart of the real time detection algorithm (LISP)

3.3 CHAPTER SUMMARY

This chapter described the methods used for the evaluation and development of real time distraction alert system. The distraction detection methods are divided into the offline detection analysis and real time detection analysis. The offline analysis means that driving experiments are still performed in real time but distraction is detected after the driving experiment is over. The steering wheel angle and the accelerator pedal position are collected from the simulator in Excel sheets. After that, MATLAB is used to calculate the jerk profile, rate of change and spikiness index of both the steering angle and accelerator pedal position. The analysis requires baseline driving experiments (non-distracted) and distraction driving experiments. The sum squared error of the jerk profile, rate of change and spikiness index of different driving experiments are used as distraction indicators. The main goal of the offline analysis is to determine the most suitable indicator for detecting distraction in real time. The real time analysis means that distraction is detected in real time while driving. The steering rate is chosen for the real time analysis since a high correlation is found between steering input and driver distraction. The real time detection methods are divided into methods. The first method uses a single steering rate threshold range determined from baseline driving experiments. However, the second method monitors the first few minutes of driving and builds a steering rate threshold range in real time. The steering rate and the real time distraction detection algorithms are added to the truck driving simulator through the LISP programming library.

CHAPTER 4

OFFLINE DETECTION OF DRIVER DISTRACTION

4.1 INTRODUCTION

This chapter presents the results for the offline detection of driver distraction. The offline detection means that the driving experiments are still done in real time but the distraction detection is done offline. The main goal of the offline analysis is to determine which driver inputs (steering wheel, accelerator pedal) are affected by driver distraction.

The jerk profile, rate of change profile as well as the spikiness index distraction indicators are used to study the effects that distraction may have on the steering wheel angle and the accelerator pedal position. The jerk profile, rate of change profile and the spikiness index of both the steering wheel angle and accelerator pedal position are compared to determine the most suitable indicator for the real time application. Additionally, the effects that driver distraction may have on the accelerator pedal position are compared with previous studies that used the pedal to detect different levels of alertness.

The results of the offline detection are determined through baseline (non-distracted) and distraction driving experiments. The driver in the distraction driving experiments is subjected to different sources of distraction to ensure that the system can detect any kind of driver distraction. The baseline driving experiments are needed to build a pattern of the non-distracted driving behaviour and show the transition of the driver state. This chapter concludes with a set of recommendations that will help in the development of the real time driver distraction alert system.

4.2 DATA COLLECTION FROM DRIVING SIMULATOR

4.2.1 Experimental Procedure

Several driving experiments are performed on the Virage VS600M motion base truck driving simulator. The experiments are carried out using a fully loaded tractor semitrailer vehicle configuration and a highway scenario shown in Figure 4-1.

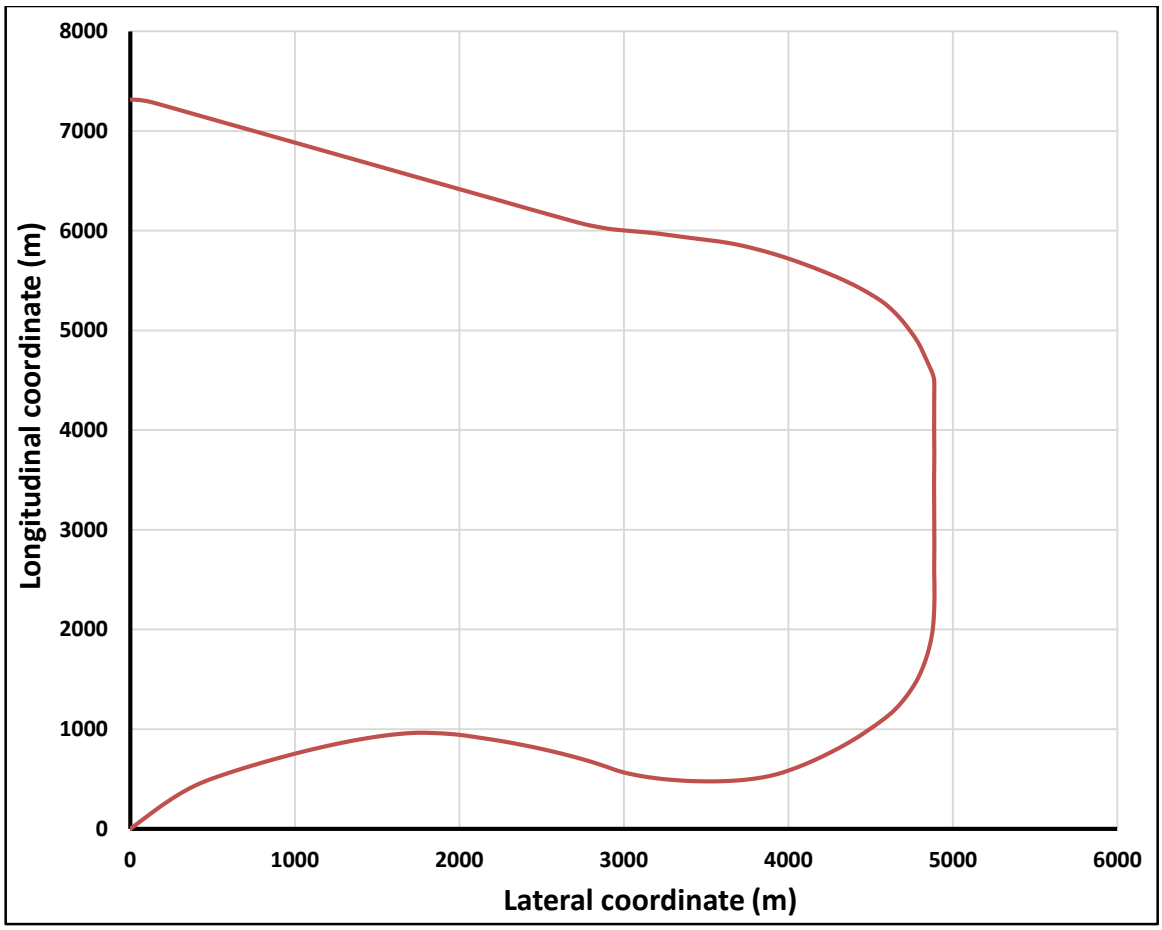

Figure 4-1 Highway scenario path coordinates used for offline driving experiments

The sources of distraction presented in [19, 103] are used in this research as shown in Figure 4-2: (a) Texting on a mobile phone, (b) reading emails, (c) checking maps (GPS), (d) talking to other occupants, (e) making a phone call, (f) picking up an object, (g) eating, (h) Adjusting radio channels.

(a) Texting on a mobile phone

(b) Reading emails while driving

(c) Checking maps (GPS)

(d) Talking to other occupants

(e) Making a phone call

(f) Picking up an object

(g) Eating while driving

(h) Adjusting radio channels

Figure 4-2 Offline distraction driving experiments performed on the simulator

The main purpose of presenting the distraction driving experiments shown in Figure 4-2 is to provide a visualization of the experimental procedure and show the reader how the aforementioned sources of distraction are actually performed on the simulator. The main purpose of the offline experiments is to evaluate the sum squared error of the jerk profile, spikiness index and the rate of change of both the steering wheel angle and the accelerator pedal position and choose the most suitable distraction indicator for the real time detection application. The conclusions of the offline driving experiments led to the development of the real time distraction detection system. The offline experiments are presented in Table 4-1. Five driving experiments are required to make sure that the baseline driving results are similar. This means that a non-distracted driver must have the same driving profile since all the other conditions are constant and the only variable is the driving behaviour. It should be noted that the traffic in each scenario is generated randomly

Table 4-1 Driving experiments needed for the offline analysis

Experiment Number	Description	Duration (minutes)
-	Five trials of baseline driving	5
1	Texting on a mobile phone while driving	
2	Reading emails while driving	
3	Checking maps (GPS) while driving	
4	Talking to other occupants while driving	
5	Making a phone call while driving	
6	Picking up an object while driving	
7	Eating while driving	
8	Adjusting radio channels while driving	

Experiments with different sources of distraction are needed to confirm that the distraction detection method is valid for all distraction sources. Driving experiments of five minutes are sufficient for the offline analysis since the main goal is to compare different files for the same period of time to determine the deviation that distraction may cause. Additionally, driver distraction can occur in seconds once drivers takes their eyes off the road [104]. Consequently, five minutes of driving while being distracted is sufficient for comparison.

4.2.2 Raw Data Recording

The steering wheel angle, accelerator pedal position and the time step datasets are collected from the simulator for the purposes of the offline analysis. The data collection from the simulator is done by editing any scenario from the library using the NotePad++ tool and then adding the data collection script to that scenario.

Two scripts for the same scenario were investigated. The first script encompassed the collecting data block whereas the second script encompassed the scenario script without the data collection block. After that, WinMerge tool has been used to compare the two scripts. This tool places each file either to the left or right of the screen and highlights the different parts of the script. The operator can then add the different parts to any scenario using the NotePad++ program and save it as a different name in order to keep the original files unmodified.

In order to check the data that will be collected from the data collection scenario, the operator has to double click on the scenario. After that, the main script and the data library shows up. The operator then has to click on the data collection block to the left side of the

library screen. By doing that, two tabs having the labels of “Normal code” and “When becomes active” will appear.

The operator can check which data will be collected by looking at the last line of script under the “Normal code” tab. The last line of the script will have the “get-steering” code template. The “get-steering code” is used to collect the steering angle. The operator can change the data collected by looking at the code templates on the upper side of the screen and then placing another template instead of “get-steering” such as “get-accelerator”.

The data is collected by running the scenario that has the data collection script and saved in an excel sheet that will be available right after stopping the scenario. Each column in this sheet represents one of the selected parameters. For example, the first column is reserved for the steering angle whereas the second column is reserved for the accelerator position. As a result, the operator has to check the last line of the script under the “When becomes active” tab to label the column for each data set collected. The labels should follow the same sequence presented in the last line of script under the “Normal code” tab.

4.2.3 Data Processing

For the offline estimation of the driver’s distraction, the raw data is collected in a Comma Separated Value (CSV) format file and converted into excel sheets to perform the necessary processing and analysis for driver’s distraction detection. The raw data of all variables is arranged in one column and each variable is separated from other variables by a semicolon. As a result, the raw data in the excel sheet is converted from text to columns and thus the raw data will have a specified column for each collected variable. After that, the total time of the simulation is calculated by adding the time steps collected from the simulator.

Furthermore, the steering angle is collected from the simulator as a ratio of the maximum steering wheel angle. The maximum steering wheel angle is 720 degrees measured from the center to the rightmost or leftmost steering wheel position. Therefore, the steering wheel angle collected from the simulator is multiplied by 720 to get the steering angle values in degrees. After that, MATLAB is used to read the processed data from excel sheets and determine the jerk profile, rate of change profile and spikiness index distraction indicators.

4.3 OFFLINE RESULTS FOR STEERING WHEEL ANGLE

4.3.1 Jerk Profile

4.3.1.1 Baseline Driving

The time history of the steering wheel jerk profile of one baseline driving experiment is shown in Figure 4-3. The driving experiment lasted for 5 minutes and the driver was not subjected to any source of distraction. It can be observed that the steering jerk profile is within the range of 2500 deg/s^3. Four additional baseline driving experiments are required to confirm that the steering jerk profile is consistent over several baseline driving experiments as shown in Figure 4-4. The steering jerk profile of the five baseline experiments is still within the same range. As a result, any steering jerk profile that exceeds this range corresponds to a distracted driver. Driving experiments of five minutes are sufficient for the offline analysis since the main goal is to compare different files for the same period of time to determine the deviation that distraction may cause. Additionally, driver distraction can occur in seconds once drivers takes their eyes off the road [104]. Consequently, five minutes of baseline driving and distracted driving are sufficient for

comparison. It should be noted that the small amplitude jerk spikes within the baseline range correspond to road curvature and normal steering profile behaviour such as changing lanes and reacting to traffic and environmental conditions.

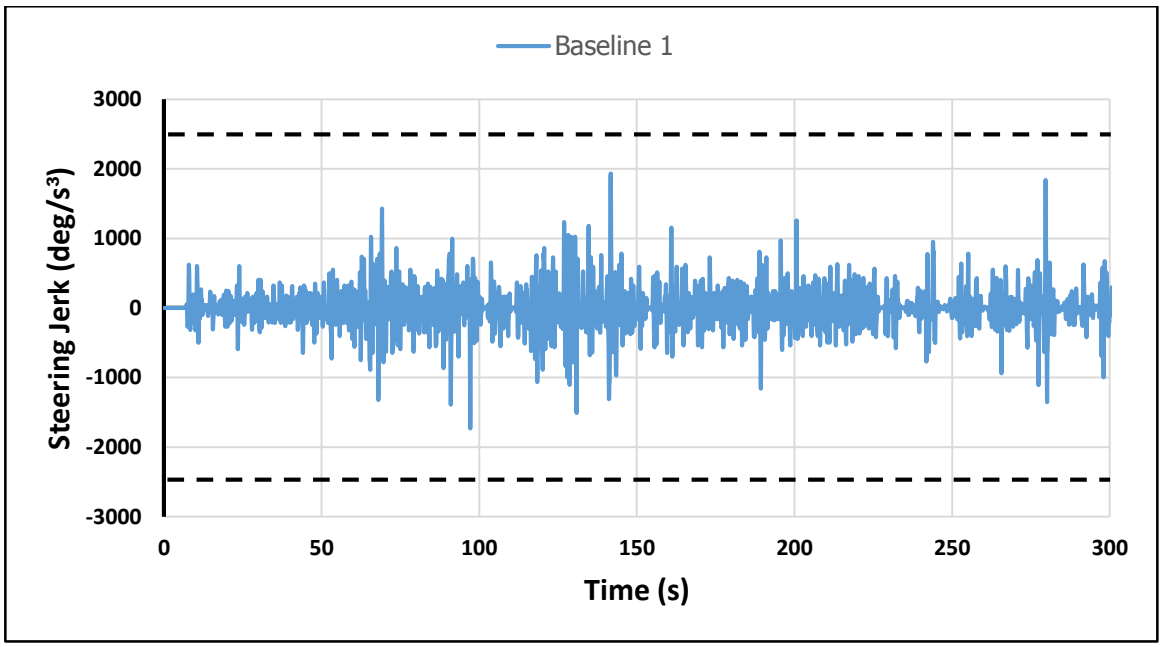

Figure 4-3 Steering jerk profile for a baseline driving experiment

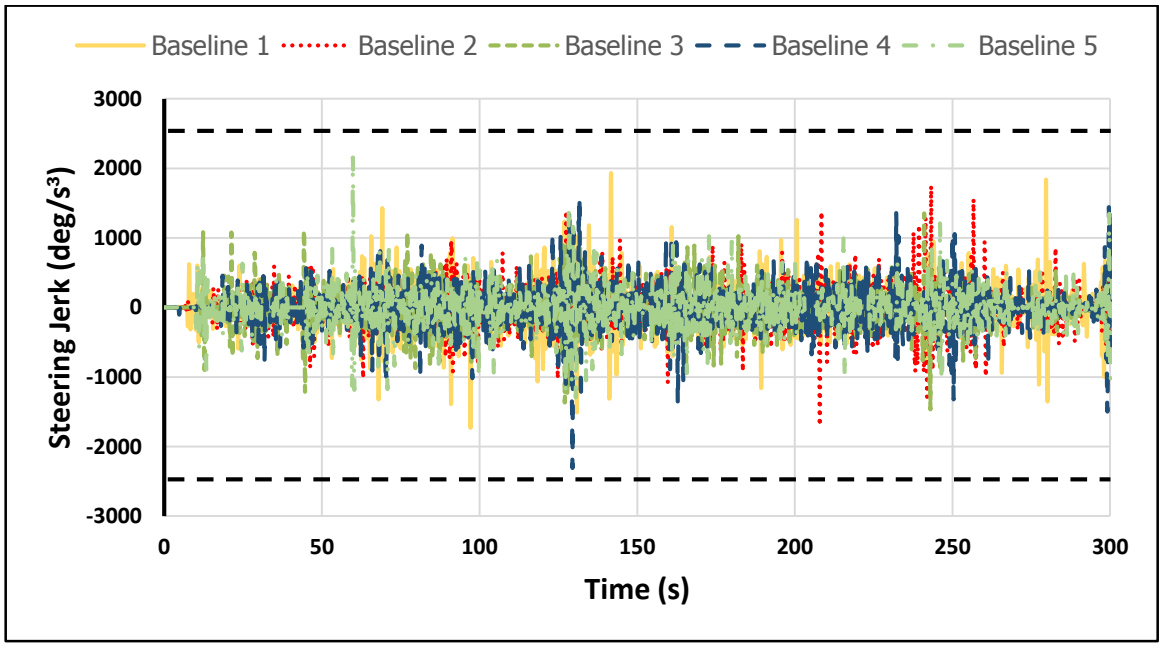

Figure 4-4 Steering jerk profile for baseline driving experiments

4.3.1.2 Distracted Driving

The time history of the steering wheel jerk profile of driving experiments with several sources of distraction is compared with one baseline driving experiment as shown in Figure 4-5. The jerk profile for all driving experiments is determined using equation 3-5. The driving experiment in which the driver is required to send text messages while driving results in steering jerk spikes of 5000 deg/s^3 as observed in Figure 4-5 (a). However, a steering jerk spike of over 4000 deg/s^3 is obtained from reading emails while driving as noticed in Figure 4-5 (b). The steering jerk spikes of a driver checking maps while driving for example lasts only for few seconds as shown in Figure 4-5 (c). This means that driver distraction can occur in seconds as discussed in [104]. The steering jerk profile of a driver talking to other vehicle occupants and a driver making a phone call are presented in Figure 4-5 (d) and (e), respectively. The steering jerk profile of a driver picking up an object while driving results in more frequent jerk spikes exceeding 6000 deg/s^3 as seen in Figure 4-5 (f). The frequent jerk spikes could be attributed to the driver not only taking their eyes off the road but also doing a physical activity that could affect the steering wheel significantly. This also applies to a driver eating while driving where a spikes will be detected frequently as shown in Figure 4-5 (g). The steering jerk profile of a driving experiment in which the driver is adjusting radio channels, results in a less frequent but high jerk spike of 11000 deg/s^3. This could be attributed to the fact that the driver does not adjust radio channels often. However, adjusting radio channels takes the driver attention since the driver has to look on a smaller screen to see the channel number. In conclusion, all distraction driving experiments result in jerk spikes that exceed the jerk profile of baseline driving experiments. As a result, the steering wheel jerk profile is indicative of driver distraction.

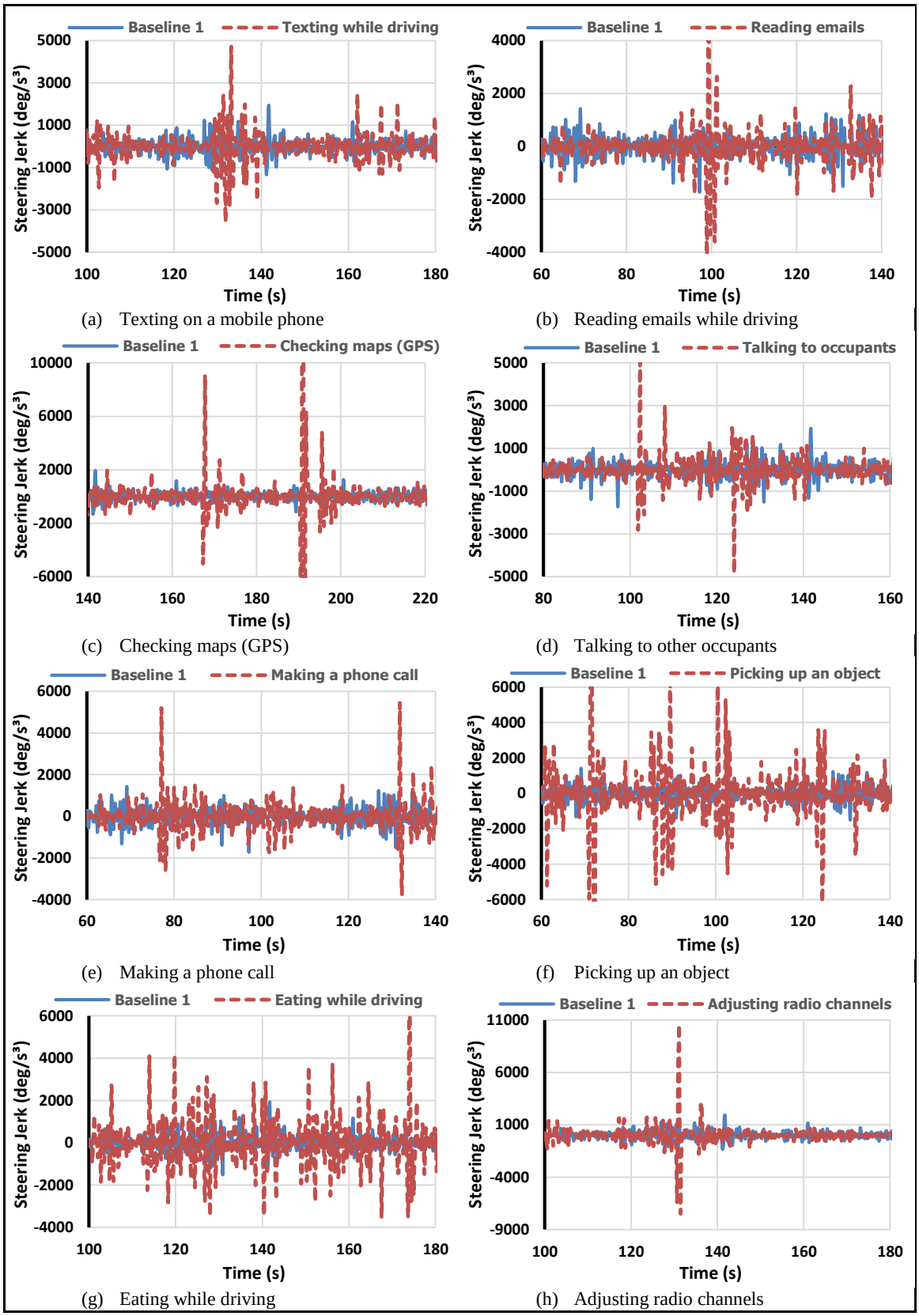

Figure 4-5 Steering jerk profile for distraction driving experiments

4.3.1.3 Distraction Indicators

The sum squared error described in equation 3-7 is used to quantify the difference between the steering jerk profiles of baseline and distraction driving experiments. The sum squared error is normalized using equation 3-8 to find the steering jerk distraction indicators. The steering jerk distraction indicator determined from the first and second sum squared error (SSE) methods is shown in Figure 4-6 (a) and (b), respectively. Simulation numbers of 1-4 in Figure 4-6 (a) represent baseline driving while numbers of 5-12 represent driving with different sources of distraction. However, simulation numbers of 1-5 in Figure 4-6 (b) represent baseline driving and numbers of 6-13 represent distraction. It should be noted that the total number of driving experiments (simulations) is 13; where 5 of which represent baseline driving experiments while the other 8 represent distraction. Nonetheless, Figure 4-6 (a) shows only 12 simulation numbers since the first SSE technique requires two driving experiments at first for the same driving maneuver and driver to find the reference SSE. The reference SSE for the first SSE technique is referred to as the encircled simulation number (1) shown in Figure 4-6 (a).

The baseline driving experiments have distraction indicator values of 1 since the sum squared error of any baseline driving experiment should be consistent and will have the same sum squared error as the reference SSE. In contrast, the sum squared error of a distraction driving experiment will result in higher sum squared error values than the reference SSE and will have distraction indicator values greater than 1. For example, a driver that sends text messages while driving has a 3 times greater sum squared error value than the reference SSE as indicated in Figure 4-6 (a). Furthermore, driving experiments

with picking up an object and checking maps (GPS) as sources of distraction result in distraction indicator values of 15.3 and 15, respectively.

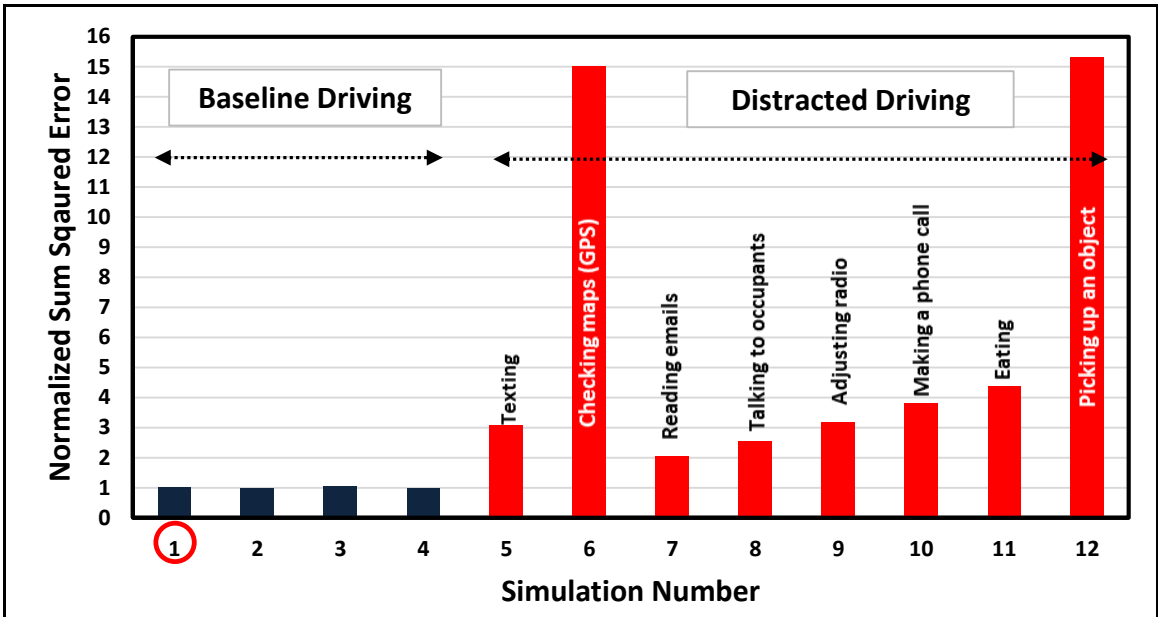

(a) Steering Jerk distraction indicator (first SSE)

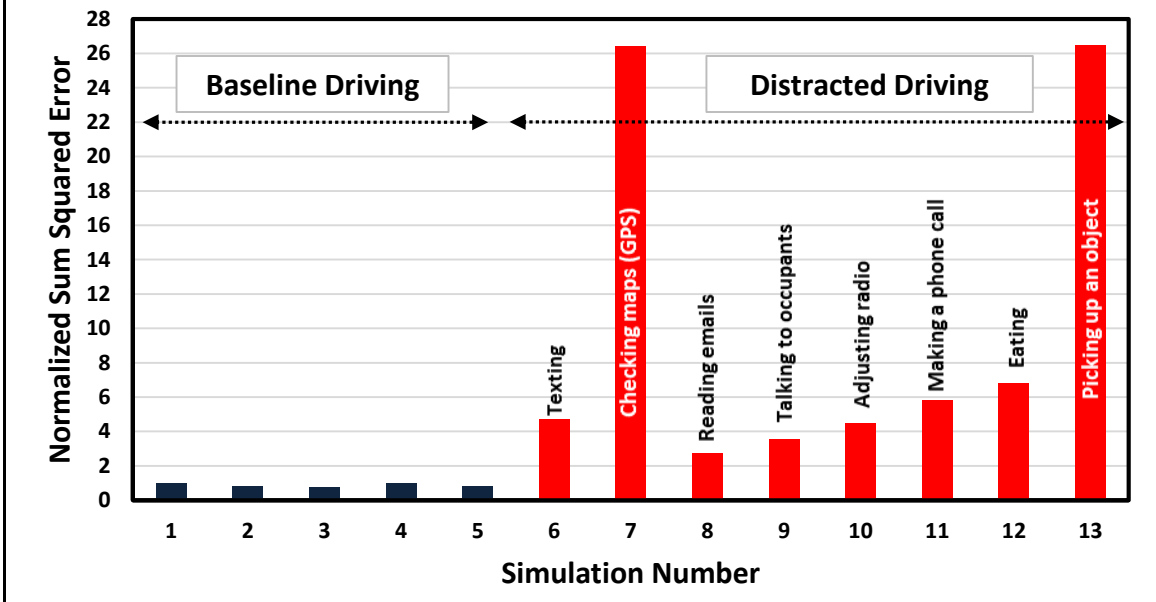

(b) Steering Jerk distraction indicator (second SSE)

Figure 4-6 Steering jerk profile distraction indicator

This could be attributed to the fact that checking maps and picking up an object force the driver to not only taking their eyes off the road but also doing a physical activity that could affect the steering wheel significantly. The distraction indicators determined using the second SSE technique result in greater distraction indicator value compared to that of the first SSE technique as demonstrated in Figure 4-6 (b). For example, a driver picking up an object or checking maps (GPS) while driving have distraction indicator values of 26.5 and 26.4, respectively. This is due to the fact that the second SSE technique uses the zero line of a curve to determine the reference SSE instead of comparing two curves. The main purpose of using the first SSE technique is to ensure that the time history of the steering jerk profile curve is consistent and the only variable is the driving behaviour. However, the second SSE technique is used to determine if the amplitude of the steering rate or jerk profile is sufficient for detecting driver distraction.

4.3.2 Rate of Change Profile

4.3.2.1 Baseline Driving

The time history of the steering rate profile of a baseline driving experiment is shown in Figure 4-7. It can be observed that the steering rate profile is within a range of 30 deg/s. This also applies to four additional baseline driving experiments as observed in Figure 4-8. This means that a consistent steering rate profile can be obtained for a non-distracted driver. As a result, a steering rate profile that exceeds this steering rate range corresponds to driver distraction. This conclusion is confirmed by the driver distraction identification method presented in [101]. This study concluded that sudden steering corrections induced by driver

distraction result in momentary high amplitude spikes in the lateral acceleration as seen in Figure 4-9.

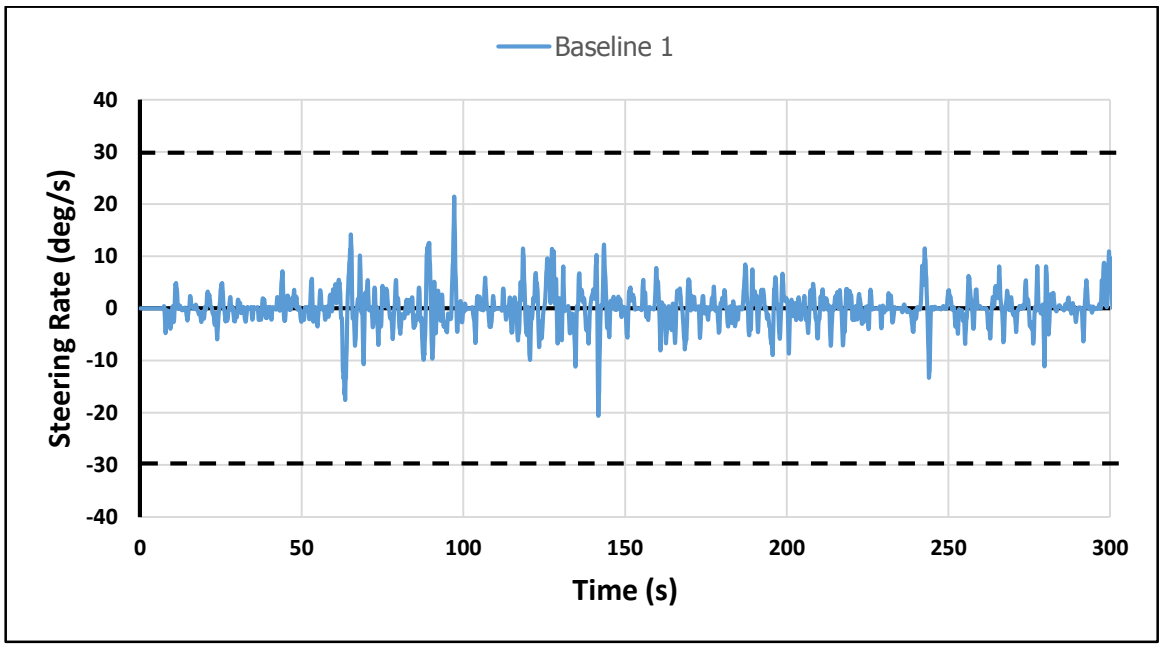

Figure 4-7 Offline Steering rate profile for a baseline driving experiment

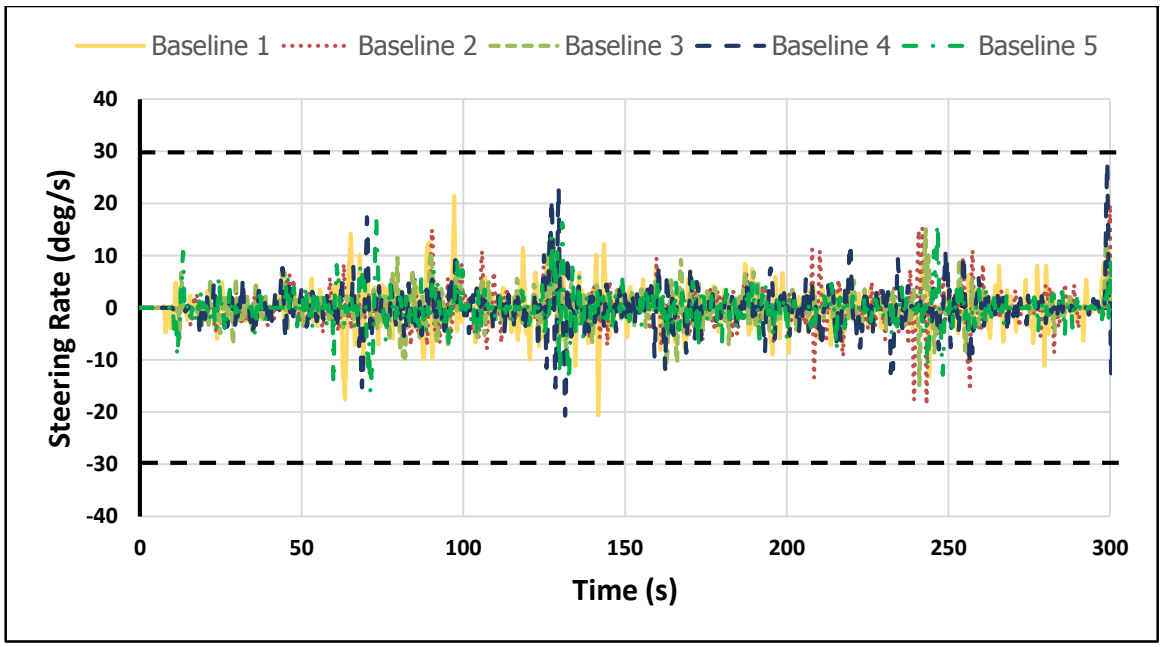

Figure 4-8 Offline Steering rate profile for baseline driving experiments

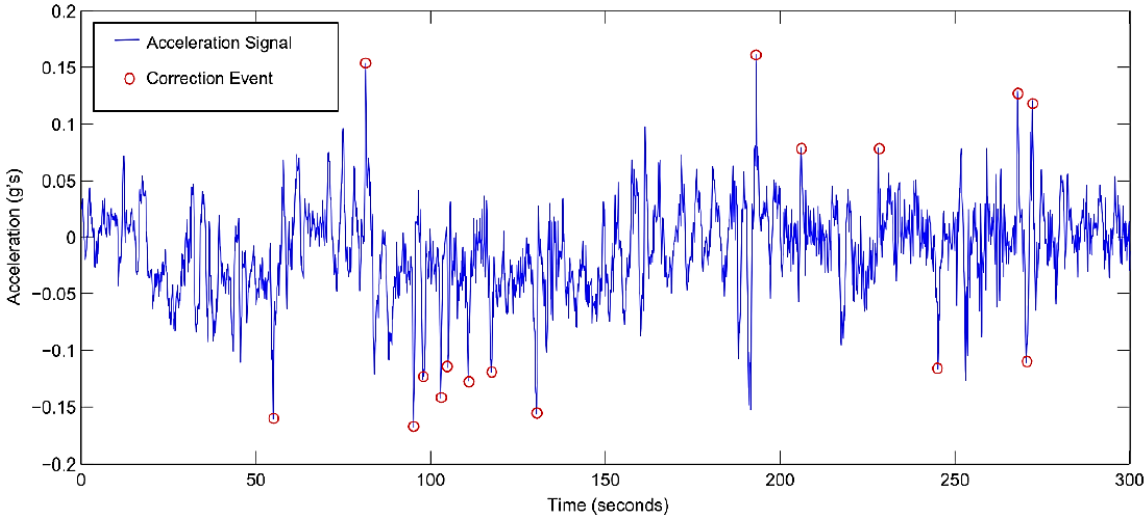

Figure 4-9 Lateral acceleration profile for a distracted driver [101]

4.3.2.2 Distracted Driving

The time history of the steering rate profile of driving experiments in which the driver is subjected to different sources of distraction is displayed in Figure 4-10: (a) Texting on a mobile phone, (b) reading emails, (c) checking maps (GPS), (d) talking to other occupants, (e) making a phone call, (f) picking up an object, (g) eating, (h) Adjusting radio channels. It is evident that the steering rate profile of all distraction driving experiments exceed the baseline steering range of 30 deg/s. Consequently, the steering rate profile is indicative of driver distraction. The steering rate for the offline analysis is determined using the Savitzky-Golay numerical differentiation method as presented in equation 3-4. It should be noted that the steering jerk and rate of change profiles indicate distraction at the same instance in time. For example, the steering jerk and rate profiles of a driver checking maps while driving indicate driver distraction after 160 and 190 seconds of driving time as observed in Figure 4-5 (c) and Figure 4-10 (c), respectively. Therefore, both the steering wheel jerk and rate of change can equally detect driver distraction and the steering jerk or rate of change can be separately used.

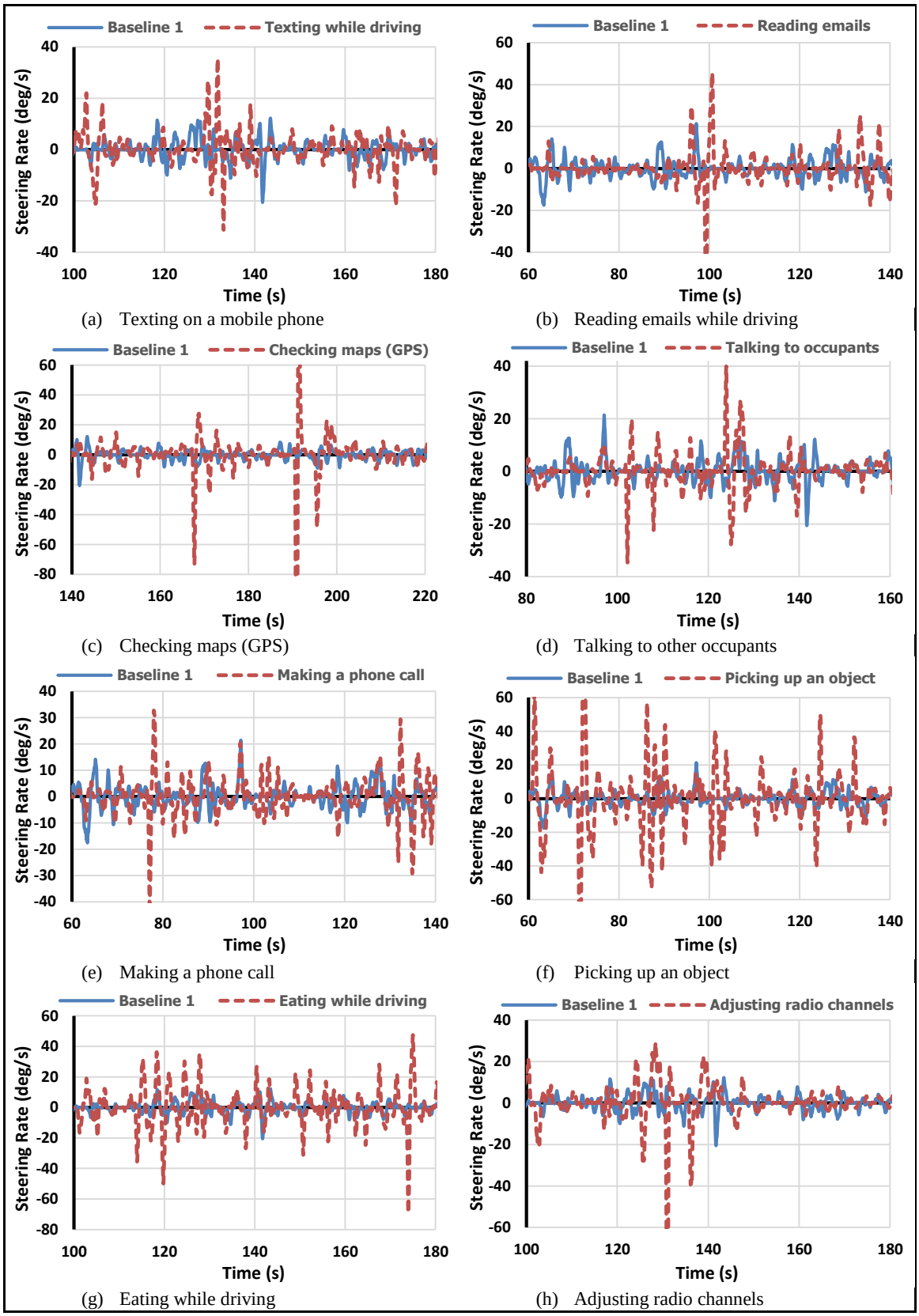

Figure 4-10 Offline Steering rate profile for distraction driving experiments

4.3.2.3 Distraction Indicators

The steering rate distraction indicators shown in Figure 4-11 are determined using the same method implemented in determining the steering jerk distraction indicators as presented in 4.3.1.3. The steering rate distraction indicators generated from the first SSE technique have values lower than distraction indicators obtained from the second SSE technique as observed in Figure 4-11 (a) and (b), respectively. For example, a driver making a phone call while driving have distraction indicator values of 3.6 and 5.4 obtained from the first and second SSE techniques, respectively. This is due to the fact that the second SSE technique uses the zero line of a curve to determine the reference SSE instead of comparing two curves. Baseline driving experiments have distraction indicator values of 1 or less as seen in simulation numbers 1-4 of Figure 4-11 (a) and simulation numbers of 1-5 of Figure 4-11 (b). This means that a non-distracted driver will have the same sum squared error as the reference SSE value. In contrast, a distracted driver will have indicators values greater than 1. For example, a driver eating while driving has a distraction indicator value of 3.7 as indicated in Figure 4-11 (a). It can be observed that the steering rate distraction indicator generates values that are similar to those obtained from the steering jerk. For example, a driver picking up an object while driving has a jerk indicator value of 15.3 and rate indicator value of 15.2 as demonstrated in Figure 4-6 (a) and Figure 4-11 (a), respectively. As a result, the steering jerk and steering rate profile can evenly detect driver distraction. However, the steering rate distraction indicator of a driver checking maps while driving has indicator value lower than that of the steering jerk indicator as observed in Figure 4-11 (a) and Figure 4-6 (a), respectively. This implies that both steering jerk and rate indicators detected distraction but the jerk had a greater amplitude spike.

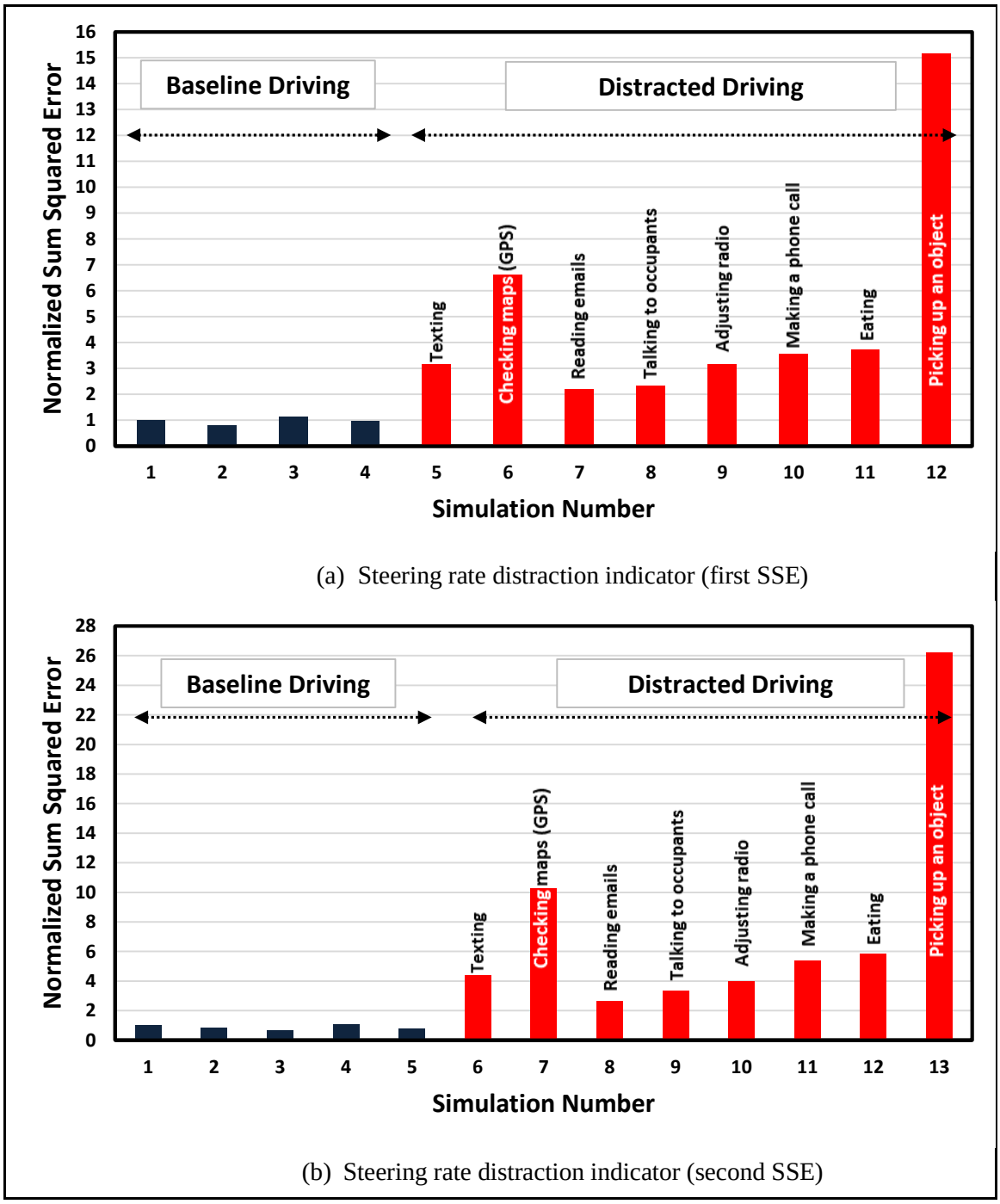

(a) Steering rate distraction indicator (first SSE)

(b) Steering rate distraction indicator (second SSE)

Figure 4-11 Steering rate profile distraction indicator

4.3.3 Spikiness Index

4.3.3.1 Baseline Driving

The steering wheel spikiness index is defined as the deviation of the instantaneous steering jerk from the general tend of the steering jerk profile. It was used in a previous study to discern different level of alertness while keeping the detection algorithm independent of environmental conditions [14]. The steering wheel spikiness index is determined using equation 3-6.

The time history of the steering wheel spikiness index for a baseline driving experiment is presented in Figure 4-12. It can be noticed that the steering wheel spikiness index is within the range of ($2.5x10^5$). In order to verify that a non-distracted driver will have a similar spikiness index over multiple driving experiments, four additional baseline driving experiments are performed as shown in Figure 4-13. The steering wheel spikiness index of all baseline driving experiments are within the same range. As a result, a driver subjected to any source of distraction will have a spikiness index above the suggested range since the spikiness index is a function of the jerk profile.

The driving experiments of the offline analysis is performed for the same driving maneuver, simulation time as well as the same driver to ensure that the deviation in the spikiness index in only caused by a degradation in the driving performance. The main goal of determining the steering wheel spikiness index is to compare it with the jerk profile and the steering rate to determine the most suitable driver distraction indicator for the real time application.

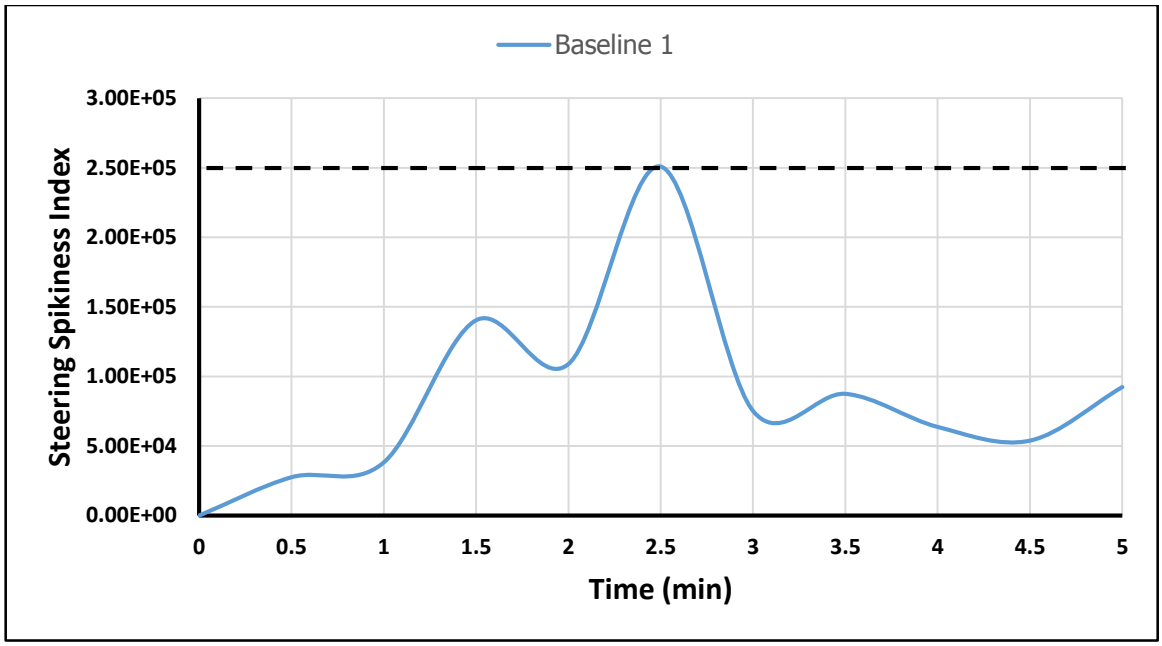

Figure 4-12 Steering spikiness index for a baseline driving experiment

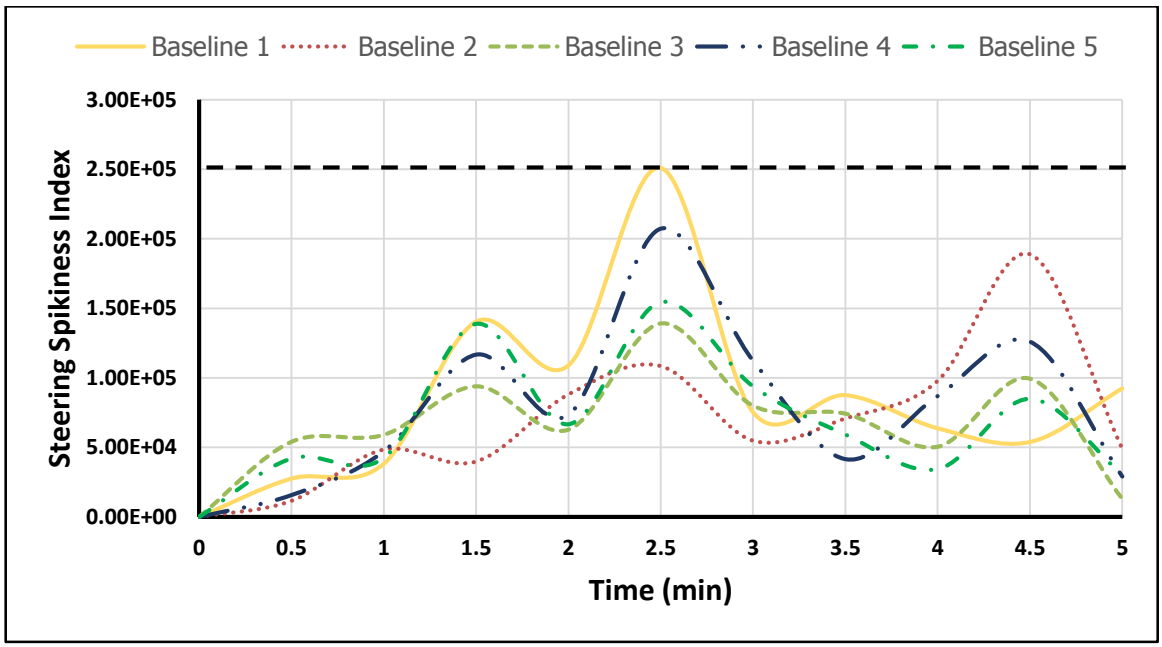

Figure 4-13 Steering spikiness index for baseline driving experiments

4.3.3.2 Distracted Driving

The time history of the steering wheel spikiness index for a driver subjected to different sources of distraction is displayed in Figure 4-14. Driving experiments in which the driver sends text messages while driving result in a spikiness index peaks of ($8.0x10^5$) while a driver that reads emails while driving result in a spikiness index peak of ($1.0x10^6$) as observed in Figure 4-14 (a) and (b), respectively. The steering spikiness index of a driver checking maps while driving results in a spikiness index peak that is 80 times higher than that of the baseline driving experiments as shown in Figure 4-14 (c). This could be attributed to the fact that one data point of the spikiness index encapsulates 30 seconds of driving time. Therefore, if several distraction jerk spikes are evident in the same 30 second time frame then a greater spikiness index is generated. The steering spikiness indices of a driver talking to other occupants inside the vehicle and a driver making phone calls while driving are demonstrated in Figure 4-14 (d) and (e), respectively.

The time history of steering spikiness index of a driver picking up an object while driving and a driver eating while driving indicate a greater area under the curve as shown in Figure 4-14 (f) and (g), respectively. This is due to the fact that the steering jerk spikes caused by driver distraction are more frequent as illustrated previously in Figure 4-5 (f) and (g), respectively. The spikiness index plot of a driver adjusting radio channels while driving presented in Figure 4-14 (h) has smaller area under the curve. This could be attributed to the less frequent jerk spikes as seen in Figure 4-5 (h). To conclude, the steering spikiness index is indicative of driver distraction since the spikiness index of the distraction driving experiments exceeds the spikiness index baseline range.

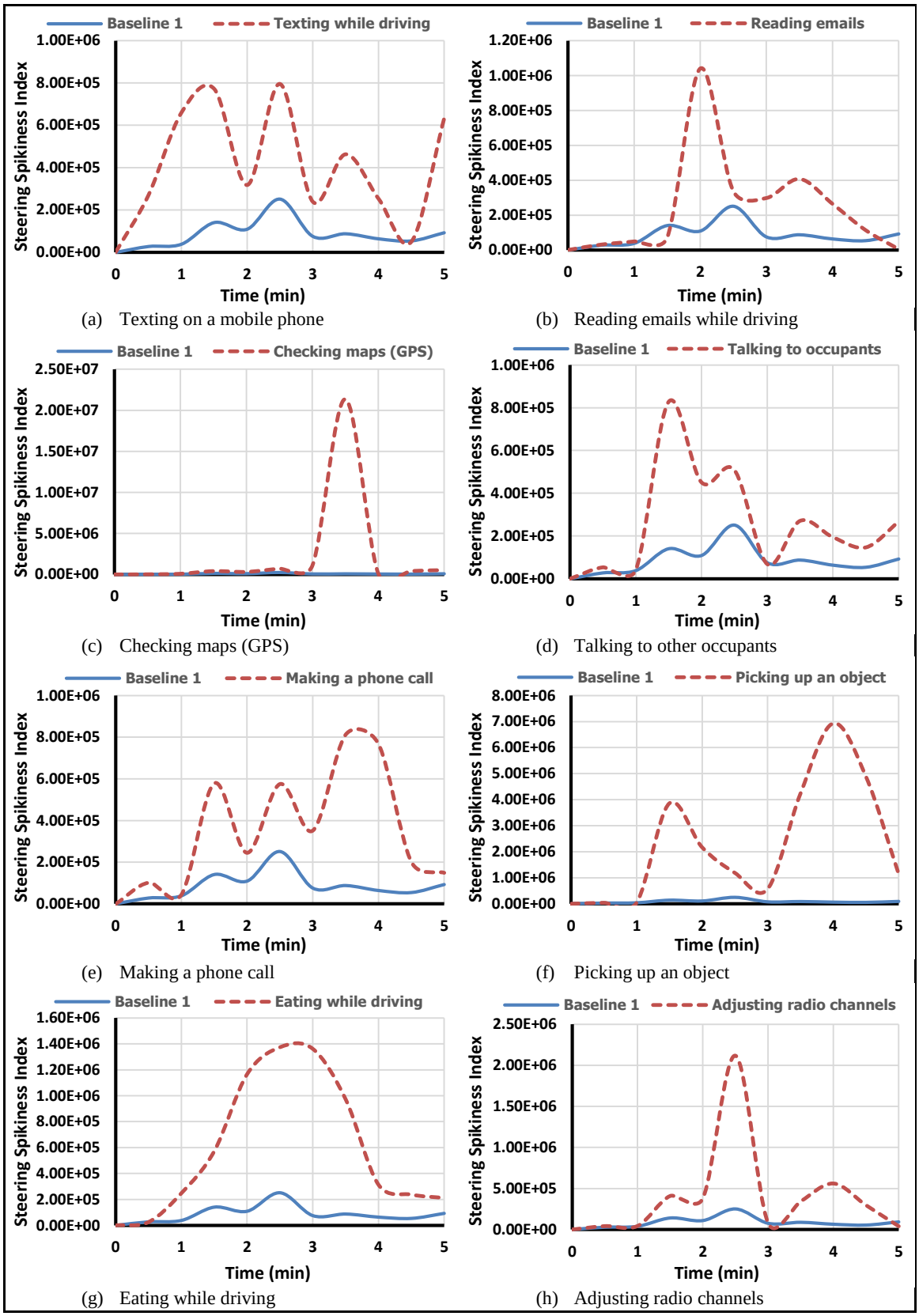

(a) Texting on a mobile phone

(b) Reading emails while driving

(c) Checking maps (GPS)

(d) Talking to other occupants

(e) Making a phone call

(f) Picking up an object

(g) Eating while driving

(h) Adjusting radio channels

Figure 4-14 Steering spikiness index for distraction driving experiments

4.3.3.3 Distraction Indicators

The steering spikiness distraction indicators for the first and second sum squared error (SSE) techniques are demonstrated in Figure 4-15 (a) and (b), respectively. The distraction indicator of the steering spikiness index is determined in similar manner to the steering jerk indicators discussed previously in section 4.3.1.3.

Simulation numbers of 1-4 in Figure 4-15 (a) represent baseline driving while numbers of 5-12 represent driving with different sources of distraction. However, simulation numbers of 1-5 in (b) represent baseline driving and numbers of 6-13 represent distraction. The steering spikiness distraction indicators have values of 1 or less for baseline driving and values greater than 1 for distracted driving experiments. It can be observed that the steering spikiness indicator obtained from the first SSE technique have higher values than that of the second SSE technique. For example, the steering spikiness index obtained from the first SSE technique for a driver that texts while driving is 30 times greater than that of a baseline experiment. In contrast, the steering spikiness indicator obtained from the second SSE technique is only 20 times greater than the baseline.

The steering spikiness indicator in Figure 4-15 shows that picking up an object and checking maps while driving result in the greatest steering spikiness distraction indicator values. The same conclusion is obtained from the steering jerk and rate distraction indicators presented previously in Figure 4-6 and Figure 4-11 since the driver in such cases is not only distracted but also exerts a physical effort that could affect the steering behaviour significantly.

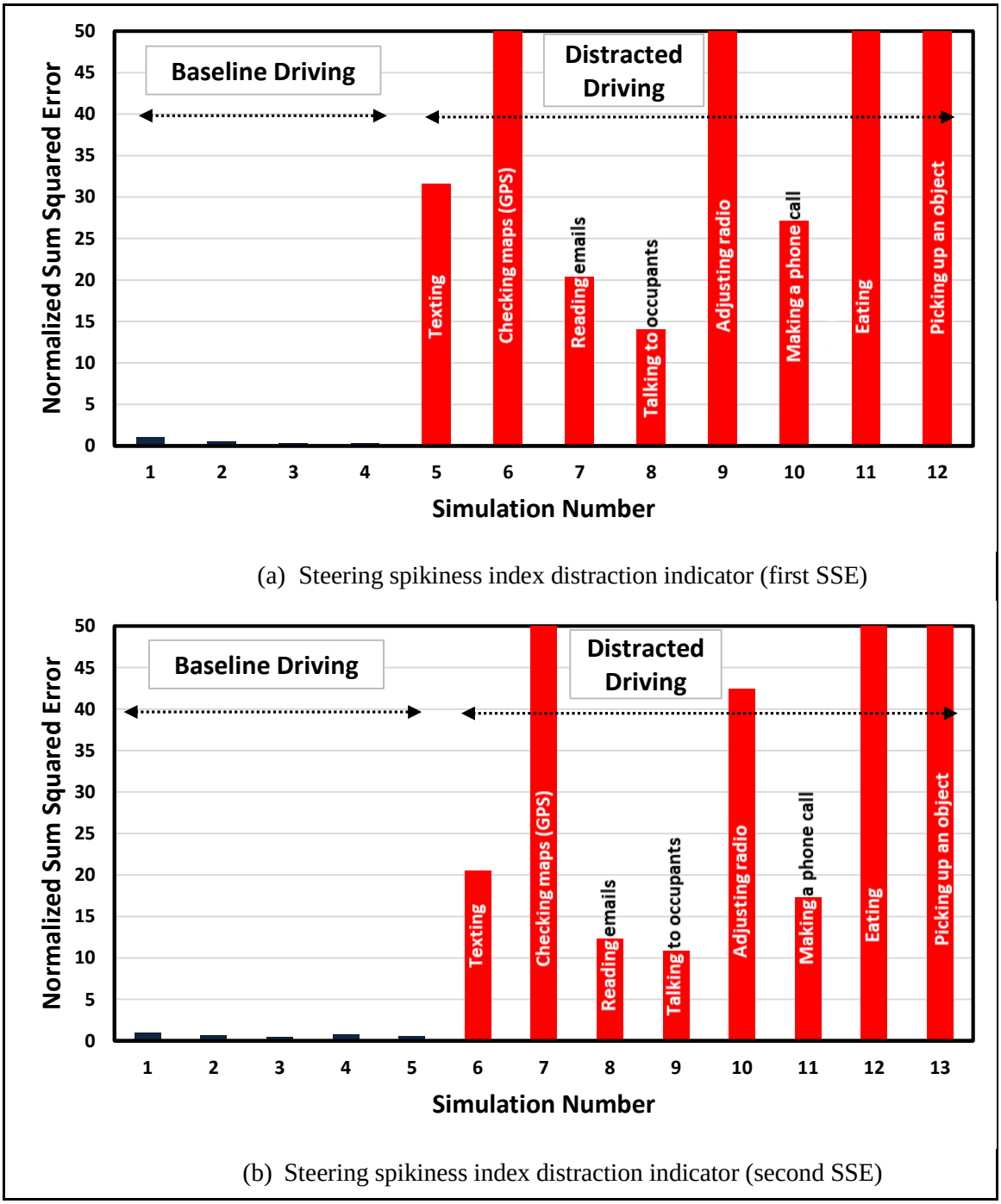

(a) Steering spikiness index distraction indicator (first SSE)

(b) Steering spikiness index distraction indicator (second SSE)

Figure 4-15 Steering spikiness index distraction indicator

4.3.4 Comparison of Steering Wheel Distraction Indicators

In summary, both the steering jerk and rate of change profiles are indicative of driver distraction. Furthermore, the steering jerk and rate of change profile indicate distraction at the same instance in time as shown in Figure 4-5 (c) and Figure 4-10 (c), respectively. The steering jerk and rate of change generate similar distraction indicator values as observed in Figure 4-6 and Figure 4-11, respectively. It should be noted that the jerk steering profile requires at least 7 data points to find the steering jerk of the middle point, which in turn requires the data to be stored over a period of time to be able to generate a steering jerk profile. This process requires storing the data for at least 20 seconds of time before being able to evaluate driver distraction. This will affect the efficiency of the driver distraction warning system since it would generate late warnings [98]. Therefore, the steering rate profile is preferred to monitor the driver distraction. Moreover, the steering rate profile equation will be modified in order to be used in real time. The steering rate profile used in the offline analysis is determined through the Savitzky-Golay numerical differentiation method. This method uses a 7-point moving window in order to preserve the characteristics of the raw data. This is needed when finding the third derivative since a higher derivative will significantly affect the characteristics of the raw data while the first derivative will not affect the characteristics of the raw data significantly. The steering rate profile has been commercially used to detect driver inattentiveness (drowsiness) as explained in [31]. Additionally, the steering wheel spikiness index is indicative of driver distraction. However, the spikiness index is excluded from the real time analysis since it requires 30 seconds of drive time to generate one data point of spikiness as observed in Figure 4-12. This is considered to be a large time frame and will generate late distraction warnings [98].

4.4 OFFLINE RESULTS FOR ACCELERATOR PEDAL POSITION

4.4.1 Accelerator Pedal Distraction Indicators

This section presents a sample of the accelerator pedal analysis results and provides the reader with visuals that can directly help in quantifying driver distraction detected through the accelerator pedal. The accelerator pedal jerk profile, rate of change and spikiness index distraction indicators obtained from the first SSE technique are chosen for the purposes of comparison. The distraction indicator figures are chosen since it is hard for the reader to observe a difference in the driver behaviour from the jerk profile, rate of change and spikiness index of the accelerator pedal position. However, the figures of the accelerator pedal jerk profile, rate of change and the spikiness are given along with all distraction indicators in Appendix B for further reference.

The distraction indicators for the jerk profile and spikiness index of the accelerator pedal are displayed in Figure 4-16 and Figure 4-17, respectively. Simulation numbers of 1-4 represent baseline driving while numbers of 5-12 represent distraction. The distraction indicator values for baseline driving should be equal or less than 1 since the sum squared error of a driver driving the same maneuver without being subjected to any sources of distraction should be consistent with the reference SSE over multiple trials. In contrast, distraction indicators generated from distraction driving experiments should have values greater than 1 or values different than baseline driving indicators. However, the jerk profile and spikiness index distraction indicators for the accelerator pedal do not show a specific trend for baseline and distracted driving experiments. This also applies to the accelerator pedal rate of change distraction indicators as indicated in Figure 4-18. For example, a non-distracted driver can have values much greater than 1 instead of having values less than or

equal to 1. Furthermore, a driver subjected to different sources of distraction can have values less than 1 instead of having values much greater than 1. As a result, the author speculates that the accelerator pedal is not indicative of driver distraction.

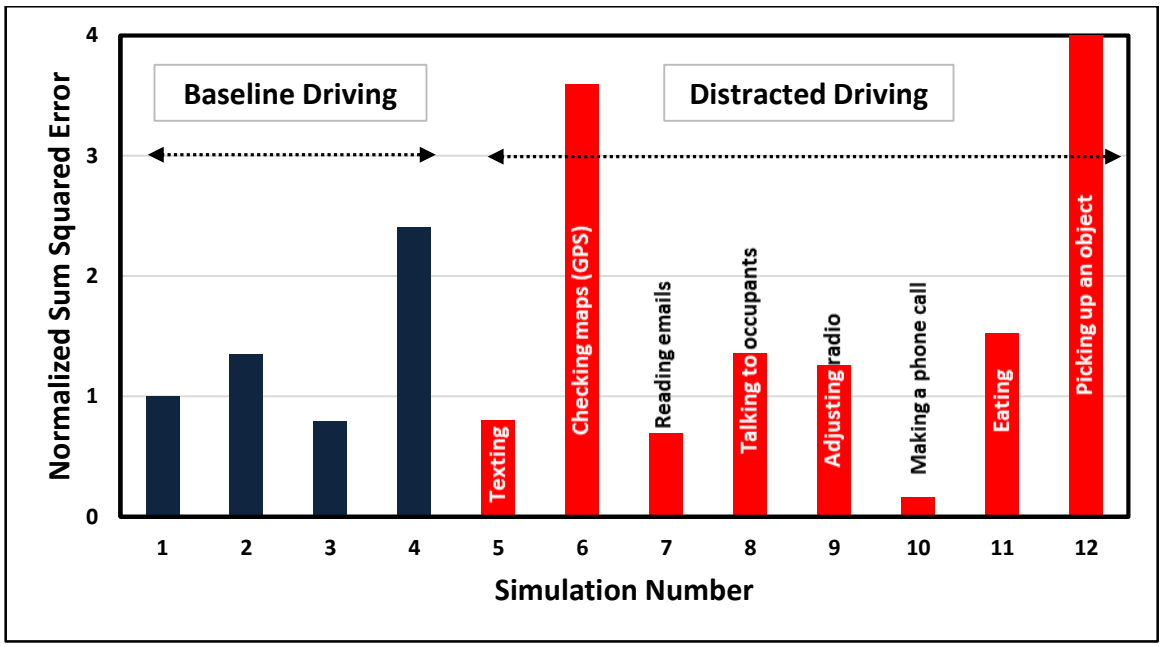

Figure 4-16 Accelerator pedal Jerk profile distraction indicator

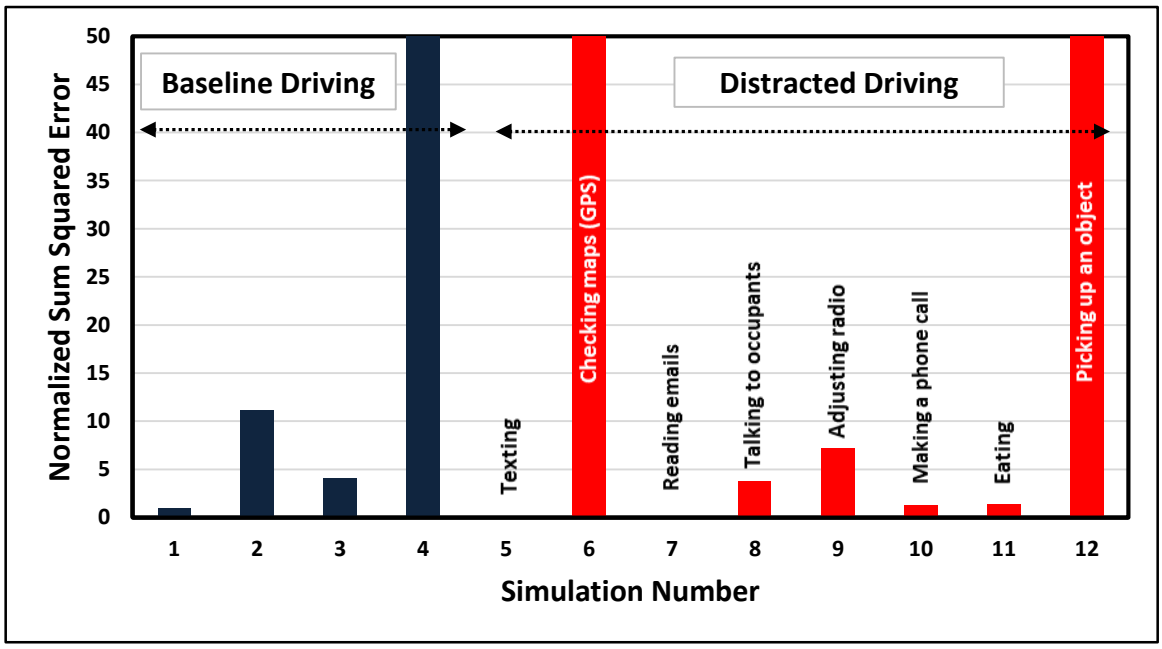

Figure 4-17 Accelerator pedal spikiness index distraction indicator

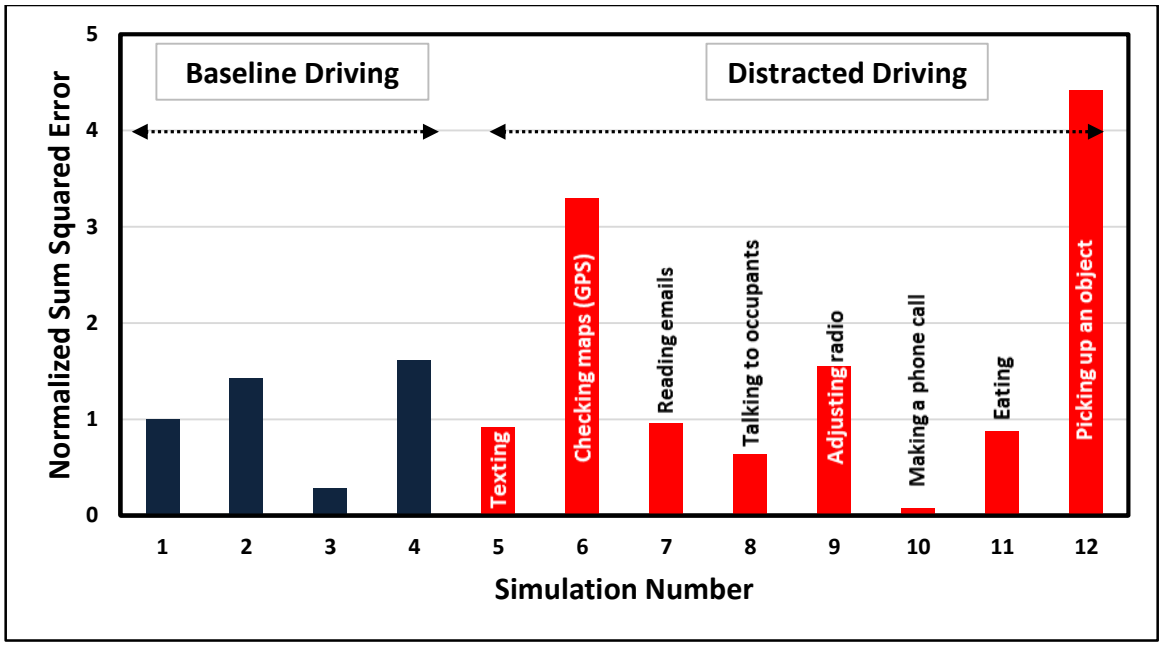

Figure 4-18 Accelerator pedal rate profile distraction indicator

4.4.2 Comparison with Published Work

The main goal of this section is to compare the accelerator pedal distraction indicators determined in this thesis with the drowsiness indicators provided in [24]. Additionally, this section is provided to discuss differences between distraction and drowsiness and how that can affect the accelerator pedal indicators. The study presented in [24] concluded that the jerk profile and spikiness index of both the steering wheel angle and accelerator pedal position are indicative of driver drowsiness. Two neural networks were trained on baseline (alert) driving behaviour. After that, the output of the trained network was compared with inputs to the network. The inputs in this case represent driving experiments with different levels of alertness. The difference between the input and output of an ANN was determined through the sum squared error. Participants were asked to drive for few minutes each hour for 24 hours. After that, the sum squared error was normalized by dividing the sum squared error of each experiment by the highest sum squared error value. The highest value

represents the worst case of drowsiness. The jerk profile and spikiness index drowsiness indicators are shown in Figure 4-19 and Figure 4-20, respectively.

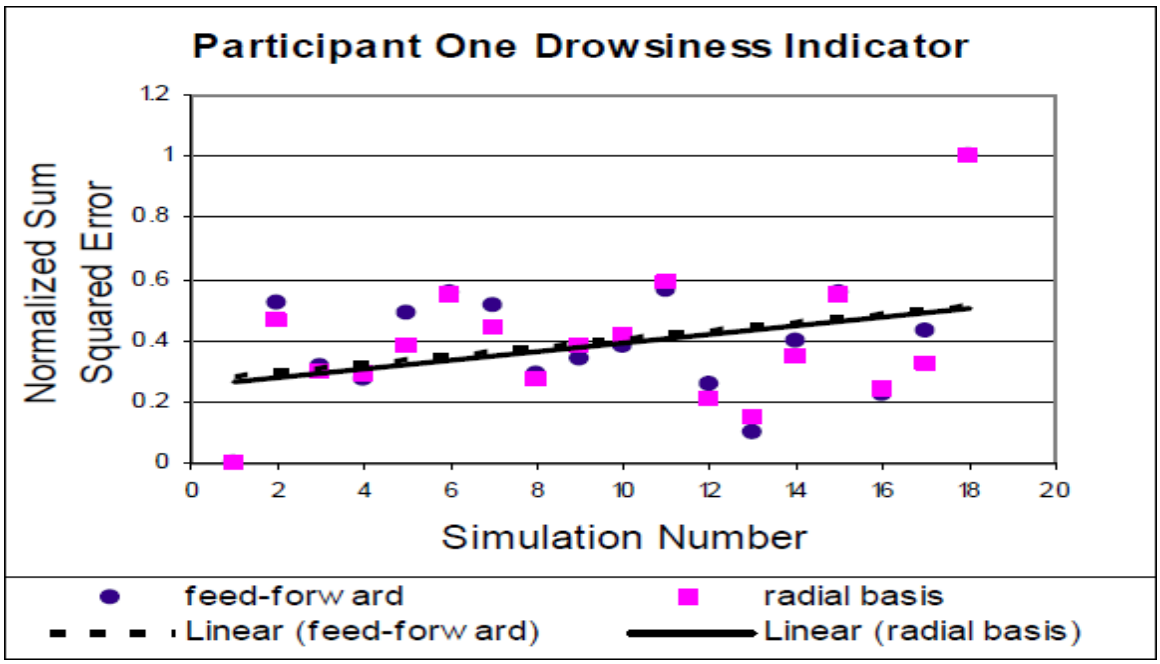

Figure 4-19 Jerk profile drowsiness indicator [24]

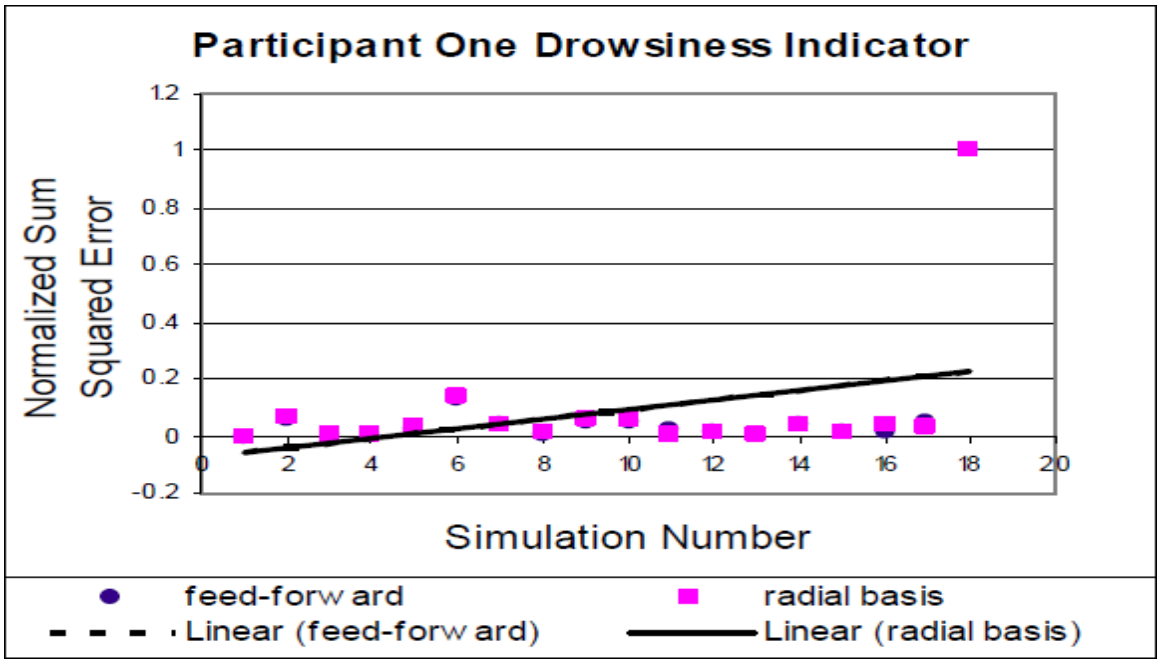

Figure 4-20 Spikiness index drowsiness indicator [24]

It can be observed that results from the jerk profile and spikiness index networks strayed further from the general drowsiness indicator trend line the further the driver stayed awake, respectively. The neural network used in [24] was trained on eight drivers and cannot accommodate all driving styles.

Although dividing the sum squared error (SSE) of each driving experiment by the SSE of the worst case scenario shows gradual reduction of the alertness level, the warning system will not be able to function without having the worst case scenario as a reference or it will generate a late warning. As a result, this thesis suggests using the SSE of the first driving experiment as the baseline as demonstrated in Figure 4-16 and Figure 4-17. This way the alert system will be able to issue a warning whenever the driver is outside of the baseline range. This approach also provides different alertness levels where a lower alertness level will indicate a higher deviation from the baseline. This new approach is suitable for distraction detection where the warning system cannot wait for the worst case of distraction and the warning should be issued instantly when needed. It should be noted that the sum squared error used in detecting driver distraction is determined by simply comparing results of baseline driving experiments with distraction driving experiments instead of using a neural network that can keep a record of the baseline driving profile.

The work presented in [24] concluded that the accelerator pedal is indicative of driver drowsiness. However, the jerk profile of the accelerator pedal was combined with the steering wheel jerk profile. This also applies to the spikiness index of the steering wheel and accelerator pedal as shown in Figure 4-19 and Figure 4-20, respectively. Consequently, the effects that drowsiness may have on the accelerator pedal were not studied independently. It should be noted that the accelerator pedal position was correlated with

driver drowsiness in another study presented in [14]. However, the driving experiment in this study was simulated on a personal computer like a video game and the steering wheel and pedals were connected externally to the computer. This simulation environment would not give the real driving feel and conditions. Additionally, distraction may have different effects on the accelerator pedal than drowsiness. Distraction is different than drowsiness. Distraction is generally caused by a triggering event that discerns driver alertness whereas drowsiness does not involve a triggering event and it can be considered as a gradual loss of driver alertness [21]. This means that distraction occurs in a matter of seconds [104] and the accelerator pedal would not show sudden variations. In contrast, drowsiness is a gradual loss of driver alertness and a change in the accelerator pedal profile can be detected over time. Additionally, the steering wheel angle has a wider operation range of 0-720˚ from center position to the rightmost or leftmost position of the steering wheel while the accelerator pedal position has a range of 0-1. As a result, sudden changes in the steering wheel angle will have significant impact on the steering rate and jerk profile whereas changes in the accelerator pedal position may not be have sensible effects on the pedal profile. Finally, up to the best of the author's knowledge there has not been any published research that independently studies the effects of driver distraction on the accelerator pedal position.

4.5 CHAPTER SUMMARY

The offline analysis investigated the effects that driver distraction can have on the steering wheel angle and accelerator pedal position. The steering jerk profile, rate of change and spikiness index were determined to find a correlation between the steering wheel and driver

distraction. The sum squared error was used to detect the deviation of the steering profile of a distracted driver from the baseline steering profile and generate distraction indicators.

It was found that the steering jerk, rate of change profiles and the spikiness index are indicative of driver distraction. The steering rate and jerk profile indicate driver distraction at the same instant in time. Moreover, the steering rate distraction indicators have similar values to the steering jerk indicators. The steering spikiness index have greater distraction indicator values than that of the steering jerk and rate of change. However, the steering wheel spikiness index needs at least 30 seconds of driving time to generate one data point of the spikiness index.

Additionally, the jerk profile is determined using the Savitzky-Golay method which requires 7 data points to determine the jerk profile of the middle point. As a result, the jerk profile requires the data to be stored in the simulator for at least 20 seconds before distraction can be detected. This will affect the efficiency of the alert system since it would generate late driver distraction warning. It should be noted that the steering rate can detect distraction instantly since the data does not have to be stored in the simulator for periods of time.

The sum squared error (SSE) compares the steering rate error for the same period of time. Therefore, the SSE of the steering rate for the real time application should be compared over a small period of time of 1-2 seconds. However, the sum squared error for the steering rate of the baseline period is not sufficient to build an accurate pattern of the driving behaviour since 2 seconds of the SSE is considered as a small time frame and more data points are needed to generate accurate results.

The accelerator pedal jerk, rate of change as well as spikiness index were also studied. However, it was found that the accelerator pedal is not indicative of driver distraction since the distraction indicators did not show a specific trend in the accelerator pedal. The work done with the accelerator pedal position in this chapter has been compared with previous studies that used the accelerator pedal to detect drowsiness. Additionally, the differences between driver distraction and driver drowsiness have been discussed in this chapter to understand their effects on the accelerator pedal position. Consequently, the author recommends using the amplitude of the steering rate as the main indicator of driver distraction in real time.

CHAPTER 5

REAL TIME DETECTION OF DRIVER DISTRACTION

5.1 INTRODUCTION

This chapter demonstrates the results of the real time detection of driver distraction. The real time detection means that distraction is detected in real time while driving. The main goal of the real time analysis is to test the suggested real time detection methods through a set of baseline and distraction driving experiments. Based on the findings of the offline analysis, the steering jerk profile and spikiness index as well as the accelerator pedal indicators are excluded from the real time analysis for the reasons discussed in the previous chapter. As a result, the steering rate of change is used to detect driver distraction in real time. The real time analysis comprises of two distraction detection methods. The first real time detection method uses a single threshold steering rate value in detecting driving distraction while the second method monitors the driver behaviour for the first 5 minutes of driving and then generates a final threshold value based on that. The first method requires baseline driving experiments at first to determine the most suitable threshold value of the steering rate and the allowance factor of the second method. The allowance factor is multiplied by the maximum absolute steering rate to account for small variations in the normal driving behaviour and reduce false distraction warnings. The chapter then compares the first real time detection method with the second real time detection method. It also discusses the effects of path and payload on the steering rate. The chapter concludes with a description of the proposed final concept of the driver distraction alert system applied on the truck driving simulator.

5.2 DATA COLLECTION FROM DRIVING SIMULATOR

5.2.1 Experimental Procedure

Several driving experiments are carried out by utilizing the Virage VS600M motion base truck driving simulator. The experiments are done using a fully loaded tractor semitrailer vehicle configuration and a highway driving scenario shown in Figure 5-1.

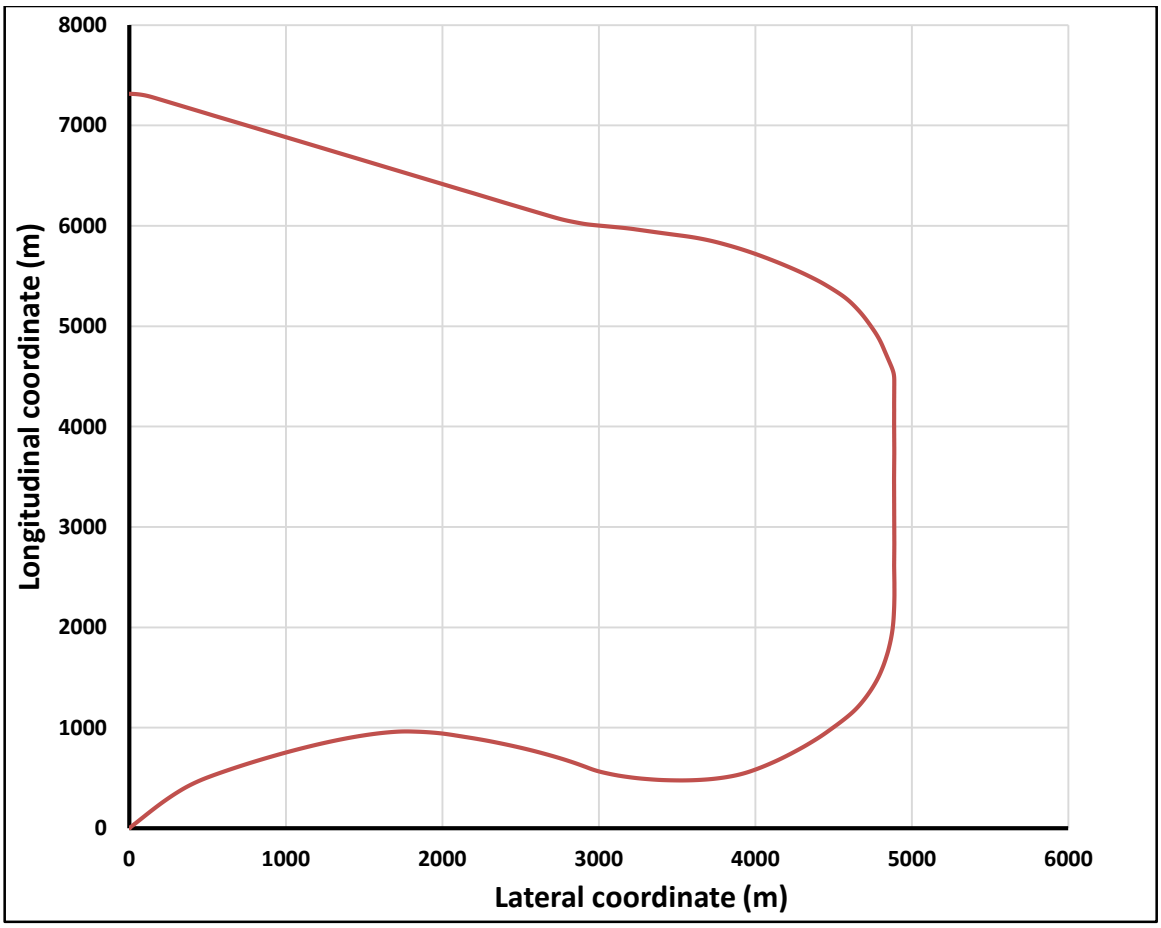

Figure 5-1 Highway scenario path coordinates used for real time driving experiments

As presented previously in chapter 4, the same sources of distraction discussed in [19, 103] are used for the real time analysis as shown in Figure 5-2: (a) Texting on a mobile phone, (b) reading emails, (c) checking maps (GPS), (d) talking to other occupants, (e) making a phone call, (f) picking up an object, (g) eating, (h) Adjusting radio channels.

(a) Texting on a mobile phone

(b) Reading emails while driving

(c) Checking maps (GPS)

(d) Talking to other occupants

(e) Making a phone call

(f) Picking up an object

(g) Eating while driving

(h) Adjusting radio channels

Figure 5-2 Real time distraction driving experiments performed on the simulator

The main purpose of presenting the distraction driving experiments shown in Figure 5-2 is to provide a visualization of the experimental procedure and show the reader how the aforementioned sources of distraction are actually performed on the simulator. The main purpose of the real time experiments is to test the suggested real time distraction detection method and make sure it can be applied to real world vehicles. The real time experiments needed to evaluate the final threshold value of the steering rate and the allowance factor for the real time detection methods are shown in Table 5-1. Eight baseline driving experiments of 10 minutes each are required to find the final threshold steering rate value and the allowance factor that will result in accurate detection of driver distraction. The final threshold steering rate value is used for the first distraction detection method while the allowance factor is used for the second real time detection method.

Table 5-1 Driving experiments needed for the real time analysis

<table>
<tr><th>Experiment Number</th><th>Description</th><th colspan="2">Duration (minutes)</th></tr>
<tr><td>-</td><td>Eight trials of baseline driving</td><td colspan="2">10</td></tr>
<tr><td>1</td><td>Texting on a mobile phone while driving</td><td rowspan="8">5</td><td rowspan="8">5</td></tr>
<tr><td>2</td><td>Reading emails while driving</td></tr>
<tr><td>3</td><td>Checking maps (GPS) while driving</td></tr>
<tr><td>4</td><td>Talking to other occupants while driving</td></tr>
<tr><td>5</td><td>Making a phone call while driving</td></tr>
<tr><td>6</td><td>Picking up an object while driving</td></tr>
<tr><td>7</td><td>Eating while driving</td></tr>
<tr><td>8</td><td>Adjusting radio channels while driving</td></tr>
</table>

The first method requires eight trials of baseline driving and experiments with different sources of distraction. The duration of the baseline experiment and the distraction experiment is 10 minutes each. However, the driver in the distraction experiment of the first detection method is asked to be vigilant during the first 5 minutes then the driver is subjected to a certain source of distraction. The purpose of the first 5 minutes of the first experiment is to ensure that the distraction detection system does not issue false warnings. The second method of distraction detection requires only 10 minutes of drive time where the first 5 minutes of the experiment are used for building the baseline automatically in real time and then the driver is subjected to a certain source of distraction during the next 5 minutes. The system will only start detecting distraction right after building the baseline. It should be noted that driver was first familiarized with driving the truck simulator before commencing the driving experiments.

5.2.2 Raw Data Recording

The steering wheel angle, steering rate, brake pedal position, total time of simulation, final threshold value of the steering rate and the time step datasets are collected from the simulator for the purposes of the real time analysis.

As discussed in chapter 4, the data collection from the simulator is done by editing any scenario from the library using the NotePad++ tool and then adding the data collection script to that scenario. Each scenario has a specific script which is compared with another script having the data collection script for the same scenario using WinMerge tool. This tool places each file either to the left or right of the screen and highlights the different parts of the two scripts. The operator can then add the different parts to any scenario using the NotePad++ program.

The operator can check the data that will be collected from the data collection scenario by double clicking on the scenario and selecting the data collection block. By doing that, two tabs having the labels of “Normal code” and “When becomes active” will appear. The operator can check which data will be collected by looking at the last line of script under the “Normal code” tab. The last line of the script will have the “get-steering” code template. The “get-steering code” is used to collect the steering angle.

The operator can change the data collected by looking at the code templates on the upper side of the screen and then placing another template instead of “get-accelerator” such as “get-steering”. However, the code templates are limited to a certain number of parameters. For example, the steering rate and the final threshold values do not have a code template. In this case the simulator steering rate algorithm is added to the script and then the data is simply collected by using the steering rate variable name instead of “get-steering” format. The data is collected by running the scenario that has the data collection script and saved in an excel sheet that will be available right after stopping the scenario. Each column in this sheet represents one of the selected parameters. For example, the first column is reserved for the steering angle whereas the second column is reserved for the accelerator position. As a result, the operator has to check the last line of the script under the “When becomes active” tab to label the column for each data set collected. The labels should follow the same sequence presented in the last line of script under the “Normal code” tab.

5.2.3 Data Processing

The raw data collected from the driving simulator for the purposes of the real time driver distraction detection required similar processing to the offline driver distraction detection. However, some of the data required processing in the LISP programming environment before collection. First, the steering rate of change algorithm is added to the simulator software. Additionally, the final steering rate threshold value of the first real time detection experiments is added manually to the LISP environment. In contrast, the maximum absolute steering rate value used for the second real time detection method is calculated automatically in the programming environment. After five minutes of driving, the maximum absolute steering rate is multiplied by the allowance factor to determine the final steering rate threshold value. The allowance factor is required to ensure that the driver does not get false distraction warnings.

As mentioned earlier in the previous chapter, the raw data collected from the simulator is saved in a Comma Separated Value (CSV) format file. This file is converted to an excel sheet and the data is then converted from text to columns so that each variable can have a specified column. The steering wheel angle is collected from the simulator as ratio of the maximum steering wheel angle where the maximum steering angle is 720 degrees measured from the center to the rightmost or leftmost steering wheel position. As a result, the steering wheel angle, steering rate of change and final threshold value are multiplied by 720 to get the steering angle and rate values in deg and deg/s, respectively. It should be noted that no further processing is required after this step and the steering rate data can be plotted in excel. The data is processed mainly in the LISP programming environment and the real time analysis does not require using MATLAB.

5.3 REAL TIME RESULTS FOR STEERING WHEEL RATE OF CHANGE

5.3.1 First Distraction Detection Method

5.3.1.1 Baseline Driving

The time history of the steering rate for eight baseline driving experiments is displayed in Figure 5-3. The steering rate profile in this chapter is determined through equation 3-9 since it only requires two data points to find the steering rate and does not require storing data in the simulator for a period of time. The maximum absolute steering rate of the first baseline driving experiment is 27 deg/s after 5 minutes of driving and 34 deg/s after 10 minutes as observed in Figure 5-3 (a). The main goal of measuring the maximum absolute steering rate of the driver after 5 and 10 minutes of driving is to determine the most suitable period of time needed to accurately study the driving pattern and build a baseline of the driver steering rate profile. It can be seen in Figure 5-3 that a final steering rate threshold of 43 deg/s can detect driver distraction for any driving experiment and at the same time reduce false driver distraction detection warnings. The maximum absolute steering rate values obtained from the eight baseline driving experiments presented in Figure 5-3 are summarized in Table 5-2. The maximum absolute steering rate of the first, fourth, fifth and seventh baseline driving experiments have greater values after 10 minutes of driving than those obtained from the first 5 minutes of driving. As a result, a baseline of 10 minutes is recommended for real life applications. However, the author suggests that 5 minutes of baseline drive time is sufficient for the simulation purposes since a final steering rate threshold of 43 deg/s accounts for small steering rate variations in the normal driving behaviour. Additionally, the allowance factor also accounts for variations in driving styles and small variations in the normal driving behaviour.

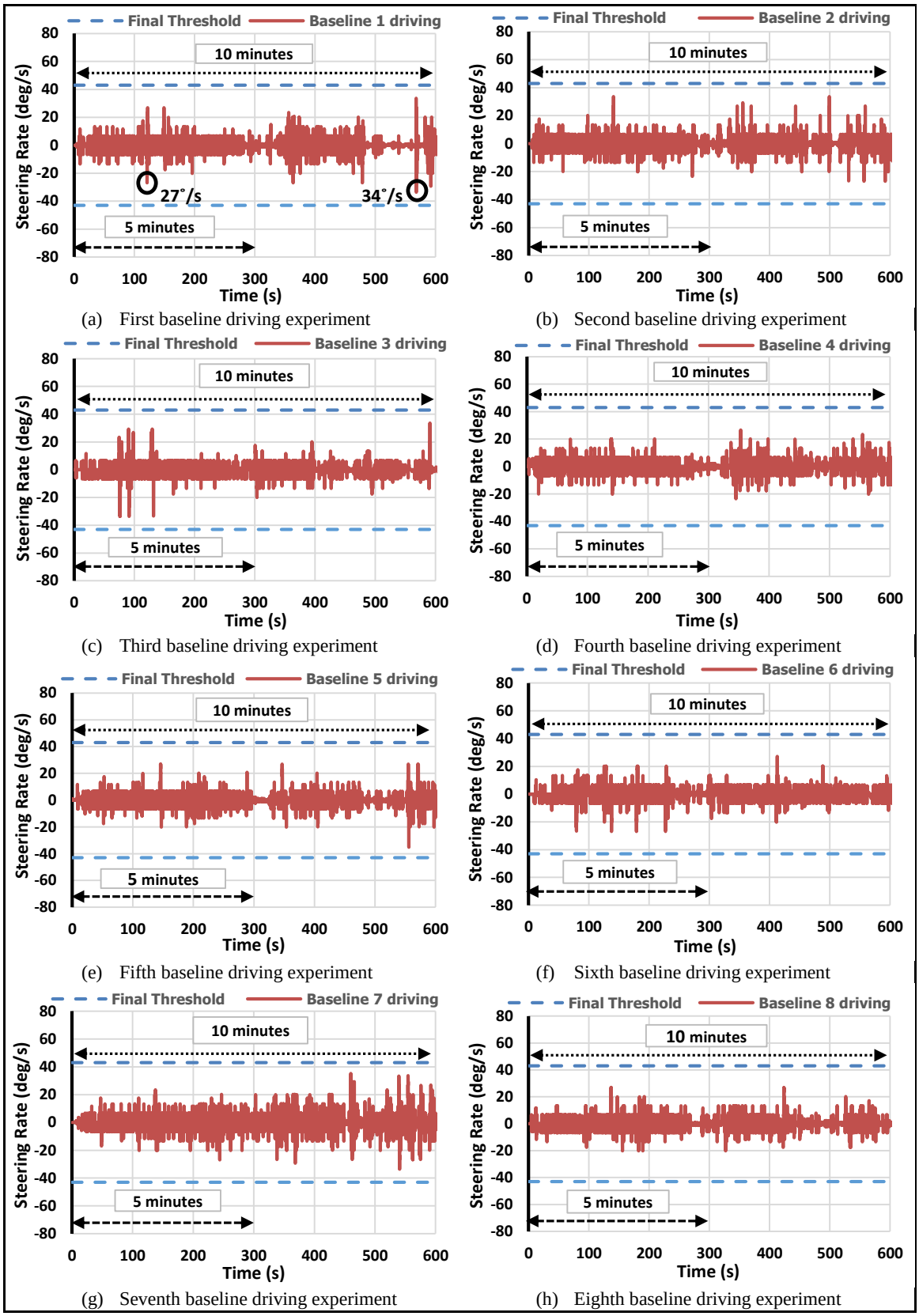

Figure 5-3 Real time Steering rate profile for baseline driving experiments

Table 5-2 Maximum absolute steering rate values for the baseline driving experiments

Experiment Number	Duration (minutes)	S_{max} (Deg/s)	Duration (minutes)	S_{max} (Deg/s)
1	5	27	10	34
2		34		34
3		34		34
4		20		27
5		27		35
6		27		27
7		27		35
8		27		27

The allowance factor is needed to find the final steering rate threshold of the second real time detection method. The allowance factor is determined by finding the average of the maximum absolute steering rate values in Table 5-2 and then multiplying it by the factor that would result in a steering rate threshold of 43 deg/s. An allowance factor of 1.4 results in the best distraction detection. As a result, the maximum absolute steering value obtained during the baseline period is multiplied by 1.4 to find the final threshold value.

The final threshold range concept has been used in [101] to identify driver distraction. The lateral acceleration was used as the main indicator of driver distraction where sudden steering corrections caused by driver distraction resulted in high spikes in the amplitude of the lateral acceleration. It was suggested that a normal threshold value should be 1.5 times the standard deviation of the lateral acceleration signal. However, the extreme lateral acceleration should be 2.5 times the standard deviations of the lateral acceleration signal

as illustrated in Figure 5-4. The lateral acceleration requires an additional sensor but the main goal of presenting this study is to show that distraction can be detected by assuming a threshold range and validating the threshold by a set of driving experiments.

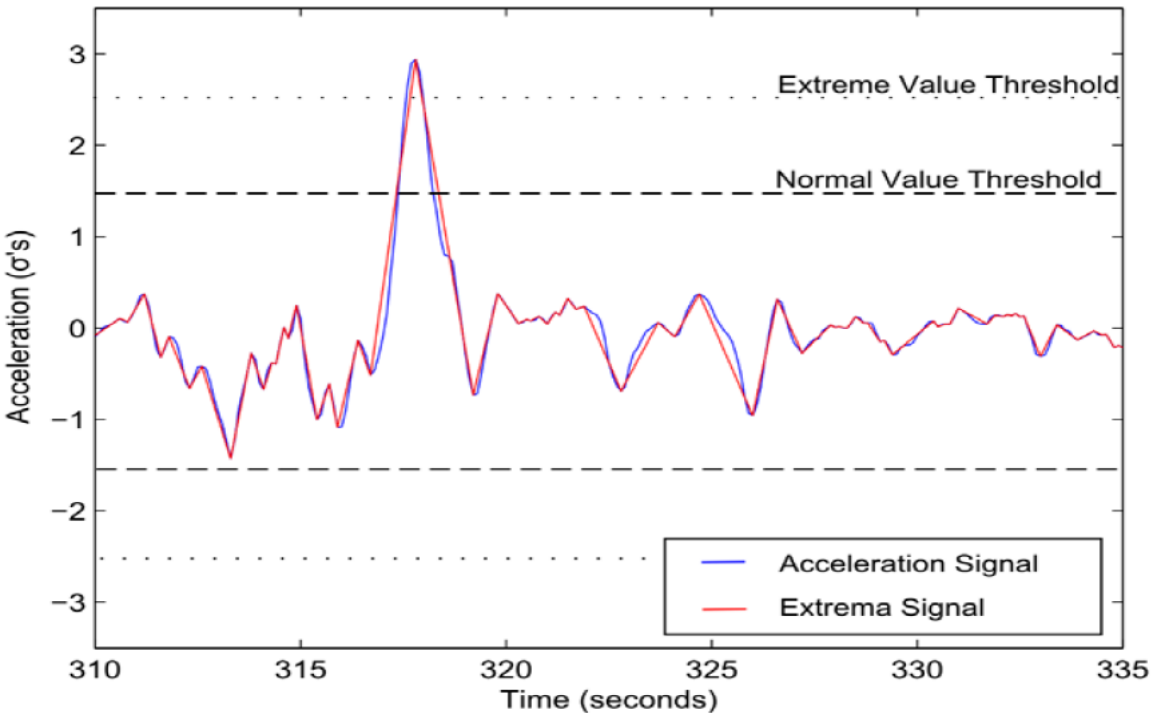

Figure 5-4 The final threshold concept for detecting driver distraction [101]

5.3.1.2 Distracted Driving

The steering rate profile obtained from eight driving experiments in which the driver is subjected to different sources of distraction is demonstrated in Figure 5-5. In order to ensure that the alert system does not issue any false warnings and show the transition of the driver state, the driver is not subjected to any source of distraction during the first 5 minutes of driving. The steering rate for a driver texting or reading emails while driving indicate small steering corrections at first. After that, the intensity of corrections increases over time if the driver continues to be distracted as observed in Figure 5-5 (a) and (b).

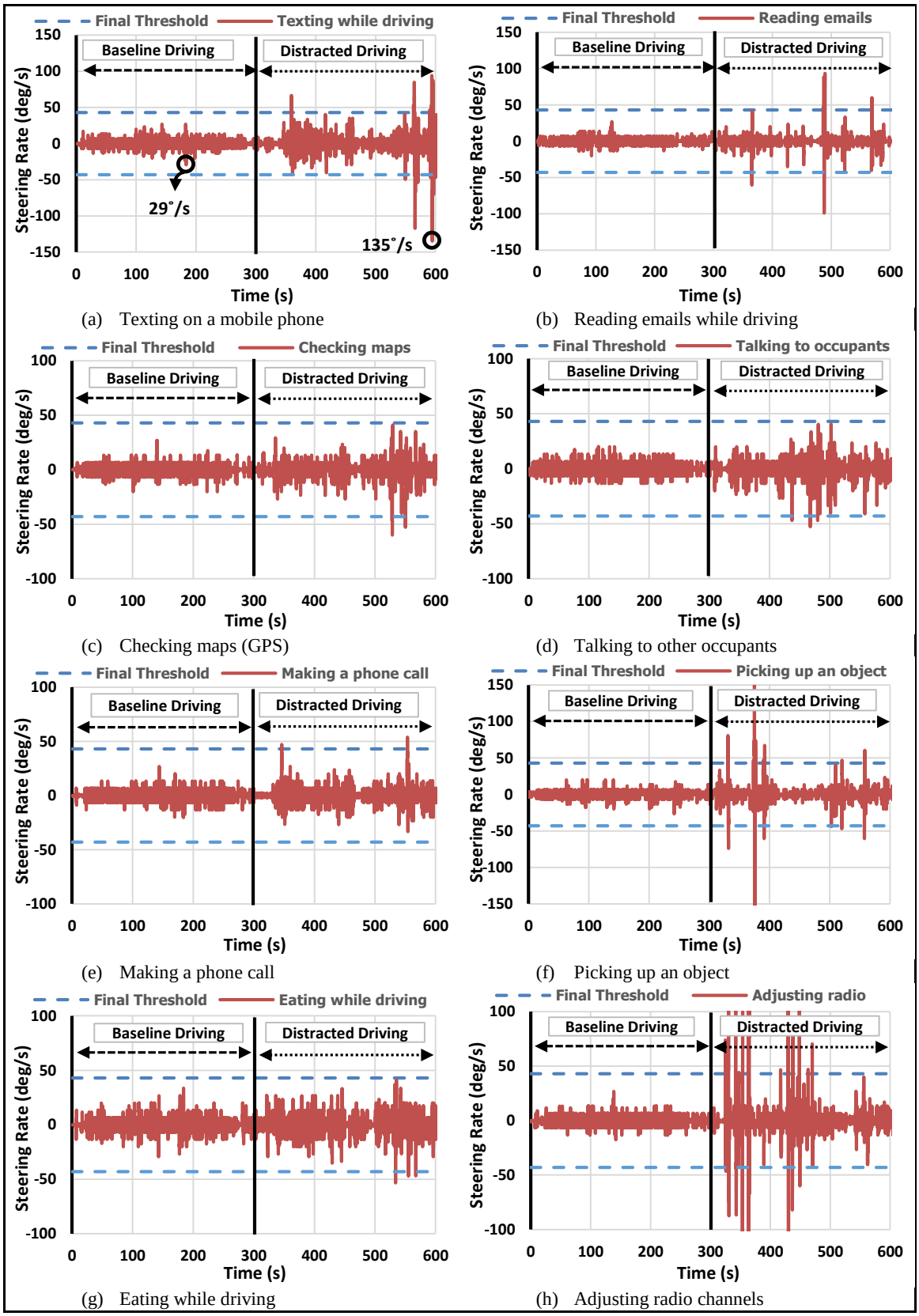

Figure 5-5 Steering rate profile of real time distraction driving experiments (1st method)

This could be attributed to the fact that drivers take their eyes off the road for seconds at first and then the driver feels more comfortable and tends to focus on the other task rather than concentrating on the driving task. The steering rate profile of a driver texting while driving has a value of 29 deg/s in the baseline period compared to a value of 135 deg/s in distraction detection period. This means that the steering rate is indicative of driver distraction in real time. The steering rate profile of drivers checking maps, talking to other occupants, making phone calls and eating while driving slightly exceed the single threshold range of 43 deg/s as seen in Figure 5-5 (c), (d), (e) and (g), respectively. This means that drivers did not take their eyes off the road that often and thus did not make large steering corrections. However, the system can still detect the distracted driving behaviour. It can be observed in Figure 5-5 (f) that a driver picking up an object while driving has a high amplitude steering rate spikes that exceed 150 deg/s. This could be attributed to the driver not only taking their eyes off the road but also doing a physical activity which can affect the steering wheel significantly. Additionally, the steering rate of a driver adjusting radio channels while driving has high amplitude and frequent spikes exceeding 100 deg/s as noticed in Figure 5-5 (h). This is due to the fact that adjusting radio channels takes the driver attention since the driver has to look on a smaller screen while driving. This could be dangerous if the driver keeps on adjusting channels frequently.

5.3.2 Second Distraction Detection Method

The time history of the steering rate profile of driving experiments in which the driver is subjected to different sources of distraction is displayed in Figure 5-6: (a) Texting on a mobile phone, (b) reading emails, (c) checking maps (GPS), (d) talking to other occupants, (e) making a phone call, (f) picking up an object, (g) eating, (h) Adjusting radio channels.

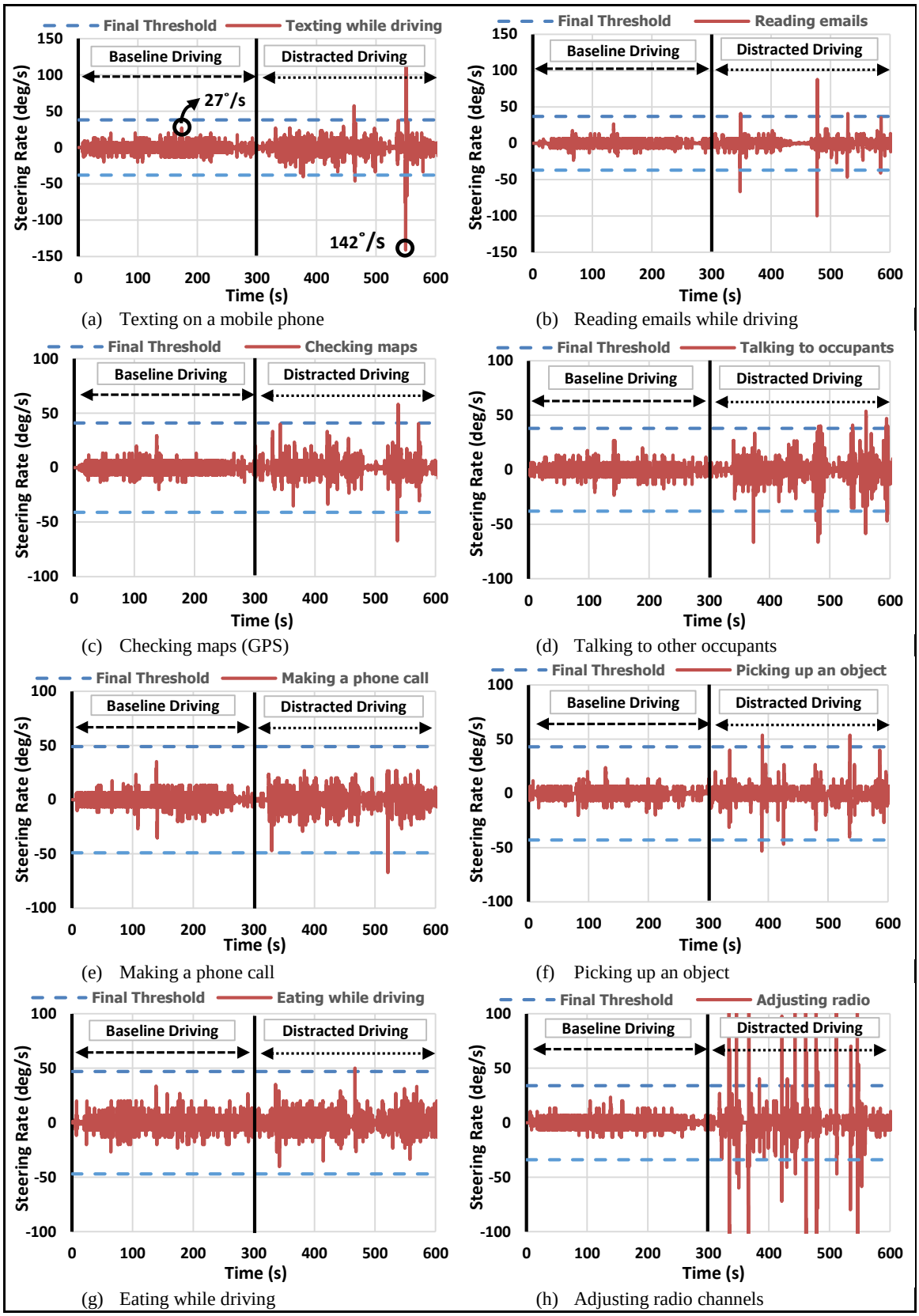

Figure 5-6 Steering rate profile of real time distraction driving experiments (2nd method)

The first 5 minutes of driving are used to build a baseline of the driving pattern and to determine the final steering rate threshold range automatically in real time. It can be observed from Figure 5-6 (a) that the maximum steering rate is 27 deg/s during the baseline period compared to 142 deg/s during the distracted driving period. This means that distraction resulted in higher steering rate profile which exceeds the threshold range and thus the system can successfully detect variations in the driving behaviour. Additionally, the final steering rate threshold range of the second real time detection method is variable compared to the constant threshold of 43 deg/s of the first real time detection method. For example, the final steering rate threshold range in Figure 5-6 (a) is 38 deg/s.

5.4 COMPARISON BETWEEN FIRST AND SECOND METHODS

The maximum absolute steering rate (S_{max}) and final threshold values obtained from the first real time distraction driving experiments are presented in Figure 5-7. It can be observed that the steering rate obtained from distraction experiments exceeds a single threshold range of 43 deg/s. This single threshold value can accommodate a variety of driving styles as demonstrated in Figure 5-5. Furthermore, this method can detect distraction without requiring a baseline driving period in the beginning of each driving experiment since the threshold range is constant. It should be noted that the single threshold range of 43 deg/s is suitable for the tractor semitrailer vehicle configuration. In contrast, the final steering rate threshold range of the second real time detection method is variable where the final threshold values range between 34 and 49 deg/s as observed in Figure 5-8. The steering rate values obtained from distraction driving experiments of the second method exceed the threshold range of 34-49 deg/s. This means that the alert system detected driver distraction successfully and did not issue false warnings. However, a

variable steering rate threshold may result in high threshold value that are close to the steering rate of a distracted driver as seen in experiment number 7 of Figure 5-8.

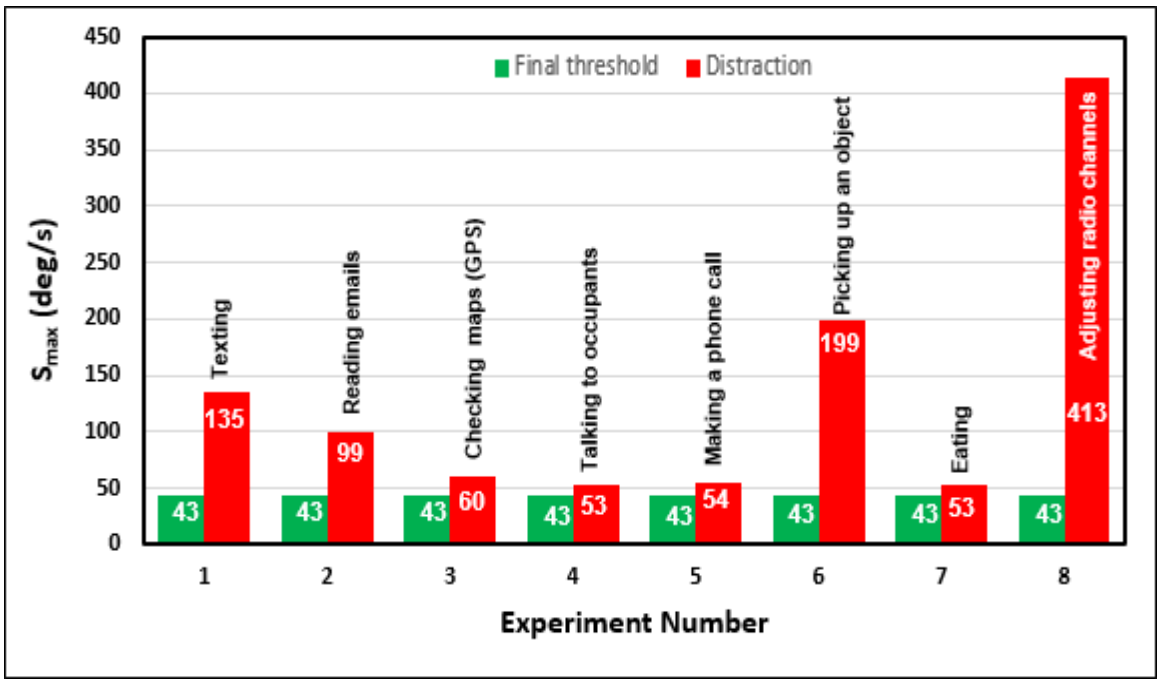

Figure 5-7 Maximum absolute steering rate values for the first method experiments

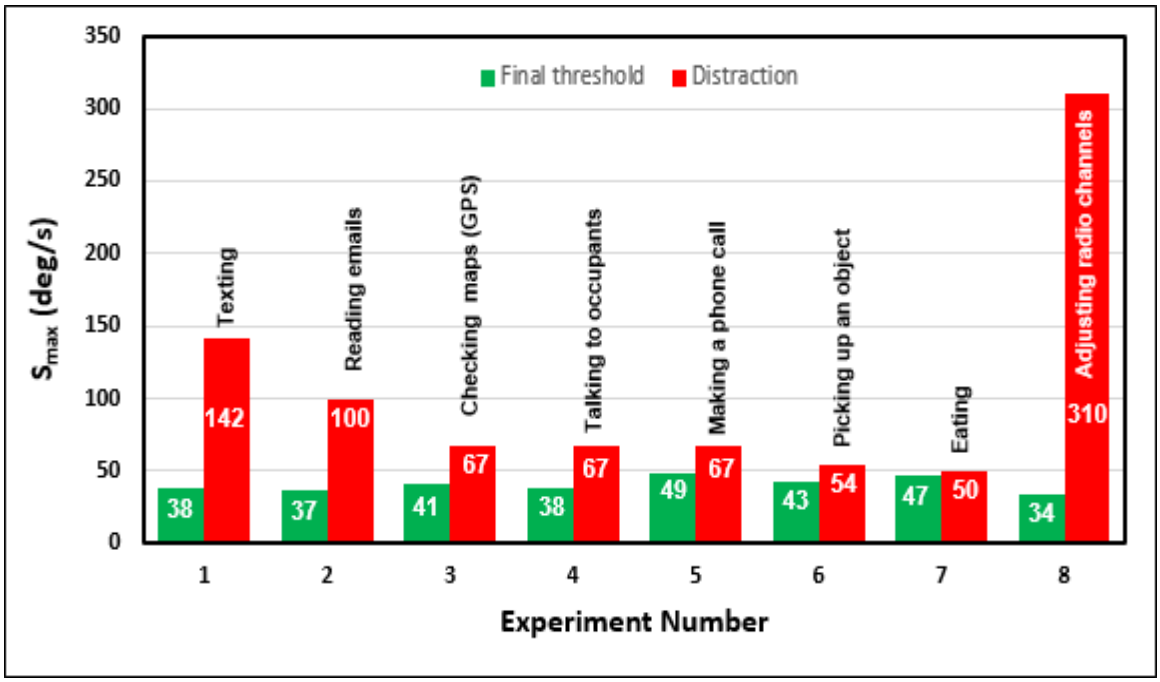

Figure 5-8 Maximum absolute steering rate values for the second method experiments

This could affect the effectiveness of the driver distraction detection system. Consequently, the first real time detection method is preferred over the second method.

5.5 EFFECTS OF PATH AND PAYLOAD ON THE STEERING RATE

In order to ensure that the steering rate threshold of the first method is suitable for any section of the highway, two baseline driving experiments of 20 minutes each are performed on the path shown in Figure 5-9. It should be noted that the first 10 minutes of the driving path were used in the baseline and distraction driving experiments of previous sections. However, the driving path starting after the first 10 minutes of driving represent a new section of the highway. The steering rate profile of the two baseline driving experiments are demonstrated in Figure 5-10.

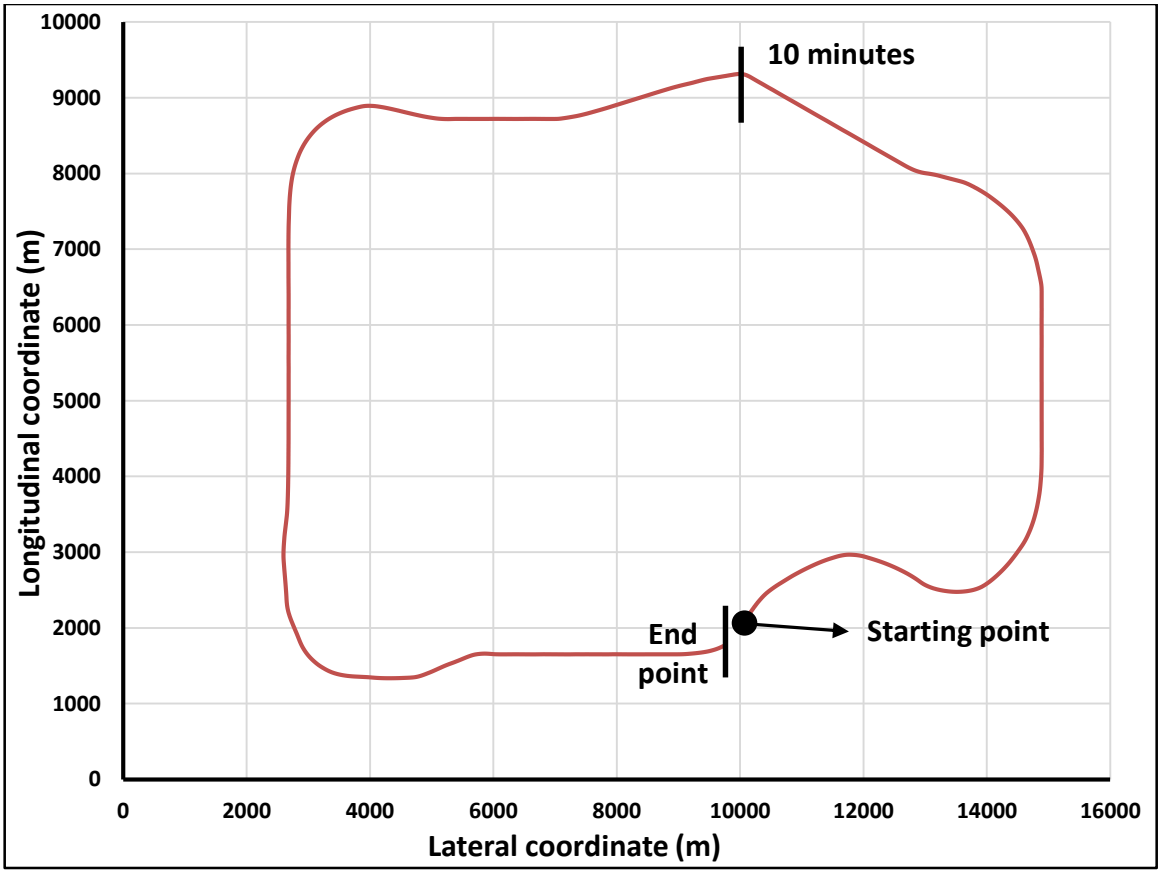

Figure 5-9 Highway path coordinates for 20 minutes of driving time

Furthermore, the same driving experiments are used to compare the empty and fully loaded tractor semitrailer vehicle configuration as illustrated in Figure 5-10 (a) and (b), respectively.

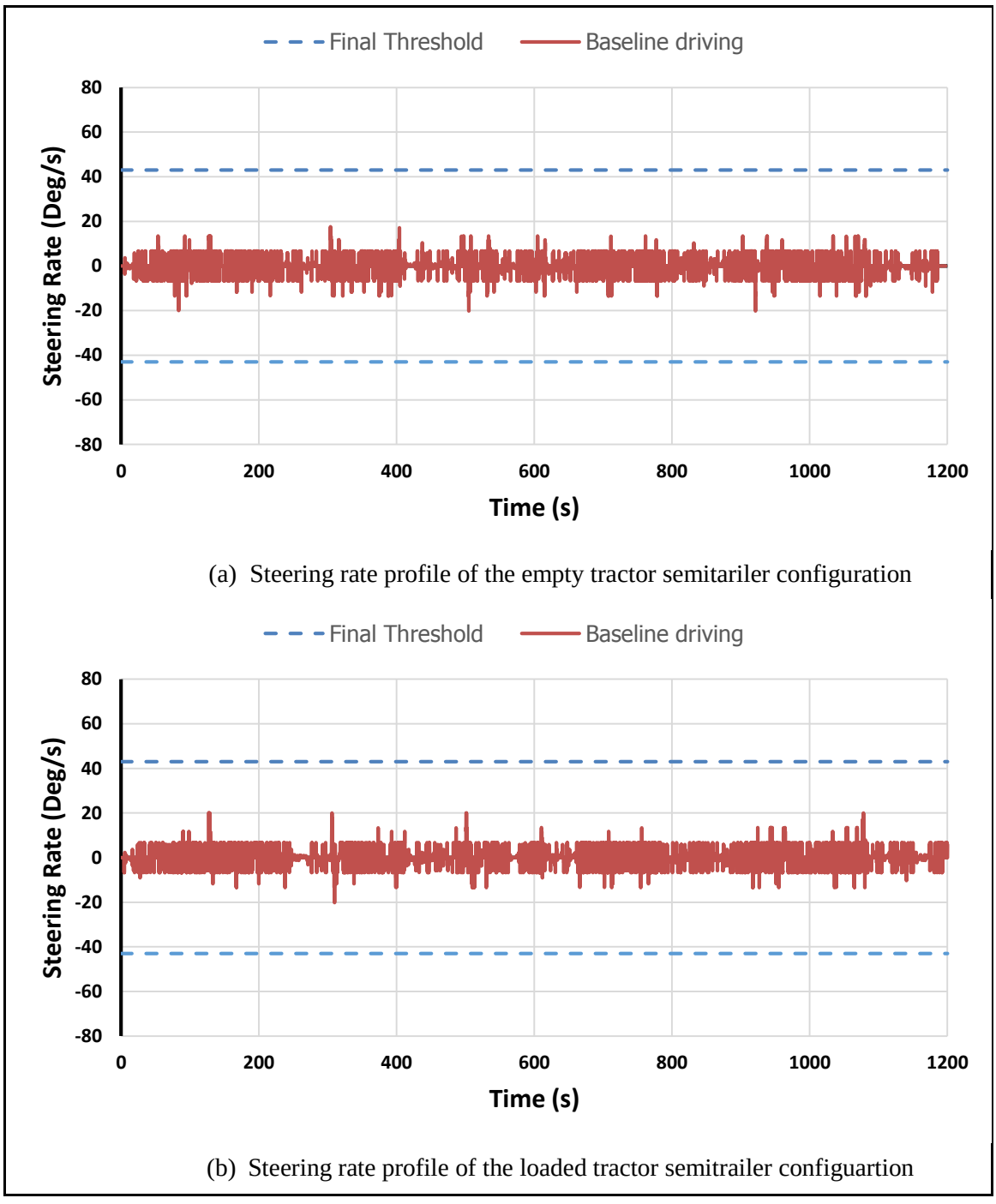

(a) Steering rate profile of the empty tractor semitariler configuration

(b) Steering rate profile of the loaded tractor semitrailer configuartion

Figure 5-10 Comparison between empty and loaded tractor semitrailer configurations

It can be observed from Figure 5-10 that the final steering rate threshold value is suitable for any section of the highway and for the empty and loaded tractor semitrailer vehicle configurations. It should be noted that the simulator can collect data for 20 minutes only and data recording stops after that.

5.6 FINAL REAL TIME DRIVER DISTRACTION ALERT SYSTEM

The findings of the offline analysis led to the development of a real time driver distraction alert system. However, the real time analysis tested the suggested real time driver distraction alert system to validate its reliability and make improvements to the system if needed. The real time analysis led to the development of the final real time driver distraction alert system. The final alert system issues a visual warning signal to notify drivers of their distracted driving behaviour as shown in Figure 5-11.

Figure 5-11 Final real time driver distraction alert system

The system also issues an audible warning signal telling the driver to look out. The first method of detection can issue the warning signal anytime while driving. Nonetheless, the second method can issue the warning signal whenever the baseline period is over and the driver will get a visual and audible warning telling the driver that the baseline is ready. This means baseline period is over and the system can detect driver distraction. The warning signal is triggered whenever the steering rate exceeds the final steering rate threshold range. It should be noted that the final real time driver distraction alert system is designed for highway driving and the system starts detecting distraction at speeds of 80 km/h and above.

5.7 CHAPTER SUMMARY

This chapter tested the suggested real time driver distraction alert system through a set of baseline and distraction driving experiments. The steering rate profile of baseline driving period was compared with distracted driving period during the same simulation and the deviation of the steering rate profile from the baseline was used as the main indicator of driver distraction.

The driving experiments of the first real time detection method revealed that a final steering rate threshold of 43 deg/s is the most suitable for distraction detection. Furthermore, the driving experiments of the second method revealed that an allowance factor of 1.4 and a threshold range of 34-49 deg/s can indicate driver distraction in real time. The comparison between the first and second distraction detection methods showed that the threshold value of the first method can accommodate a variety of driving styles. Additionally, this threshold value is suitable for the tractor semitrailer vehicle configuration. However, the variable

threshold range of the second method can have high threshold values that are close to the steering rate of a distracted driver and can affect the effectiveness of the detection system.

It was found that the final steering rate threshold is applicable to any section of the highway. Moreover, the steering rate threshold is applicable to the empty and fully loaded tractor semitrailer vehicle configurations since the steering rate profile of both configurations is in the same range. The final real time driver distraction alert system issues a visual and audible warning signal whenever the steering rate of the driver exceeds the final steering rate threshold range.

CHAPTER 6

CONCLUSIONS AND FUTURE WORK

6.1 ACCOMPLISHEMENTS

The thesis proposed a novel algorithm for estimating driver distraction by monitoring the steering wheel angle rate. This algorithm, has been tested using a commercial driving simulator and applied for a tractor semitrailer combination driven on paved highways during different driving experiments. For this purpose, the following goals have been accomplished:

- The Virage VS600M truck driving simulator model has been validated by comparing the results with TruckSim package to ensure that the simulator model is comparable to real trucks and can be used to study distraction effectively.
- Modified the offline drowsiness detection methods to be applicable for the detection of driver distraction. Therefore, the most appropriate driver input and distraction indicator for the real time application have been identified.
- Proposed two real time driver distraction detection methods that use the amplitude of the steering rate as the main indicator of driver distraction. Additionally, the steering rate threshold range has been established to discern between normal and distracted driving behaviour.
- The proposed algorithms have been successfully implemented in the truck driving simulator software in order to monitor the driving behaviour and determine the steering rate, maximum absolute steering rate and the final steering rate threshold values.

- Developed a real time driver distraction alert system that issues a visual and audible warning signal to notify the driver whenever the steering rate exceeds the final threshold range. Additionally, the proposed real time driver distraction alert system has been added as a new feature to the Virage VS600M truck driving simulator.

6.2 GENERAL CONCLUSIONS

Vehicle accidents related to driver distraction have resulted in injuries, fatalities and economic losses worldwide. The objective of this study is to develop a real time driver distraction alert system that can detect distraction at an early stage and prevent vehicle accidents. The thesis first reviewed truck simulator validation techniques used in previous studies and the causes of driver inattentiveness such as; sleepiness, fatigue, monotony as well as distraction. The driver inattentiveness monitoring techniques were divided into vehicle, driver and vehicle-driver interface monitoring techniques. The vehicle monitoring techniques such as the lane departure warning system require image processing and may not function properly if the lane markings are not clear. Furthermore, driver monitoring techniques such as the percentage of eye closure may not work under different illumination conditions plus this technique demands high computational power due to image processing. In contrast, the vehicle-driver monitoring techniques such as using the steering wheel to discern levels of driver alertness is simple, non-intrusive and cheap since it requires low computational power. As a result, the vehicle-driver interface monitoring technique has been chosen to develop a real time driver distraction alert system.

The Virage VS600M truck driving simulator model was validated with TruckSim by implementing identical technical specifications and identical vehicle speeds and driving maneuvers. The main goal of the validation was to ensure that simulator model generates

realistic results and can be used to accurately study the effects of distraction on the driving performance. The simulator validation was evaluated by comparing the steering wheel angle generated from the driver model in TruckSim with the human driver in the simulator. The low speed, double lane change and the highway driving maneuvers were sufficient for evaluating the validity of the simulator. The validation revealed that the simulator model is valid for different vehicle speeds and driving maneuvers.

The offline analysis investigated the effects that distraction can have on the steering wheel and accelerator pedal driving inputs. The jerk profile, rate of change and spikiness index of both the steering angle and pedal position were used to discern the level of driver distraction. The sum squared error was used to quantify the difference between baseline and distracted driving profile and generate distraction indicators. The main goal of the offline analysis was to determine the most suitable distraction indicator for the real time application. The offline analysis revealed that the steering jerk profile, rate of change and spikiness index are indicative of driver distraction. However, the steering jerk profile and spikiness index require storing data for at least 20 seconds which would result in late distraction warnings. It was also found that the accelerator pedal indicators are not indicative of driver distraction. As a result, the amplitude of the steering rate profile has been chosen to indicate driver distraction in real time.

The real time analysis was comprised of two real time distraction detection methods. The main goal of the real time analysis was to test and compare the suggested real time distraction detection methods and provide a description of the real time driver distraction alert system implemented on the truck driving simulator. The first detection method utilized a single steering rate threshold range to detect distraction while the second method

monitors the first few minutes of driving and generates a final steering rate threshold automatically in real time. The real time analysis of the first detection method revealed that a steering rate threshold of 43 deg/s is the most suitable for distraction detection and can accommodate a variety of driving styles. Moreover, the analysis of the second method revealed that an allowance factor of 1.4 and final threshold of 34-49 deg/s can detect distraction. However, the first method is preferred over the second since the second method can result in high threshold values that are comparable to steering rate of a distracted driver. It was also found that the steering rate threshold range is independent of the payload added to the tractor semitrailer and the path profile.

6.3 CONSIDERATION FOR FUTURE WORK

The distraction detection alert system should be tested extensively on a large pool of drivers to confirm that this system can accommodate all driving styles. Further work should be done to improve the baseline driving concept. The first real time detection method can detect driver distraction for a variety of driving styles. The second real time detection method can build a steering rate threshold for a specific driver but it requires the first few minutes of driving to create a baseline. The issue with the second method is that the system requires a perfect baseline to function properly. This problem can be solved by using a combination of both the first and second real time detection methods. The system starts with a single steering rate threshold value during the first few minutes of driving and after the baseline period is over, the threshold value will be adjusted to a specific driving style. Furthermore, the single steering rate threshold can be used to determine if the high threshold values represent a driving style or distraction occurrence. For example, if the

maximum absolute steering rate values stay higher than the threshold value for a while this represent a driving style.

Additionally, the relationship between the steering rate and the different vehicle configurations should be investigated thoroughly especially if the first real time detection method or a combination of both methods will be used to detect driver distraction since the single steering rate threshold value may differ based on the vehicle configuration used.

Finally, the driver distraction detection alert system presented in this thesis should be implemented in real vehicles. This could be done by having a steering wheel angle sensor, Arduino board and a light bulb or any warning signal. The steering rate algorithm can be programmed into the Arduino board. Implementing the real time distraction detection system in real vehicles will give a better understanding of how the system would perform in a real driving environment compared to the simulation environment.

PUBLICATIONS

L. Dababneh and M. El-Gindy, "Driver vigilance level detection systems: a literature survey," *International Journal of Vehicle Performance*, vol. 2, pp. 1-29, 2015.

L. Dababneh, A.H.M Sharaf and M. El-Gindy, "Real-Time Non-Intrusive Monitoring and Prediction of Driver Distraction," *International Journal of Vehicle Systems Modelling and Testing*, (accepted).

Note that parts of the above publications are contained in this work. All of the content in this work and publications were completed by the author. The co-authors provided technical support and reviews when needed to the work.

REFERENCES

[1] P. Strohl, J. Blatt, F. Council, K. Georges, J. Kiley, R. Kurrus, A. McCarrt, S. Merrit, A. Pack, S. Rogus, T. Roth, J. Stutts, P. Waller and D. Willis, "Drowsy driving and automobile crashes," National Highway Traffic Safety Administration, Washington DC, 1998.

[2] R. Grace, V. E. Byrne, D. M. Bierman, J.-M. Legrand, D. Gricourt, B. Davis, J. J. Staszewski and B. Carnahan, "A drowsy driver detection system for heavy vehicles," *Proceedings of the AIAA/IEEE/SAE Digital Avionics Systems Conference*, vol. 2, pp. I36/1-I36/8, 31-7 October- November 1998.

[3] J.-S. Wang, R. R. Knipling and L. J. Blincoe, "Motor vehicle crash involvements: A multi-dimensional problem size assessment," *Proceedings of the 1996 Annual Meeting of ITS America*, pp. 958-965, 1996.

[4] Transport Canada, "Road Safety in Canada," 2011. [Online]. Available: http://www.tc.gc.ca/eng/motorvehiclesafety/tp-tp15145-1201.htm. [Accessed 9 November 2015].

[5] ROSPA, "Driver Fatigue and Road Accidents: A Literature Review and Position Paper," 2001. [Online]. Available: http://www.rospa.com/. [Accessed 9 November 2015].

[6] Chris Hall, "OPP continue to investigate Hwy. 401 crash that killed three in Whitby," 4 October 2015. [Online]. Available:

http://www.durhamregion.com/news-story/5944202-opp-continue-to-investigate-hwy-401-crash-that-killed-three-in-whitby. [Accessed 30 December 2015].

[7] A. Rose, R. Evans and G. Wheaton, Methodological approaches for simulator evaluations, San Diego, California: Academic Press, 1987.

[8] H. Jamson, "Curve negotiation in the Leeds Driving Simulator: the role of driver experience," *Engineering in psychology and cognitive ergonomics*, vol. 3, pp. 351-358, 1999.

[9] S. Espié, P. Gauriat and M. Duraz, "Driving simulator validation: The issue of transferability of results acquired on simulator," *Proceeding of the Driving Simulator Conference*, pp. 149-156, 2005.

[10] F. Panerai, J. Droulez, J. Kelada, A. Kemeny, E. Balligand and B. Favre, "Speed and safety distance control in truck driving: comparison of simulation and real-world environment," *Proceedings of the driving simulation conference*, pp. 91-107, 2001.

[11] A. H. Hoskins, "Development and validation of the Pennsylvania truck driving simulator," The Pennsylvania State University, Pennsylvania, USA, 2002.

[12] J. P. Chrstos and G. J. Heydinger, "Evaluation of VDANL and VDM RoAD for predicting the vehicle dynamics of a 1994 Ford Taurus," SAE Technical Paper, 1997.

[13] A. Hoskins and M. El-Gindy, "Technical report: Literature survey on driving simulator validation studies," *International journal of heavy vehicle systems*, vol. 13, no. 3, pp. 241-252, 2006.

[14] A. V. Desai and M. A. Haque, "Vigilance monitoring for operator safety: A simulation study on highway driving," *Journal of safety research*, vol. 37, no. 2, pp. 139-147, 2006.

[15] Oxford Dictionary, [Online]. Available: http://www.oxforddictionaries.com/. [Accessed 9 November 2015].

[16] F. Sagberg, P. Jackson, H.-P. Krüger, A. Muzet and A. Williams, "Fatigue, sleepiness and reduced alertness as risk factors in driving," Institute of Transport Economics, Oslo, Norway, 2004.

[17] D. F. Dinges, "An overview of sleepiness and accidents," *Journal of sleep research*, vol. 4, no. 2, pp. 4-14, 1995.

[18] J. C. Stutts, J. W. Wilkins and B. V. Vaughn, "Why do people have drowsy driving crashes: Input from drivers who just did," American Automobile Association Foundation for Traffic Safety, Washington DC, 1999.

[19] "Mobile phone use: a growing problem of driver distraction," World Health Organization, Geneva, Switzerland, 2011.

[20] M. A. Regan, J. D. Lee and K. L. Young, "Introduction," in *Driver Distraction: Theory, Effects and Mitigation*, Boca Raton, FL, USA, CRC Press Taylor & Francis Group, 2009, pp. 3-7.

[21] National Cooperative Highway Research Program, "Drowsy and Distracted Drivers," 2005. [Online]. Available: http://safety.transportation.org/htmlguides/DDD/Section03.htm. [Accessed 30 December 2015].

[22] . T. Brandt, R. Stemmer and A. Rakotonirainy , "Affordable visual driver monitoring system for fatigue and monotony," *Proceedings of the IEEE International Conference on Systems, Man and Cybernetics*, vol. 7, pp. 6451-6456, 10-13 October 2004.

[23] G. W. Williams and R. E. Shor, "A historical note on highway hypnosis," *Accident Analysis & Prevention*, vol. 2, no. 3, pp. 223-225, 1970.

[24] J. Culp, M. El-Gindy and M. Haque, "Non-Intrusive Driver Drowsiness Monitoring Via Artificial Neural Networks," *SAE International SP 2164*, 2008.

[25] S.-Y. Kim and S.-Y. Oh, "A driver adaptive lane departure warning system based on image processing and a fuzzy evolutionary technique," *Proceedings of the IEEE Intelligent Vehicles Symposium*, pp. 361-365, 9-11 June 2003.

[26] Y. Yim and S.-Y. Oh, "Three-feature based automatic lane detection algorithm (TFALDA) for autonomous driving," *Proceedings of the IEEE/IEEJ/JSAI*

International Conference on Intelligent Transportation Systems, pp. 929-932, 5-8 October 1999.

[27] C. R. Jung and C. R. Kelber, "A lane departure warning system using lateral offset with uncalibrated camera," *Proceedings of the IEEE Conference on Intelligent Transportation Systems,* pp. 102-107, 13-15 September 2005.

[28] C. Kreucher, S. Lakshmanan and K. Kluge, "A driver warning system based on the LOIS lane detection algorithm," *Proceedings of the IEEE International Conference on Intelligent Vehicles,* vol. 1, pp. 17-22, 1998.

[29] D. J. LeBlanc, G. E. Johnson, P. T. Venhovens, G. Gerber, R. DeSonia, R. Ervin, C.-F. Lin, A. Ulsoy and T. Pilutti, "CAPC: An implementation of a road-departure warning system," *Proceedings of the IEEE International Conference on Control Applications,* pp. 590-595, 15-18 September 1996.

[30] Volvo Car Group, "Volvo Cars introduces new systems for alerting tired and distracted divers," 28 August 2007. [Online]. Available: https://www.media.volvocars.com/global/en-gb/media/pressreleases/12130. [Accessed 9 November 2015].

[31] Daimler AG, "TecDay Real Life Safety," 12 November 2008. [Online]. Available: http://media.daimler.com/dcmedia/0-921-658892-1-1147922-1-0-0-0-0-1-12759-614216-0-0-0-0-0-0-0.html?TS=1447105960862. [Accessed 9 November 2015].

[32] Daimler AG, "Lane Keeping Assist: Always on the Right Track | Daimler >Technology & Innovation > Safety > Prevention," 15 June 2015. [Online]. Available: http://www.daimler.com/dccom/0-5-1210218-1-1210351-1-0-0-1210228-0-0-135-0-0-0-0-0-0-0-0.html. [Accessed 9 November 2015].

[33] American Honda Motor, "Honda CR-V Sensing," 2015. [Online]. Available: http://automobiles.honda.com/cr-v/honda-sensing.aspx. [Accessed 9 November 2015].

[34] Acura Canada, "Lane Keeping Assist System," 2015. [Online]. Available: https://www.acura.ca/rlx/technology. [Accessed 5 November 2015].

[35] Ford of Europe, "Ford Technology Newsbrief (Driver Alert)," August 2010. [Online]. Available: http://technology.fordmedia.eu/documents/newsletter/FordTechnologyNewsletter082010.pdf. [Accessed 9 November 2015].

[36] Cadillac Canada, "Cadillac ATS - 2015," 2015. [Online]. Available: http://media.cadillac.com/media/us/en/cadillac/vehicles/ats/2015.html. [Accessed 6 November 2015].

[37] Toyota, "Toyota Lane Keeping Assist," 2015. [Online]. Available: http://www.toyota-global.com/innovation/safety_technology/safety_technology/technology_file/active/lka.html. [Accessed 9 November 2015].

[38] C.-T. Lin, C.-J. Chang, B.-S. Lin, S.-H. Hung, C.-F. Chao and I.-J. Wang, "A real-time wireless brain–computer interface system for drowsiness detection," *IEEE Transactions on Biomedical Circuits and Systems,* vol. 4, no. 4, pp. 214-222, 2010.

[39] N. R. Pal, C.-Y. Chuang, L.-W. Ko, C.-F. Chao, T.-P. Jung, S.-F. Liang and C.-T. Lin, "EEG-based subject-and session-independent drowsiness detection: an unsupervised approach," *EURASIP Journal on Advances in Signal Processing,* vol. 2008, p. 192, 2008.

[40] A. Picot, S. Charbonnier and A. Caplier, "On-line automatic detection of driver drowsiness using a single electroencephalographic channel," *Proceedings of the 30th Annual International Conference of the IEEE Engineering in Medicine and Biology Society,* pp. 3864-3867, 20-25 August 2008.

[41] C.-T. Lin, Y.-C. Chen, T.-Y. Huang, T.-T. Chiu, L.-W. Ko, S.-F. Liang, H.-Y. Hsieh, S.-H. Hsu and J.-R. Duann, "Development of wireless brain computer interface with embedded multitask scheduling and its application on real-time driver's drowsiness detection and warning," *IEEE Transactions on Biomedical Engineering,* vol. 55, no. 5, pp. 1582-1591, 2008.

[42] V. Savchenko, "Monitoring of an operator's vigilance level by skin resistance response," *Control Engineering Practice,* vol. 4, no. 1, pp. 67-72, 1996.

[43] A. Azman, Q. Meng and E. Edirisinghe, "Non intrusive physiological measurement for driver cognitive distraction detection: Eye and mouth movements," *3rd*

International Conference on Advanced Computer Theory and Engineering (ICACTE), vol. 3, pp. V3-595-V3-599, 2010.

[44] W. W. Wierwille, S. Wreggit, C. Kirn, L. Ellsworth and R. J. Fairbanks, "Research on vehicle based driver status/performance monitoring: development, validation, refinement of algorithms for detection of driver drowsiness," National Highway Traffic Safety Administration, Washington DC, USA, 1994.

[45] D. F. Dinges and R. Grace, "PERCLOS: A valid psychophysiological measure of alertness as assessed by psychomotor vigilance," Federal Highway Administration. Office of motor carriers, USA, 1998.

[46] I. Park, J.-H. Ahn and H. Byun, "Efficient measurement of eye blinking under various illumination conditions for drowsiness detection systems," *Proceedings of the IEEE 18th International Conference on Pattern Recognition,* vol. 1, pp. 383-386, 2006.

[47] D. Tock and I. Craw, "Tracking and measuring drivers' eyes," *Image and Vision Computing,* vol. 14, no. 8, pp. 541-547, 1996.

[48] M. Kaneda, H. Obara and T. Nasu, "Adaptability to ambient light changes for drowsy driving detection using image processing," *JSAE Review,* vol. 20, no. 1, pp. 133-136, 1999.

[49] M. Eriksson and N. P. Papanikolopoulos, "Driver fatigue: a vision-based approach to automatic diagnosis," *Transportation Research Part C: Emerging Technologies,* vol. 9, no. 6, pp. 399-413, 2001.

[50] T. Hong and H. Qin, "Drivers drowsiness detection in embedded system," *Proceedings of the IEEE International Conference on Vehicular Electronics and Safety,* pp. 1-5, 13-15 December 2007.

[51] H. Ueno, M. Kaneda and M. Tsukino, "Development of drowsiness detection system," *Proceedings of the IEEE Conference on Vehicle Navigation and Information Systems,* pp. 15-20, 31 August 1994.

[52] T. Ito, S. Mita, K. Kozuka, T. Nakano and S. Yamamoto, "Driver blink measurement by the motion picture processing and its application to drowsiness detection," *Proceeding of the IEEE 5th International Conference on Intelligent Transportation Systems,* pp. 168-173, 3-6 September 2002.

[53] S. Hu and G. Zheng, "Driver drowsiness detection with eyelid related parameters by Support Vector Machine," *Expert Systems with Applications,* vol. 36, no. 4, pp. 7651-7658, 2009.

[54] A. Picot, S. Charbonnier and A. Caplier, "Drowsiness detection based on visual signs: blinking analysis based on high frame rate video," *Proceedings of the IEEE Instrumentation and Measurement Technology Conference,* pp. 801-804, 3-6 May 2010.

[55] K. Sugiyama, T. Nakano, S. Yamamoto, T. Ishihara, H. Fujii and E. Akutsu, "Method of detecting drowsiness level by utilizing blinking duration," *JSAE Review,* vol. 17, no. 2, pp. 159-163, 1996.

[56] H. Dikkers, M. Spaans, D. Datcu, M. Novak and L. J. Rothkrantz, "Facial recognition system for driver vigilance monitoring," *Proceedings of the IEEE International Conference on Systems, Man and Cybernetics* , vol. 4, pp. 3787-3792, 2004.

[57] E. Vural, M. Çetin, A. Erçil, G. Littlewort, M. Bartlett and J. Movellan, "Automated drowsiness detection for improved driving safety," *Proceedings of the 4th international conference on automotive technologies,* 2008.

[58] S. Abtahi, B. Hariri and S. Shirmohammadi, "Driver drowsiness monitoring based on yawning detection," *IEEE Instrumentation and Measurement Technology Conference,* pp. 1-4, 10-12 May 2011.

[59] P. Smith, M. Shah and N. da Vitoria Lobo, "Monitoring head/eye motion for driver alertness with one camera," *Proceedings of the International Conference on Pattern Recognition,* vol. 4, p. 4636, 2000.

[60] Q. Ji and X. Yang, "Real-time eye, gaze, and face pose tracking for monitoring driver vigilance," *Real-Time Imaging,* vol. 8, no. 5, pp. 357-377, 2002.

[61] Q. Ji, Z. Zhu and P. Lan, "Real-time nonintrusive monitoring and prediction of driver fatigue," *IEEE Transactions on Vehicular Technology*, vol. 53, no. 4, pp. 1052-1068, 2004.

[62] . L. M. Bergasa, R. Barea, E. L. Guillén, . M. S. Escudero, L. Boquete and J. . I. Pinedo, "Facial Features Tracking Applied to Drivers Drowsiness Detection," *Proceedings of the 21st IASTED International Conference on Applied Informatics*, pp. 231-236, 10-13 February 2003.

[63] . L. M. Bergasa, J. Nuevo , M. A. Sotelo and M. Vazqeuz, "Real-time system for monitoring driver vigilance," *Proceedings of the IEEE Intelligent Vehicles Symposium*, pp. 78-83, 14-17 June 2004.

[64] Leon Kelion, "Caterpillar backs eye-tracker to combat driver fatigue," 2013. [Online]. Available: http://www.bbc.com/news/technology-22640279. [Accessed 9 November 2015].

[65] T. C. Chieh, M. M. Mustafa, A. Hussain, E. Zahedi and B. Majlis, "Driver fatigue detection using steering grip force," *Proceedings of the IEEE Student Conference on Research and Development*, pp. 45-48, 25-26 August 2003.

[66] J. Fukuda, E. Akutsu and K. Aoki, "An estimation of driver's drowsiness level using interval of steering adjustment for lane keeping," *JSAE review*, vol. 16, no. 2, pp. 197-199, 1995.

[67] A. Polychronopoulos, A. Amditis and E. Bekiaris, "Information data flow in awake multi-sensor driver monitoring system," *Proceedings of the IEEE Intelligent Vehicles Symposium*, pp. 902-906, 14-17 June 2004.

[68] Nissan, "Nissan's "Driver Attention Alert" Helps Detect Erratic Driving Caused By Drowsiness and Inattention," April 2015. [Online]. Available: http://nissannews.com/en-US/nissan/usa/releases/nissan-s-driver-attention-alert-helps-detect-erratic-driving-caused-by-drowsiness-and-inattention. [Accessed 9 November 2015].

[69] M. H. Hassoun, Fundamentals of artificial neural networks, Cambridge, MA: MIT press, 1995.

[70] M. Sivanandam, Introduction to artificial neural networks, New Delhi, India: vikas publishing House PVT LTD, 2009.

[71] K. L. Priddy and P. E. Keller, Artificial neural networks: an introduction, vol. 68, Bellingham,Washington: SPIE Press, 2005.

[72] G. A. Carpenter, "Neural network models for pattern recognition and associative memory," *Neural networks*, vol. 2, no. 4, pp. 243-257, 1989.

[73] . B. Carswell and . V. Chandran, "Automated recognition of drunk driving on highways from video sequences," *Proceedings of the IEEE International Conference on Image Processing*, vol. 2, pp. 306-310, 13-16 November 1994.

[74] K. Hayashi, K. Ishihara, H. Hashimoto and K. Oguri, "Individualized drowsiness detection during driving by pulse wave analysis with neural network," *Proceedings of the IEEE Conference on Intelligent Transportation Systems,* pp. 901-906, 13-16 September 2005.

[75] M. M. Bundele and R. Banerjee, "Detection of fatigue of vehicular driver using skin conductance and oximetry pulse: a neural network approach," *Proceedings of the 11th International Conference on Information Integration and Web-based Applications and Services,* pp. 739-744, 2009.

[76] P.-Y. Tsai, W. Hu, T. B. Kuo and L.-Y. Shyu, "A portable device for real time drowsiness detection using novel active dry electrode system," *Proceedings of the IEEE Annual International Conference of the Engineering in Medicine and Biology Society,* pp. 3775-3778, 3-6 September 2009.

[77] L. King, H. T. Nguyen and S. Lal, "Early driver fatigue detection from electroencephalography signals using artificial neural networks," *Proceedings of the IEEE 28th Annual International Conference of the Engineering in Medicine and Biology Society,* pp. 2187-2190, 30 August 2006.

[78] R. K. Sinha, "Artificial neural network and wavelet based automated detection of sleep spindles, REM sleep and wake states," *Journal of medical systems,* vol. 32, no. 4, pp. 291-299, 2008.

[79] S. Makeig, T.-P. Jung and T. J. Sejnowski, "Using feedforward neural networks to monitor alertness from changes in EEG correlation and coherence," *Advances in neural information processing systems,* pp. 931-937, 1996.

[80] A. Gevins and M. E. Smith, "Detecting transient cognitive impairment with EEG pattern recognition methods," *Aviation, space, and environmental medicine,* vol. 70, no. 10, pp. 1018-1024, 1999.

[81] A. Subasi, "Automatic recognition of alertness level from EEG by using neural network and wavelet coefficients," *Expert Systems with Applications,* vol. 28, no. 4, pp. 701-711, 2005.

[82] E. O. Andreeva, P. Aarabi, M. G. Philiastides, K. Mohajer and M. Emami, "Driver drowsiness detection using multimodal sensor fusion," *Proceeding of the SPIE-Multisensor,Multisource Information Fusion: Architectures, Algorithms, and Applications,* pp. 380-390, 2004.

[83] M. Tylee, M. Popovic, S. Yu and C. Craven, "Human responses to vibration therapy," *Proceedings of the 25th Annual International Conference of the IEEE Engineering in Medicine and Biology Society,* vol. 2, pp. 1705-1708, 17-21 September 2003.

[84] J. Rosen and M. Arcan, "Modeling the human body/seat system in a vibration environment," *Journal of biomechanical engineering,* vol. 125, no. 2, pp. 223-231, 2003.

[85] M. Wöllmer, C. Blaschke, T. Schindl, B. Schuller, B. Färber, S. Mayer and B. Trefflich, "Online driver distraction detection using long short-term memory," *IEEE Transactions on Intelligent Transportation Systems,* vol. 12, no. 2, pp. 574-582, 2011.

[86] R. Sayed and A. Eskandarian, "Unobtrusive drowsiness detection by neural network learning of driver steering," *Proceedings of the Institution of Mechanical Engineers, Part D: Journal of Automobile Engineering,* vol. 215, no. 9, pp. 969-975, 2001.

[87] A. Eskandarian and A. Mortazavi, "Evaluation of a smart algorithm for commercial vehicle driver drowsiness detection," *Proceedings of the IEEE Intelligent Vehicles Symposium,* pp. 553-559, 13-15 June 2007.

[88] J. Son and S. Park, "Cognitive workload estimation through lateral driving performance," SAE Technical Paper 0148-7191, 2011.

[89] B. B. Thompson, R. J. Marks, J. J. Choi, M. A. El-Sharkawi, M.-Y. Huang and C. Bunje, "Implicit learning in autoencoder novelty assessment," *Proceedings of the International Joint Conference on Neural Networks,* vol. 3, pp. 2878-2883, 12-17 May 2002.

[90] I. G. Daza, L. M. Bergasa, S. Bronte, J. J. Yebes, J. Almazán and R. Arroyo, "Fusion of optimized indicators from Advanced Driver Assistance Systems (ADAS) for driver drowsiness detection," *Sensors,* vol. 14, no. 1, pp. 1106-1131, 2014.

[91] L. Li, K. Werber, C. F. Calvillo, K. D. Dinh, A. Guarde and A. König, "Multi-sensor soft-computing system for driver drowsiness detection," in *Soft Computing in Industrial Applications*, Switzerland, Springer, 2014, pp. 129-140.

[92] Virage Simulation Incorporations, "TRUCK DRIVING SIMULATOR – VS600M," 2015. [Online]. Available: https://viragesimulation.com/vs600m-truck-simulator. [Accessed 2 January 2016].

[93] G. Sayer, "The Acute and Residual Effects of Cannabis on Driving and the Risk of Collision for People who Drive after using Alcohol and Drive after using Cannabis," 2014.

[94] Mechanical Simulation Corporation, "TruckSim handout," 2013. [Online]. Available: http://carsim.com/downloads/pdf/trucksim_handout.pdf. [Accessed 9 November 2015].

[95] M. El–Gindy, "An overview of performance measures for heavy commercial vehicles in North America," *International Journal of Vehicle Design,* vol. 16, no. 4-5, pp. 441-463, 1995.

[96] J. Wong, "Handling Characteristics of Road Vehicles," in *Theory of Ground Vehicles,* New Jersey, USA, John Wiley & Sons Inc., 2008, pp. 363-382.

[97] A. Savitzky and M. J. Golay, "Smoothing and differentiation of data by simplified least squares procedures," *Journal of Analytical Chemistry,* vol. 36, no. 8, pp. 1627-1639, 1964.

[98] Road Injury Prevention & Litigation Journal, "Audible Warning Systems Alert Drivers to Potential Dangers When Backing Up," 1 June 1998. [Online]. Available: http://www.usroads.com/journals/p/rilj/9806/ri980603.htm. [Accessed 9 November 2015].

[99] Tutorials Point, "LEARN LISP," 2014. [Online]. Available: http://www.tutorialspoint.com/lisp/lisp_tutorial.pdf. [Accessed 7 January 2016].

[100] Gordon S. Novak Jr., "Lisp Programming Lecture Notes," 1985. [Online]. Available: ftp://www.cs.utexas.edu/pub/AI-Lab/tech-reports/UT-AI-TR-85-6.pdf. [Accessed 7 January 2016].

[101] C. Rainey and S. McLaughlin, "Identifying Distraction: Kinematic Detection of Off-Road Eye GLances," National Surface Transportation Safety Center for Excellence, Blacksburg, Virginia, 2015.

[102] S. Singh, "Distracted driving and driver, roadway, and environmental factors," National Highway Traffic Safety Administration, Washington DC, 2010.

[103] M. A. Regan, J. D. Lee and K. L. Young, "Sources of Driver Distraction," in *Driver Distraction: Theory, Effects and Mitigation*, Boca Raton, FL, USA, CRC Press Taylor & Francis Group, 2009, pp. 249-279.

[104] National Highway Traffic Safety Administration (NHTSA), "Overview of the National Highway Traffic Safety Administration's Driver Distraction Program," 2010.[Online].Available:www.nhtsa.gov/staticfiles/nti/distracted_driving/pdf/811299.pdf. [Accessed 9 November 2015].

APPENDIX A– SAVITZKY-GOLAY FILTER

COEFFICIENTS

Table A-1 First derivative filter coefficients [96]

CONVOLUTES	1ST DERIVATIVE			CUBIC	QUARTIC		A31	A41			
POINTS	25	23	21	19	17	15	13	11	9	7	5
-12	30866										
-11	8602	3938									
-10	-8525	815	84075								
-09	-20982	-1518	10032	6936							
-08	-29236	-3140	-43284	68	748						
-07	-33754	-4130	-78176	-4648	-98	12922					
-06	-35003	-4567	-96947	-7481	-643	-4121	1133				
-05	-33450	-4530	-101900	-8700	-930	-14150	-660	300			
-04	-29562	-4098	-95338	-8574	-1002	-18334	-1578	-294	86		
-03	-23806	-3350	-79564	-8179	-902	-17842	-1796	-532	-142	22	
-02	-16649	-2365	-56881	-5363	-673	-13843	-1489	-503	-193	-67	1
-01	-8558	-1222	-29592	-2816	-358	-7506	-832	-296	-126	-58	-8
00	0	0	0	0	0	0	0	0	0	0	0
01	8558	1222	29592	2816	358	7506	832	296	129	58	8
02	16649	2365	56881	5363	673	13843	1489	503	193	67	-1
03	23806	3350	79504	8179	902	17842	1796	532	142	-22	
04	29562	4098	95338	8574	1002	18334	1578	294	-86		
05	33450	4530	101900	8700	930	14150	660	-300			
06	35003	4567	96947	7481	643	4121	-1133				
07	33754	4130	78176	4648	98	-12922					
08	29236	3140	43284	-68	-748						
09	20982	1518	-10032	-6936							
10	8525	-815	84075								
11	-8602	-3938									
12	-30866										
NORM	1776060	197340	3634092	255816	23256	334152	24024	5148	1188	252	12

Table A-2 Third derivative filter coefficient [96]

CONVOLUTES	3RD DERIVATIVE			CUBIC	QUARTIC		A33	A43			
POINTS	25	23	21	19	17	15	13	11	9	7	5
-12	-506										
-11	-253	-77									
-10	-55	-35	-285								
-09	93	-3	-114	-204							
-08	196	20	12	-68	-28						
-07	259	35	98	28	-7	-91					
-06	287	43	149	89	7	-13	-11				
-05	285	45	170	120	15	35	0	-30			
-04	258	42	166	126	18	58	6	6	-14		
-03	211	35	142	112	17	61	8	22	7	-1	
-02	145	25	103	83	13	49	7	23	13	1	-1
-01	77	13	54	44	7	27	4	14	9	1	2
00	0	0	0	0	0	0	0	0	0		0
01	-77	-13	-54	-44	7	-27	-4	-14	-9	-1	-2
02	-149	-25	-103	-83	13	-49	-7	-23	-13	-1	1
03	-211	-35	-142	-112	17	-61	-8	-22	-7	1	
04	-258	-42	-166	-126	18	-58	-6	-6	14		
05	-285	-45	-170	-120	15	-35	0	30			
06	-287	-43	-149	-89	7	13	11				
07	-259	-35	-98	-28	-7	91					
08	-196	-20	-12	68	28						
09	-93	3	114	204							
10	55	35	285								
11	253	77									
12	506										
NORM	296010	32890	86526	42636	3876	7956	572	858	198	6	2

APPENDIX B– ACCELERATOR PEDAL RESULTS

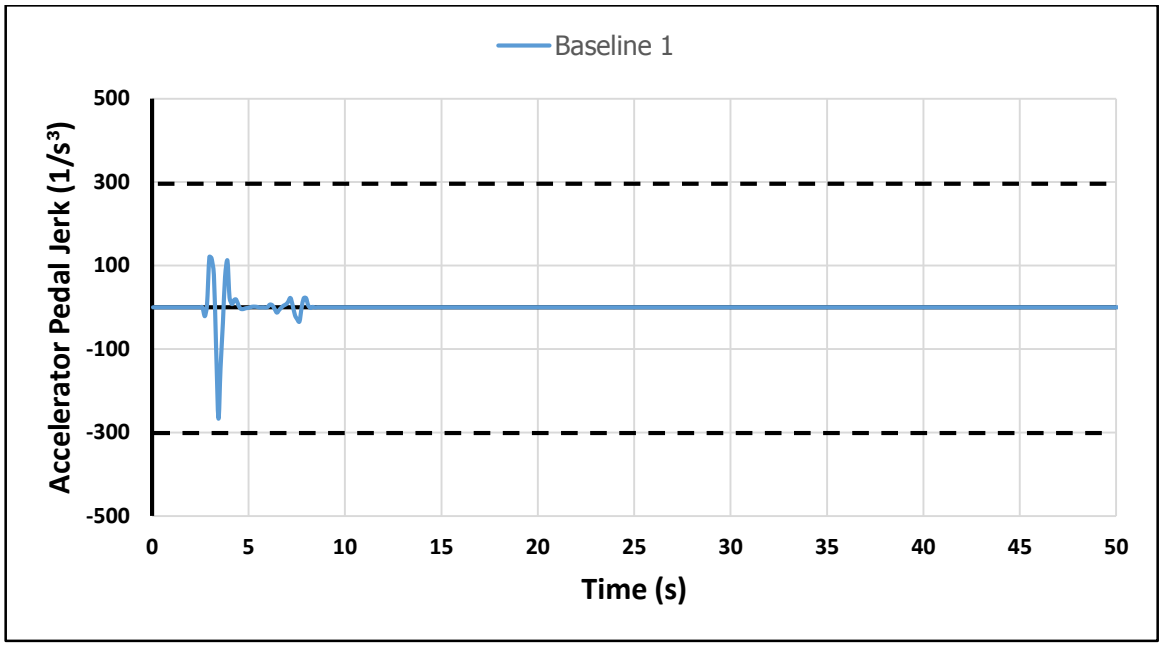

Figure B-1 Accelerator pedal jerk profile for a baseline driving experiment

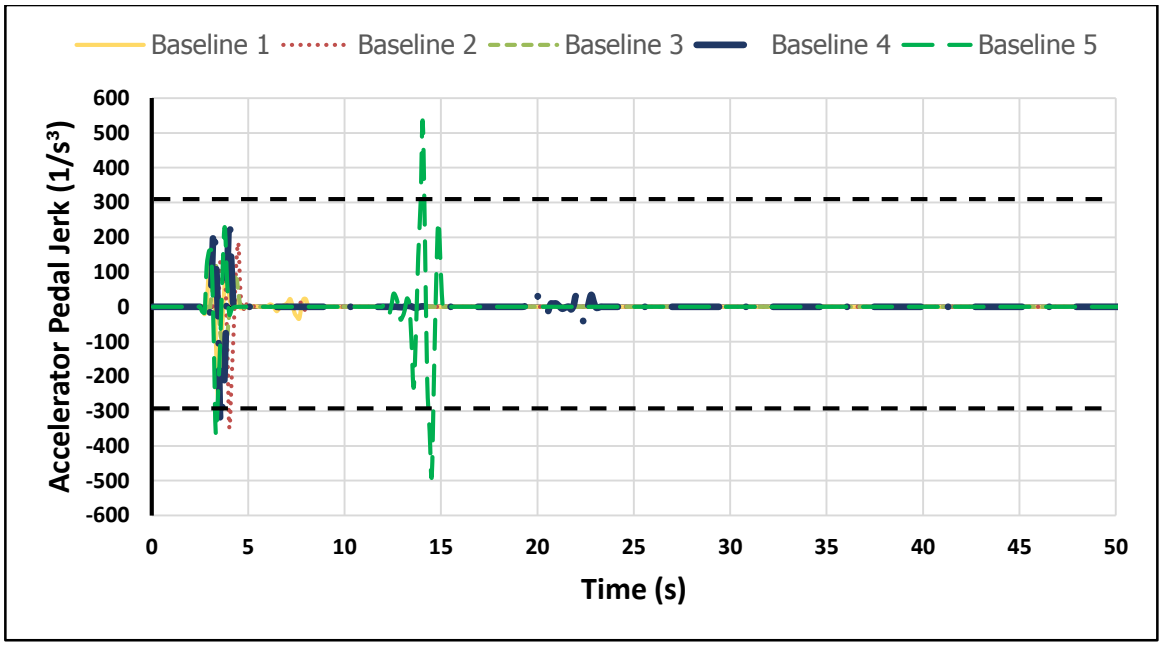

Figure B-2 Accelerator pedal jerk profile for baseline driving experiments

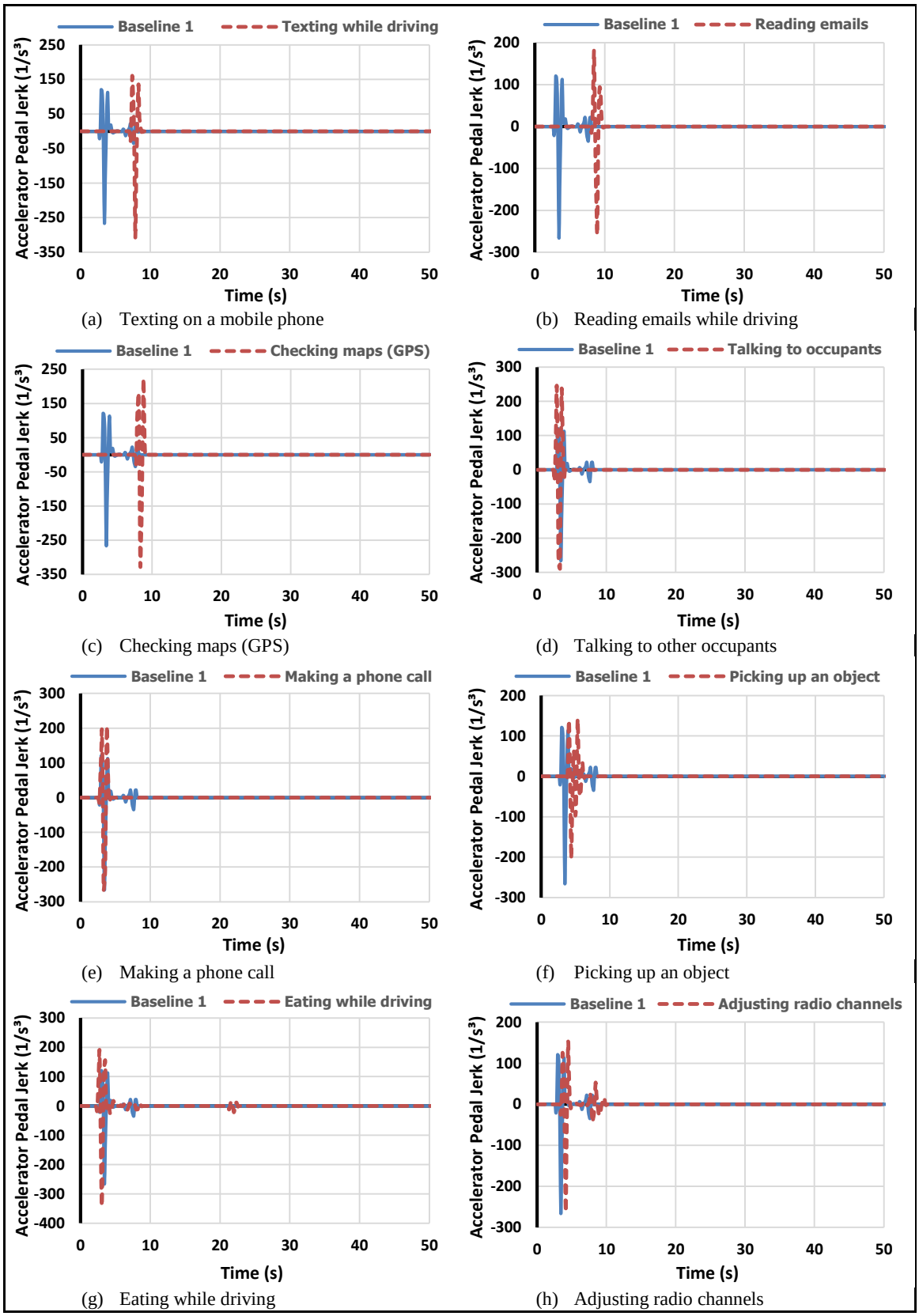

Figure B-3 Accelerator pedal jerk profile for distraction driving experiments

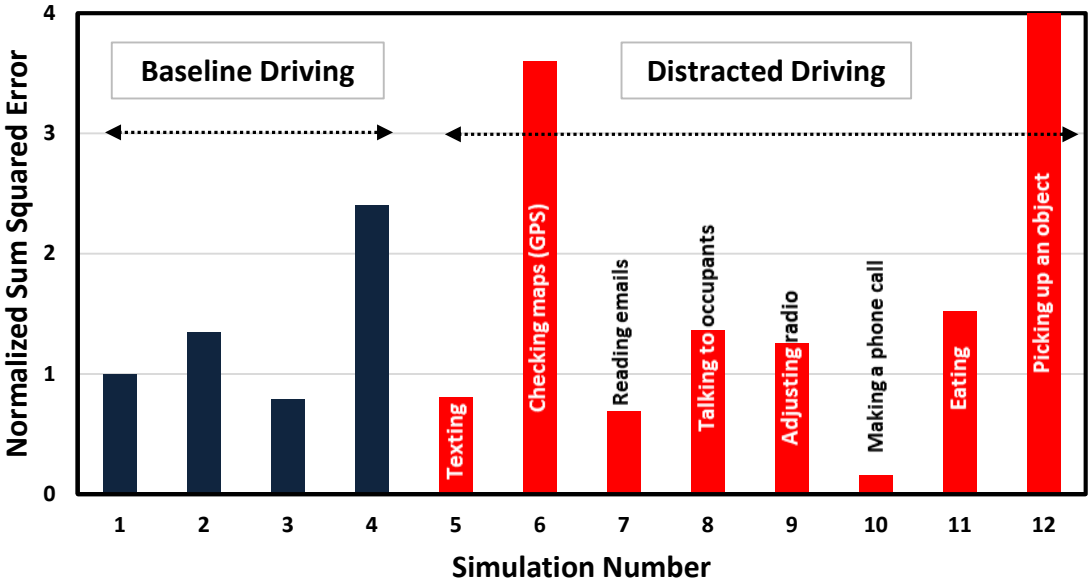

(a) Accelerator Pedal Jerk distraction indicator (first SSE)

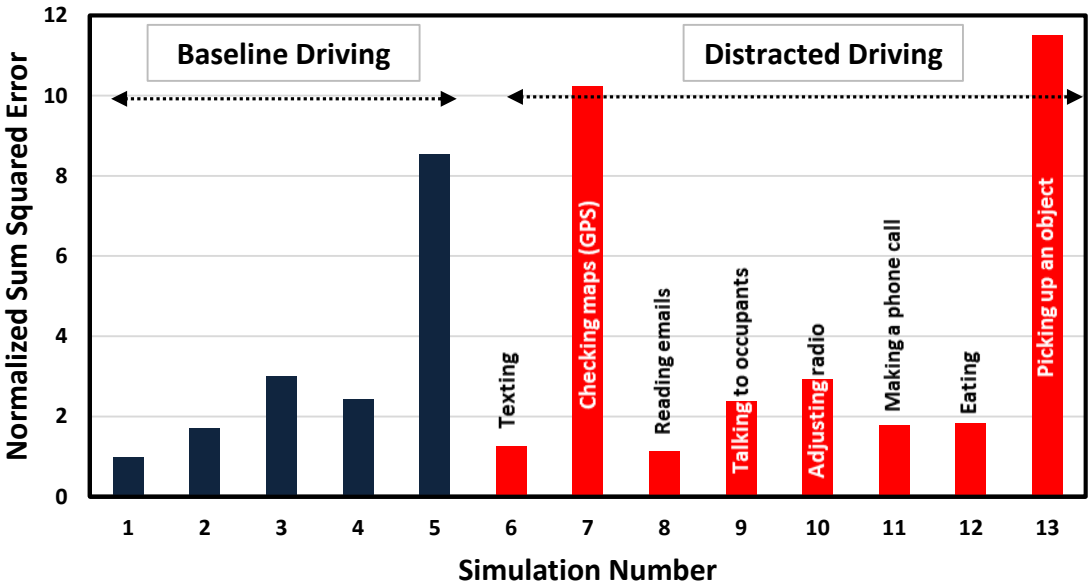

(b) Accelerator Pedal Jerk distraction indicator (second SSE)

Figure B-4 Accelerator pedal jerk profile distraction indicator

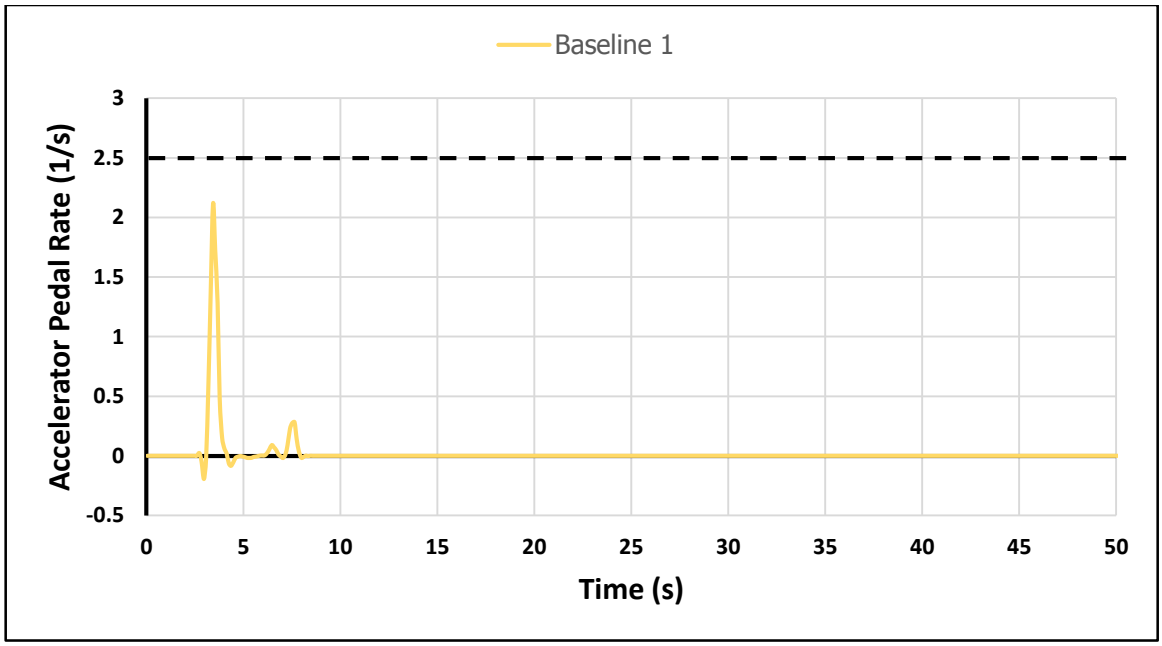

Figure B-5 Accelerator pedal rate profile for a baseline driving experiment

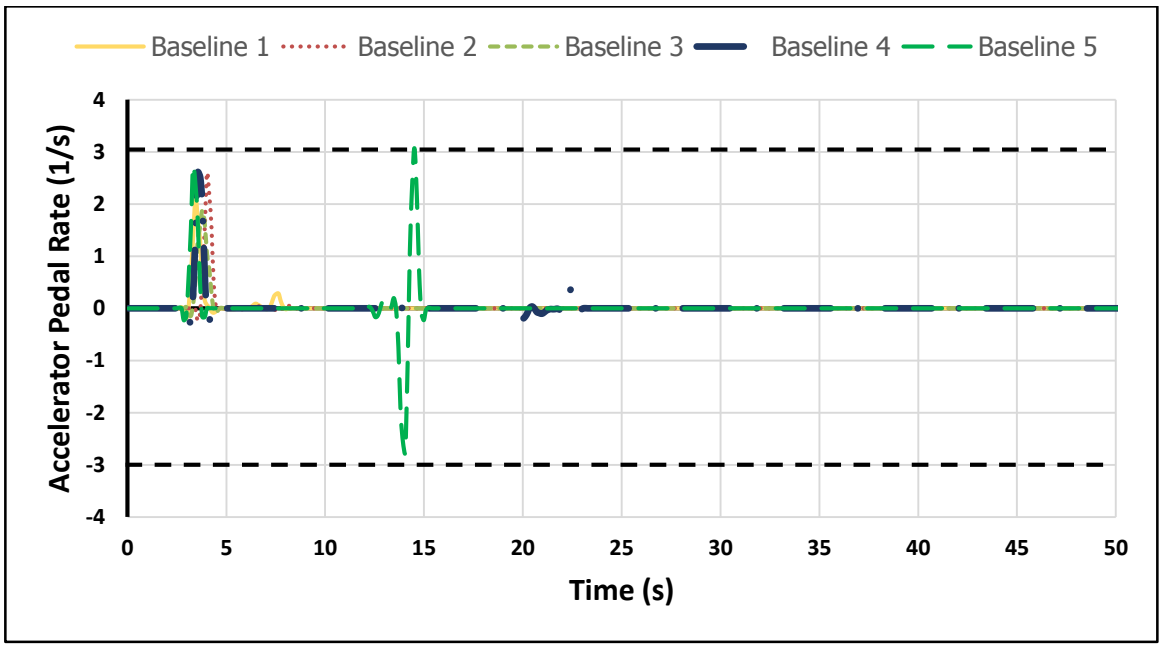

Figure B-6 Accelerator pedal rate profile for baseline driving experiments

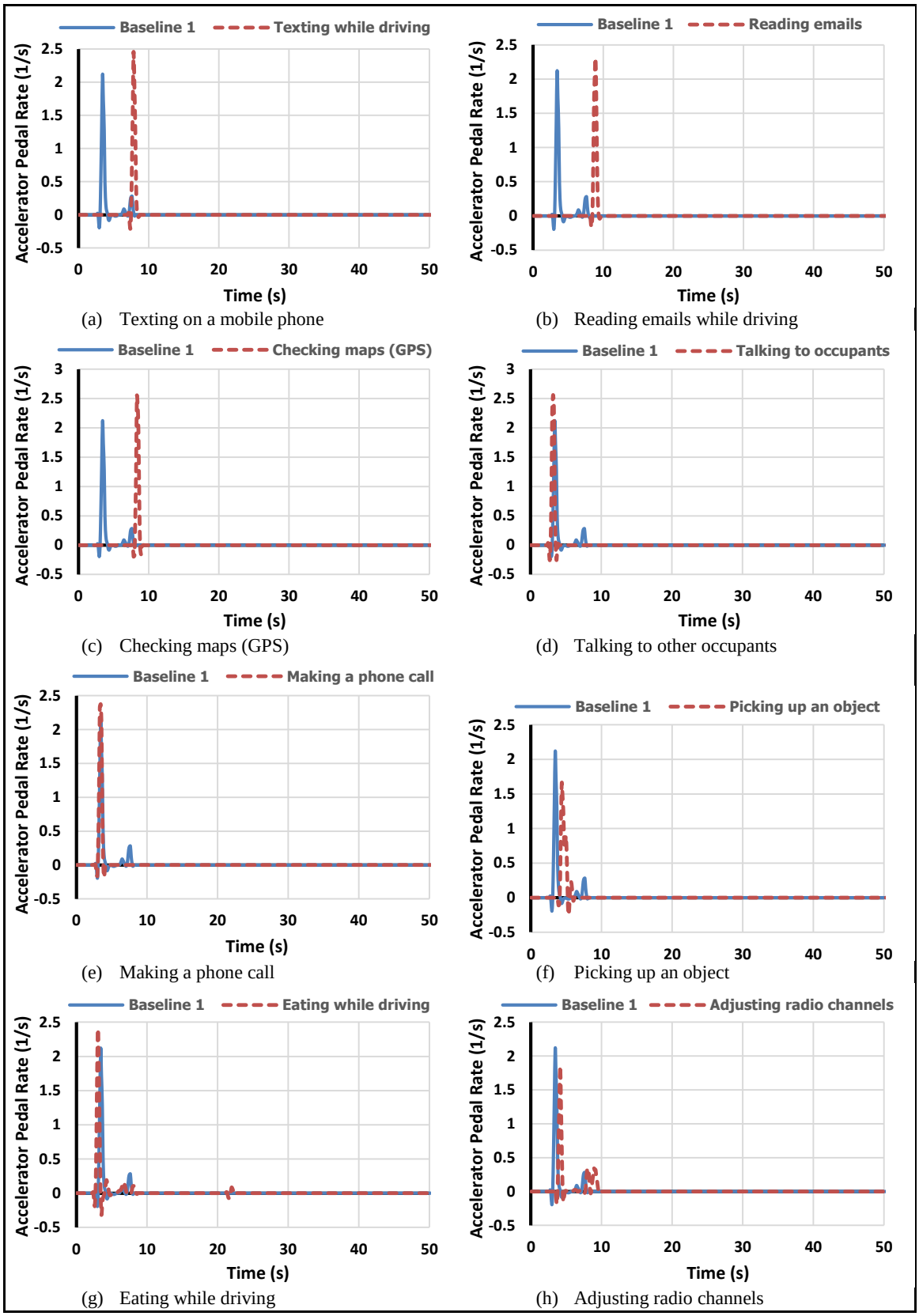

(a) Texting on a mobile phone

(b) Reading emails while driving

(c) Checking maps (GPS)

(d) Talking to other occupants

(e) Making a phone call

(f) Picking up an object

(g) Eating while driving

(h) Adjusting radio channels

Figure B-7 Accelerator pedal rate profile for distraction driving experiments

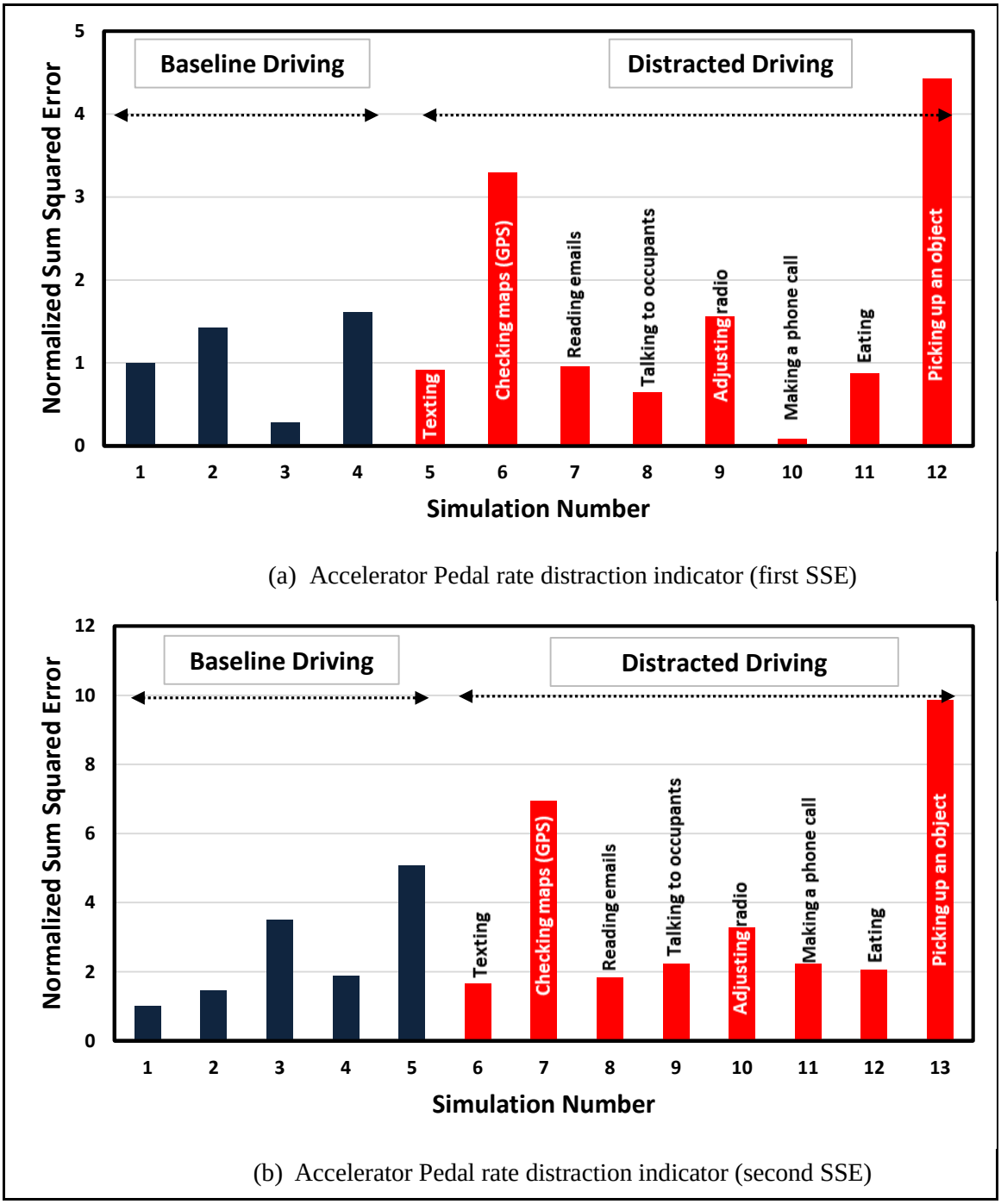

(a) Accelerator Pedal rate distraction indicator (first SSE)

(b) Accelerator Pedal rate distraction indicator (second SSE)

Figure B-8 Accelerator pedal rate distraction indicator

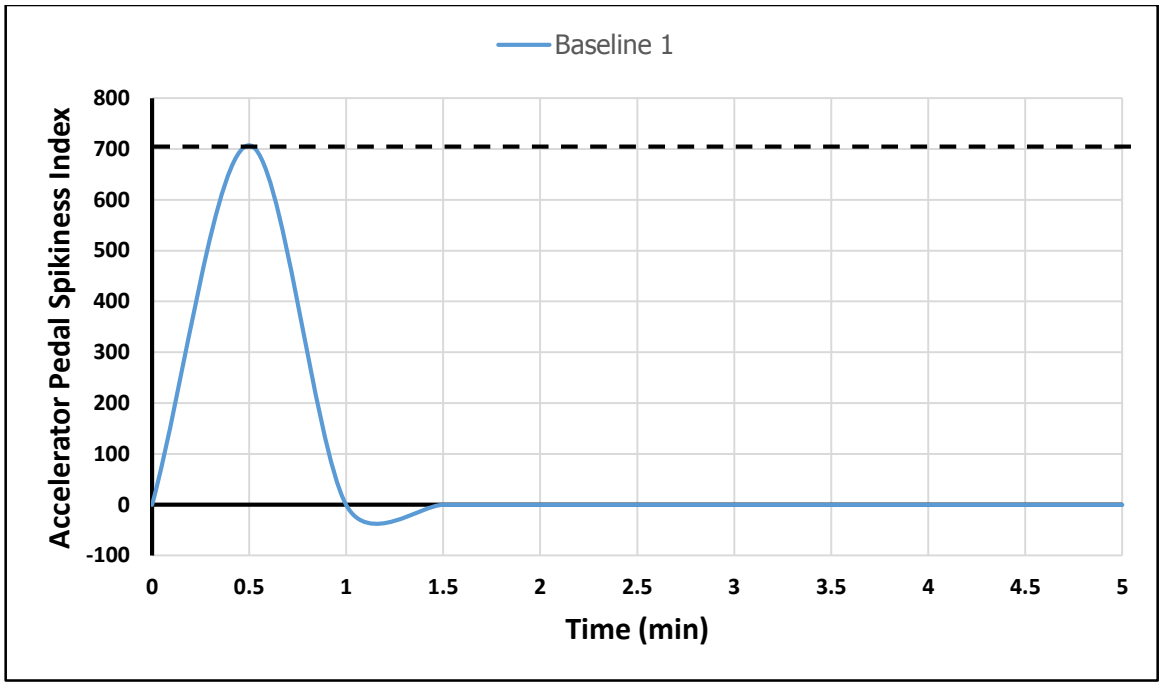

Figure B-9 Accelerator pedal spikiness index for a baseline driving experiment

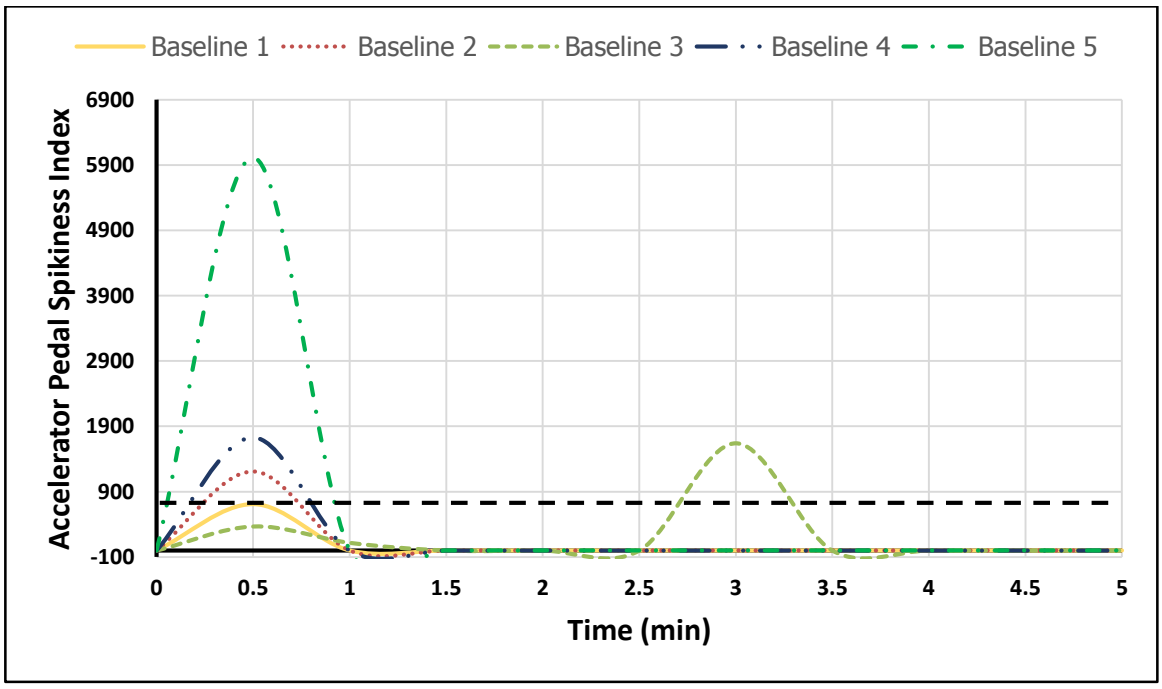

Figure B-10 Accelerator pedal spikiness index for baseline driving experiments

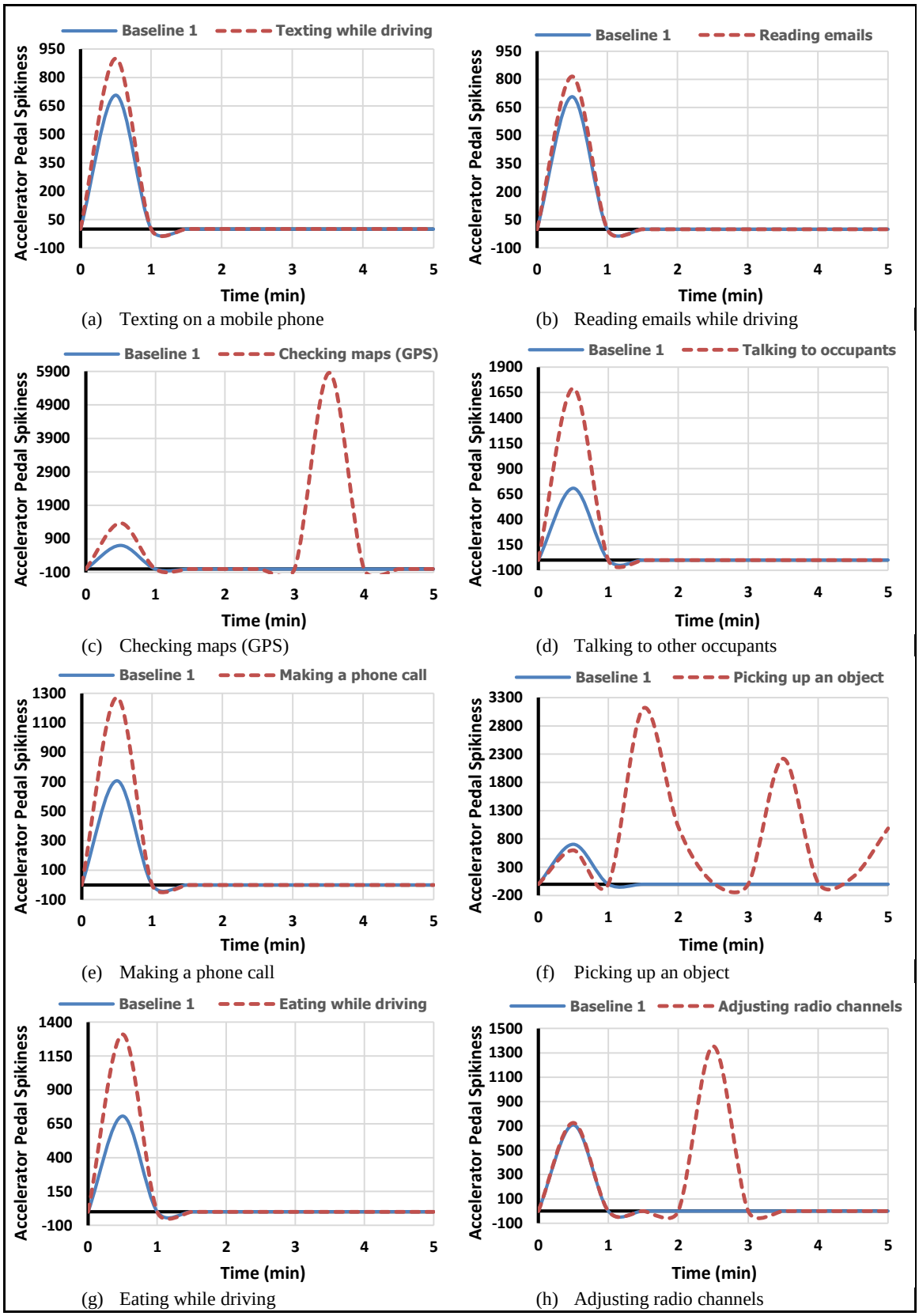

Figure B-11 Accelerator pedal spikiness index for distraction driving experiments

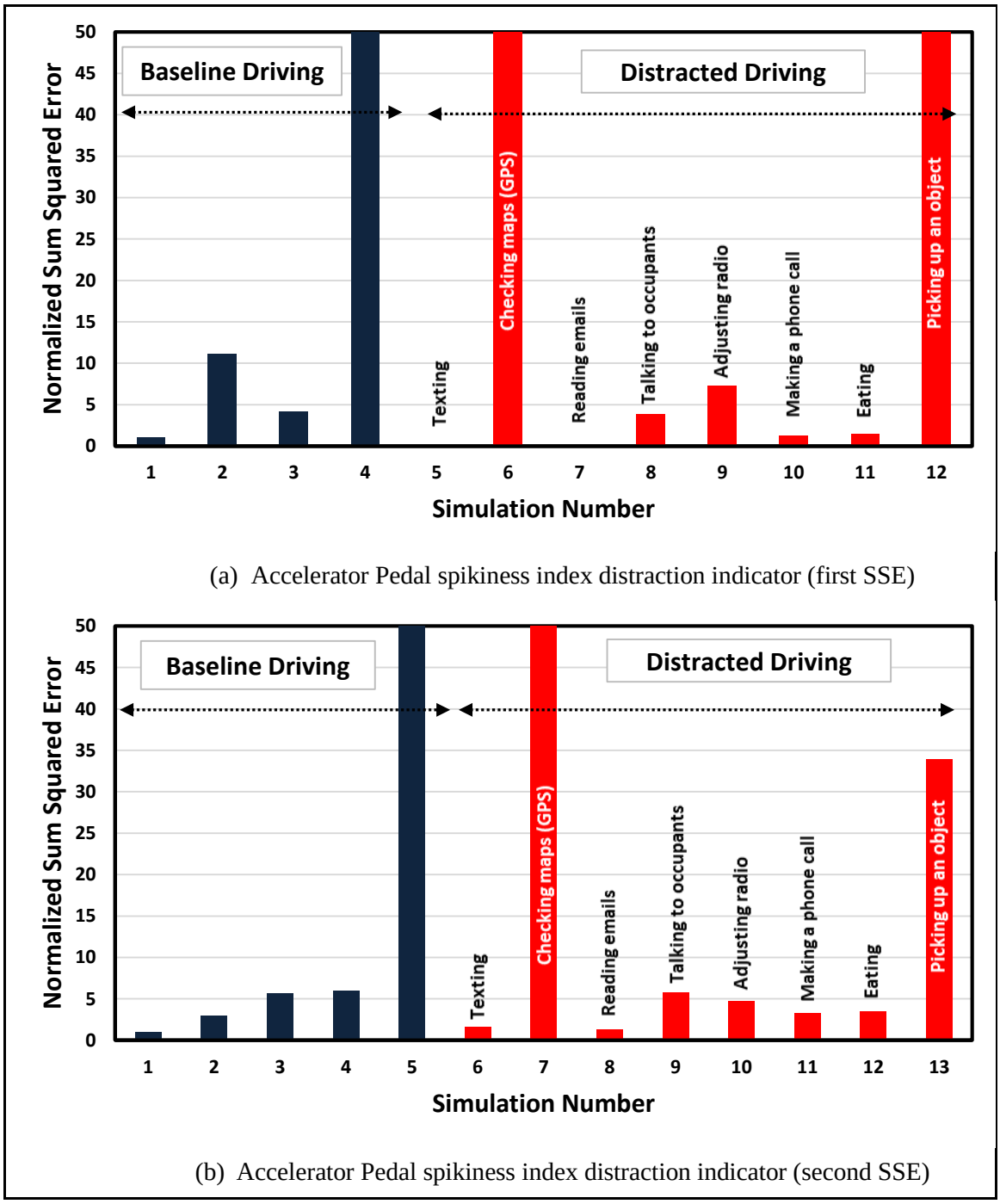

(a) Accelerator Pedal spikiness index distraction indicator (first SSE)

(b) Accelerator Pedal spikiness index distraction indicator (second SSE)

Figure B-12 Accelerator pedal spikiness index distraction indicator

APPENDIX C– PANEL ON RESEARCH ETHICS

CERTIFICATE OF COMPLETION

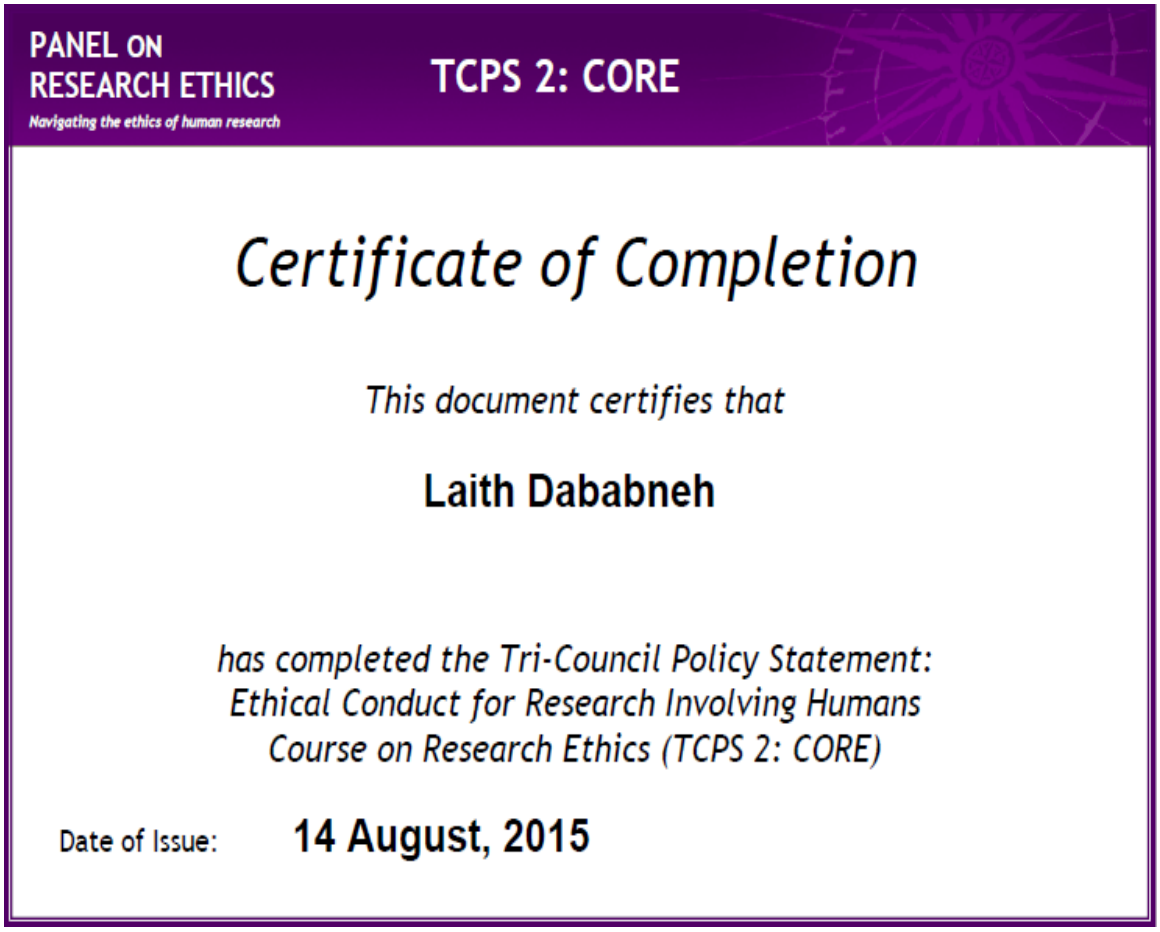

PANEL ON RESEARCH ETHICS

Navigating the ethics of human research

TCPS 2: CORE

Certificate of Completion

This document certifies that

Laith Dababneh

has completed the Tri-Council Policy Statement:
Ethical Conduct for Research Involving Humans
Course on Research Ethics (TCPS 2: CORE)

Date of Issue: **14 August, 2015**